COORDINATED IgG ANTIBODY AND CD8+ T CELL RECOGNITION OF TUMOR ANTIGENS

By

Tyler William Hulett

A DISSERTATION

Presented to the Department of Molecular Microbiology and Immunology and the Oregon Health & Science University School of Medicine in partial fulfillment of the requirements for the degree of Doctor of Philosophy

May 2018

OREGON HEALTH & SCIENCE UNIVERSITY

SCHOOL OF MEDICINE – GRADUATE STUDIES

School of Medicine

Oregon Health & Science University

CERTIFICATE OF APPROVAL

This is to certify that the PhD dissertation thesis of

Tyler William Hulett

has been approved by

Dr. Bernard A. Fox / Advisor

Dr. Larry David / Chair

Dr. Michael Gough

Dr. Paul Spellman

Dr. Owen McCarty

Dr. Evan Lind

TABLE OF CONTENTS

List of Figures:

Abbreviations:

Human leukocyte antigen (HLA)

Major histocompatibility complex class I (MHCI)

Major histocompatibility complex class II (MHCII)

Microsatellite instable (MSI)

Programmed death-ligand 1 (PD-L1)

Programmed cell death protein 1 (PD-1)

Interleukin-2 (IL-2)

Interferon gamma (IFNγ)

T cell receptor (TCR)

Transporter associated with antigen processing proteins (TAP)

Defective ribosomal products (DRiPs)

Short-lived proteins (SLiPs)

Lymphocytic choriomeningitis virus (LCMV)

Antigen presenting cell (APC)

DRiPs and SLiPs autophagosome-enriched vaccine (DRibbles)

Poly-ubiquitinated (Ubb)

Velcade (Bortezomib)

p62 (Sqstm1)

Methylcholanthrene (MCA)

Toll-like receptor (TLR)

Type 1 CD4+ T helper cells (Th1)

Type 2 CD4+ T helper cells (Th2)

Interleukin-5 (IL-5)

Interleukin-4 (IL-4)

Damage-associated molecular patterns (DAMPs)

B cell receptor (BCR)

Immunoglobulin G (IgG)

Tandem mass tag liquid chromatography-tandem mass spectrometry (TMT LC-MS/MS)

Single nucleotide variant (SNV)

Wild-type (WT)

P-value (P)

Melanoma-associated antigen glycoprotein 100 (gp100)

Tumor protein P53 (TP53)

The Cancer Genome Atlas (TCGA)

Size exclusion chromatography-microsphere-based affinity proteomics (SEC-MAP)

Bacteriophage immunoprecipitation sequencing (PhIP-seq)

Frontotemporal dementia (FTD)

Amyotrophic lateral sclerosis (ALS)

Human endogenous retrovirus K (HERV-K)

Acknowledgements:

If there is one skill you absolutely must acquire in pursuit of a Ph.D. – it is the confidence and intellectual rigor to teach yourself to become an expert at just about anything. To my advantage, I enjoy this. To the occasional frustration of others, I often develop confidence in my new interests in advance of the actual expertise. The first to suffer through this were my parents, Tom & Teresa, who have always encouraged my endless interests. Mom's over-encouragement extended so far as to suggest I could also find a cure for dementia as part of this cancer thesis. While unsuccessful, I have not forgotten that suggestion. She can read more about my thoughts on dementia and cancer on Page 107.

Norb Wiech didn't help much with dampening my spirits, and someday I will forgive him for talking me into graduate school. Until then, I will have to simply thank him for teaching me that the point of medical science it to get new treatments into real people. Norb taught me 'it's the science stupid' – and that to help people, your work needs to be rigorous, creative, and have an end goal of not more grant applications, but a business plan….oh and that you needed a Ph.D. first. Norb is thus to blame for me understanding just how special a science environment was built by Bernie Fox at the all-immunotherapy Providence Cancer Center. The labs of Notre Dame and Sloan-Kettering have nothing on this place, and the moment I met Bernie it became unacceptable for me to have joined any other group in Portland.

To properly thank all of the family and friends who have supported, loved, and counseled me in this endeavor would be impossible without a hundred additional pages. I apologize for not talking to all of you much recently, for not listing all of the Siebers' or Hulett's by name, nor having space to thank my brother Dane, my grandmother, our favorite German, or my favorite Aunt Nancy. I do however need to thank Tamara for always seeming so excited to listen to me talk about work again – and also my adoptive Notre Dame family – especially Mike Vogel and Mark & Bridget Hubbard. I'm not sure if I'll be able to pass on as much support and knowledge as you've given me, but do I intend to try.

A gracious thank you to my dissertation committee and all current and former members of the Earle A. Chiles Research Institute. In particular, to Dr. Bernard Fox for having the audacity to suggest I could actually do something – today – to help find the cure for cancer. To Dr. Shawn Jensen, Michael Afentoulis, Dr. Sachin Puri, Dr. Chris Twitty, Dr. Sandra Aung, Dr. Traci Hilton, Dr. Sarah Church, Dr. David Messenheimer, Dr. Reineke Van de Ven, Dr. Keith Wegmann, Dr. Carmen Ballesteros-Merino and Dr. Christopher Paustian for teaching me how science is done in the Fox Lab. To Dr. Walter Urba, Dr. Eric Tran, Dr. Will Redmond, Dr. Andrew Weinberg, Dr. Andrew Gunderson, Dr. Michael Gough, Dr. Marka Crittenden, Dr. Hong-Ming Hu, and Dr. David Page for teaching me to think like a scientist. And a thank you to Jessica Brown, Samantha Kaiser, Katie Robb, Molly Brown, Marlene Riske, and Vernetta Parker for helping me to stay sane during the process.

Tyler W. Hulett – April 19th, 2018

Sections of this document are adapted from the following previously published works by this author:

Hulett, T. W. Coordinated responses to individual tumor antigens by IgG antibody and CD8+ T cells following cancer vaccination. *Journal for ImmunoTherapy of Cancer* 14, (2018).

Page, D. B. & Hulett, T. W. *et al.* Glimpse into the future: harnessing autophagy to promote anti-tumor immunity with the DRibbles vaccine. *Journal for ImmunoTherapy of Cancer* 4, (2016).

Contributions:

Immunologic assays, integrated analysis, text, graphics, and figure preparation by Tyler Hulett. Senior oversight by Dr. Shawn Jensen and Dr. Bernard Fox. Support with immunologic assays provided by Michael Afentoulis, Dr. Shawn Jensen, and Dr. Bernard Fox. Support with multispectral immunohistochemistry by Dr. Carmen Ballesteros-Merino and Dr. Shawn Jensen. All TMT mass spectrometry and analysis by Dr. Larry David, Dr. Ashok Reddy, and Dr. Phillip Wilmarth. 4T1 exome analysis and variant calls by Dr. Christopher Dubay. Peptide array normalization and support by Dr. Christopher Dubay.

Support:

Financial support for these studies was provided by the Chiles Foundation, Robert W. and Elise Franz, Lynn and Jack Loacker, Wes and Nancy Lematta, M.J. Murdock Charitable Trust, the Harder Family, and the Providence Medical Foundation. Support for Tyler W. Hulett additionally provided by OCTRI-OSLER TL1 and the ARCS Foundation – Portland. Mass spectrometric analysis by Larry L. David, Ashok P. Reddy, and Phillip A. Wilmarth performed by the OHSU Proteomics Shared Resource with partial support from NIH core grants P30EY010572, P30CA069533 and shared instrument grant S10OD012246.

Abstract:

What properties, at the level of individual molecules, are responsible for allowing the adaptive immune system to differentiate cancerous cells from surrounding healthy tissue? This question is the bedrock of tumor immunology, for without some method of differentiation it would be impossible for immunity to recognize and kill tumor cells without simultaneously damaging normal organ systems. Thankfully, there are many potential avenues available by which tumors can appear unique. This often results from the evolutionary processes that either directly leads cells to become cancerous or as passengers that occur in concert with that evolutionary process. Such distinguishable features include: dramatic overexpression of normal proteins, ectopic expression of tissue or development-specific proteins, neoantigens from oncogenic or passenger mutations unique to the cancer cell lineage, aberrant glycosylation, metabolite, or lipid profiles, activation of non-canonically transcribed DNA such as endogenous retroviruses, and loss of MHCI loading or surface expression.

Most modern immunotherapies are prescribed blind to these processes based on the hypothesis that immunity to tumor-specific features already exists and simply needs to be boosted or released from suppression – or alternatively, that the therapy itself can create an environment which results in new adaptive immunity. This hypothesis has proven true for many patients since the time of William Coley, and has resulted in the widespread and growing adoption of cancer immunotherapies such as checkpoint blockade, costimulatory agonists, and cytokine therapies – as well as the established successes of traditional surgery, radiation, and chemotherapies. Unfortunately however, many of today's breakthrough immune-oncology treatments still regularly fail in the clinic. Therefore, a deeper

understanding of what tumor-specific immunity exists prior to therapy, whether such immunity is induced or aided by therapy, and which targets are missed entirely by both the natural and therapy-aided immune responses – all provide opportunities whereby additional interventions can improve outcomes and save lives. Perhaps the largest of these gaps, and the greatest opportunity, lies in better defining and monitoring antigen-specific adaptive immunity to cancer proteins and peptides by T cells and antibody. There is already a great deal of evidence that such protein and peptide antigens are both aberrantly expressed by tumors and important for successful anti-tumor adaptive immunity – but technological feasibility and cost hurdles have kept such antigen-specific humoral and cellular responses from being defined and monitored in most cases.

The primary hypothesis underlying this document is that an improved ability to measure and monitor antigen-specific adaptive immunity will lead to improved outcomes for patients with cancer. Such monitoring will allow gaps in both natural and therapy-induced anti-tumor immunity to be identified and exploited with additional therapies such as generalized or personalized cancer vaccines – and may eventually allow for the design of prophylactic cancer prevention vaccines which improve upon observations of natural anti-tumor immune surveillance. This thesis progresses towards this goal by demonstrating antigen-specific correspondence between IgG antibody and CD8+ T cell responses to cancer vaccines – a result that has important implications for high-throughput discovery and monitoring of antigen-specific anti-tumor immunity.

CHAPTER 1

INTRODUCTION

Cancer and immunity

Although the origins of each cancerous tumor are unique and complex, the problem posed by cancer is itself quite simple. Most typically, cancer can be defined as a continuously growing mass of autologous cellular tissue which ignores normal parameters of resource use and spatial regulation at the expense of a host organism. This growth will continue to surround or intrude into the margins of important tissues, organs, and blood vessels – reducing the organism's overall fitness and often eventually resulting in death. Typically, these cancerous tumors are not transmissible between people for the same reason other tissues and organs are not transplantable without careful histocompatibility matching and immunosuppression: the adaptive immune system will acutely reject any cells with foreign human leukocyte antigen (HLA) – which refers to the immune system's major histocompatibility complex class I (MHCI) peptide presentation machinery found on most all somatic cells, and major histocompatibility complex class II (MHCII), which is typically found only on the antigen-presenting cells required for the activation of adaptive immunity. Though there are dramatic naturally occurring examples of infectious cancers such as transmissible venereal tumor in domestic canines [1] and Tasmanian devil facial tumor disease [2] – these exceptions have unique immunologic profiles and are restricted to transmission within genetically homogeneous populations that do not have a parallel in humans.

The main goal of clinical tumor immunology – also termed cancer immunology, immune oncology, and immuno-oncology – is to halt and reverse the growth of human tumors by utilizing the adaptive immune system. In order to discuss how exactly it is that the adaptive immune system is able to recognize and destroy tumor cells, it is important to more

thoroughly describe the origin of tumors themselves. Most cancers start as a single defective progenitor cell, which by chance has been mutated or epigenetically dysregulated in such a way as to cause continuous aberrant cell division. The human body is estimated to be composed of tens of trillions of cells [3], many of which are replaced regularly, and yet the lifetime incidence risk for cancer is only around 40% in a long-lived Western population such as the United States [4]. This means the chances of any particular cell becoming cancerous across a lifetime are vanishingly small. When one cell does become cancerous, it typically has won a genetic lottery of sorts – with mutations knocking out or activating just the right oncogenes in combination with epigenetic dysregulation which helps the cancer grow and evade the immune system. Interestingly, sequencing studies of older individuals have shown that aged tissues regularly contain numerous colonies of cells harboring oncogenic mutations [5], and yet most of these cells still behave properly because not quite enough has gone wrong for them to become cancerous.

Cancer is most often found originating from cells that have a higher likelihood of acquiring the genetic and epigenetic aberrations that lead to cancer. In otherwise healthy adults, this often means epithelial tissue such as can be found in the skin, lung, colon, breast, and prostate or leukemias originating in the bone marrow. These carcinomas and leukemias occur more often than sarcomas of the soft tissue and bone in part because they require more cell divisions as a part of their normal function. Additionally, epithelial layers often serve as protective barriers and will have increased exposure to mutagens, viruses, and inflammation associated with the external environment – giving these cells additional evolutionary opportunities to acquire the genetic and epigenetic modifications which lead to cancer. To a tumor immunologist, the most interesting part of this so-called process of oncogenesis is how

it impacts the way that a tumor becomes either observable or hidden from the immune system. The longer an individual lives, and the more environmental insults such as smoking or ultraviolet radiation that they experience, the more chances they have of one cell acquiring just the right combination of factors which lead to cancer. This accumulated experience of both age and environment also increases the chance that when a cell does become cancerous it will contain more 'passenger' mutations and epigenetic modifications. Such 'passenger' features, though unrelated to the process that directly resulted in the cell becoming cancerous, can still appear foreign to the immune system. Both these passenger mutations and modifications along with the oncogenic mutations and modifications provide candidate antigens for tumor cell recognition by the adaptive immune system.

For this reason, clinicians are observing the apparent contradiction that smokers actually respond better to checkpoint blockade immunotherapy than non-smokers [6], possibly for the simple reason that smoking-associated carcinogens create a more highly mutated and epigenetically dysregulated cancer cell than a non-smoker's cancer cell. Similar results have been observed with the treatment of microsatellite instable (MSI) colorectal tumors and malignant melanomas – these cancers have a high abundance of genetic modifications which give them more obviously foreign antigen profiles. This, in turn, correlates with an increased susceptibility to checkpoint blockade therapies [7–10]. It might be that some of these tumors are so immunogenic that they cannot exist without simultaneously overexpressing immunologic checkpoint proteins such as programmed death-ligand 1 (PD-L1). Normally functioning as a regulator against overzealous immune responses, PD-L1 overexpression by tumors can directly suppress anti-tumor T cell responses via programmed cell death protein 1 (PD-1), and is thus susceptible to anti-PD-1 checkpoint

blockade therapy with drugs such as nivolumab (Opdivo) and pembrolizumab (Keytruda). Through these therapies and other immune checkpoint treatments, some of the most feared and previously untreatable cancers have proven to be low-hanging fruit for tumor immunologists: more severely mutated cancers are simultaneously more antigenic and more likely to be utilizing checkpoint immune evasion mechanisms, making them susceptible to systemic checkpoint blockade immunotherapy. Similar results have been observed with older cytokine therapies such as interleukin-2 (IL-2), where a systemic dose of this T cell growth factor can lead to dramatic responses for melanoma patients that endure for decades [11–13].

The real work going forward will be helping patients that fail these simple systemic treatments. Even the combination of the two checkpoint drugs ipilimumab (anti-CTLA-4) and nivolumab (anti-PD-1) leaves many patients with progressive disease [14]. Developing effective immunotherapy interventions for the majority of cancer patients will require a deep knowledge of the antigens available in a tumor to target, a method of boosting or creating responses to those targets via therapy or vaccines, and a method of confirming and continuing the therapy's success by monitoring a patient's humoral and cellular adaptive immune responses to those antigenic targets. The purpose of this document is to advance new methods and knowledge toward accomplishing these goals.

Tumor antigens

Genetic sequencing studies demonstrate that the evolutionary processes which lead to cancer typically result in a single progenitor from which all daughter cells in a tumor are descended. Though most tumors will typically become polyclonal and diversify as they grow and metastasize, there is a unique 'trunk' of genetic and epigenetic features shared by all these daughter cells that differentiates the tumor and its descendants from the rest of an

individual's somatic cells [15,16]. Although many other antigens and targets will become available as the tumor diversifies, and some of the shared epigenetic features may become silenced, many of these trunk antigens – the genetic changes in particular – will remain common across all new tumor sites. These tumor-specific passenger and oncogene neoantigens are increasingly recognized as an important feature of successful anti-tumor immunity [17–19], and are sometimes even a necessary component of oncogenesis which cannot be silenced by a growing tumor. These shared trunk neoantigens in both oncogenic and passenger mutations are unique differentiators whereby a tumor can be recognized and destroyed via adaptive immunity.

Epigenetic modifications come in a greater variety and diversity but can also result in aberrant or ectopic protein expression that can be passed along to descendent cells. Some of these aberrantly expressed genes are normally expressed at specific times in development or in immunologically protected tissues such as the testis. So-called cancer-testis antigens have long been recognized as a unique antigenic differentiator of tumor cells [20–22]. Additionally, there are non-canonically transcribed regions of DNA such as endogenous retroviruses which can become activated and serve as tumor antigens [23,24]. Additional ways tumor cells can stand out are by aberrant glycosylation and other post-translational modifications, altered metabolite production, and loss of MHCI loading or surface expression – but these are beyond the scope of this document. The primary focus of this thesis will be upon adaptive immune recognition of protein and peptide antigens by T cells and B cell secreted antibody.

Tumor recognition and killing

For a patient with cancer, the ideal outcome of antigen-specific tumor recognition is it leading to the destruction and clearance of a recognized tumor cell. In many cases, the cell completing this final recognition and killing is a cytotoxic effector CD8+ T cell. CD8+ T cells are well established as among the most important populations of adaptive immune cells in a successful anti-tumor immune response [25–27], and CD8+ T cells accomplish this by utilizing their T cell receptors (TCR), in combination with their MHCI recognizing CD8+ co-receptors, to recognize an antigenic peptide-MHCI complex presented by tumor cells. This peptide-MHCI interface is exceptionally important, and understanding why tumors present the antigenic peptides that they do, and how CD8+ T cells are selected and activated to recognize and kill cells bearing them, is essential to acquiring a deeper understanding of how some antigens might be missed and thus available for therapeutic intervention with a cancer vaccine or other immunotherapy.

Cancer cells, like healthy mammalian cells, are composed of thousands of unique proteins of varying median lifespans (Fig. 1.1A). Due to failed translation, protein damage, misfolding, oxidation, or as part of their intended structure and function – these cellular components will regularly be degraded into short peptides via the ubiquitin-proteasome system. First an E3 ubiquitin ligase identifies some aberrant or otherwise unique feature on the target protein and tags it for poly-ubiquitination and targeting to the proteasome for destruction (Fig. 1.1B) where the proteins are degraded into short peptides (Fig. 1.1C). In the context of interferon gamma (IFNγ), a cytokine that is secreted by tumor-recognizing CD8+ T cells and is associated with improved outcomes for patients receiving cancer immunotherapy [7], the cancer cell will upregulate expression of both MHCI and alternate

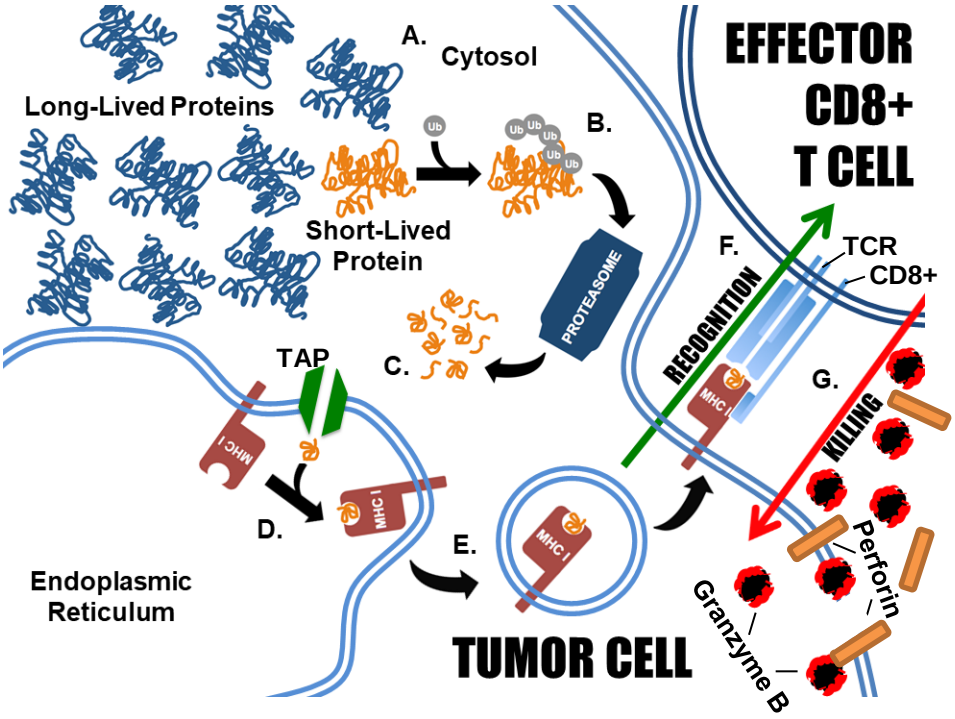

Fig. 1.1 – Overview of CD8+ T cell recognition and killing of a tumor cell. (A) Tumors are composed of thousands of unique proteins of varying abundance and lifetime. These can be divided into long-lived proteins with low turnover and short-lived proteins with high turnover. (B) E3 ubiquitin ligases tag proteins for poly-ubiquitination and degradation via the proteasome. (C) After proteasome digestion, these short peptide fragments are transported via TAP transporters into the endoplasmic reticulum where ~8-11mer peptides are (D) loaded onto MHCI molecules. These MHCI molecules are (E) delivered via vesicles to the tumor cell surface. (F) Activated CD8+ effector T cells whose T cell receptors (TCR) match the peptide-MHCI complex are triggered (G) to induce tumor killing via perforin and granzymes.

proteasome subcomponents that form a structure called the immunoproteasome. The immunoproteasome is a proteasome isoform that increases the likelihood of this ubiquitin-proteasome degradation process creating peptides that bind MHCI. Appropriately sized peptides digested by either the proteasome or immunoproteasome are transported across the endoplasmic reticulum via the transporter associated with antigen processing proteins (TAP) (Fig. 1.1D), where peptides are loaded onto empty MHCI molecules [28,29]. These peptide-MHCI complexes are then transported via vesicles (Fig. 1.1E) to the cell surface, where they then become available to passing activated effector CD8+ T cells. If an effector CD8+ T cell

happens to have a cognate TCR matching the peptide-MHCI complex on the tumor cell (Fig. 1.1F) – and there are no regulatory or other microenvironment effects inhibiting its function – the T cell will then proceed to kill the tumor cell via inducing Fas-mediated apoptosis or directly disrupting the membrane with perforin and granzyme-induced killing (Fig. 1.1G).

Even in a tumor microenvironment free from immunosuppression, there are many factors which determine whether a tumor-specific effector CD8+ T cell will be able to recognize a peptide-MHCI complex. The availability of a peptide for loading onto MHCI is determined not by its overall abundance in the tumor cell, but its throughput of proteasome degradation. While true that an abundant protein will be overrepresented in this degradation in relation to a rare protein with the same median turnover rate, proteins with extremely short half-lives are over-represented. In particular, peptides from defective ribosomal products from failed translation (DRiPs) and short-lived proteins (SLiPs) are abundant on MHCI in relation to their overall static abundance [30–33]. It has been hypothesized that in cancer cells, such DRiPs and SLiPs may be especially prevalent due to a dysregulation of normal mRNA translation [34], and be over-represented in tumor peptide-MHCI complexes.

In addition to being digested by the proteasome, peptides must be of the correct amino acid composition to bind the individual person's unique profile of MCHI isoforms. While some features of peptide-MHCI binding are somewhat general – such as a length preference for 8-11mer peptides – many others are highly individualized to the specific MHCI isoforms encoded in an individual's genetics. Wet lab experiments have enabled MHCI binding prediction algorithms which allow the estimation of expected MHCI binding for common supertypes [35,36], which like other biochemical processes can vary by logarithmic values across different antigen candidates. It is in this way that peptides from

seemingly rare proteins can become very prevalent in surface peptide-MHCI complexes: by either high-proteasomal turnover of the parent protein and/or out-competition of other digested peptides for the available MHCI binding sites due to a dramatically higher MHCI binding affinity. In short – the most common protein within a tumor cell is not necessarily the most available tumor antigen for CD8+ T cell recognition via a peptide-MHCI complex. Some groups have interrogated this by directly precipitating these short MHCI binding peptides from tumor cells and identifying them with mass spectrometry [37,38].

Since each CD8+ T cell only expresses a single and often entirely unique form of T cell receptor, the abundance of available cognate peptide-MHCI complexes are the limiting factor for how many T cell receptor / peptide-MHCI pairs can be made during an interaction with any particular tumor cell. The cumulative binding strength of these T cell receptor / peptide-MHCI pairs, or avidity, determines whether the immunologic synapse they create is strong enough to trigger tumor cell killing by the effector CD8+ T cell [39,40]. Unfortunately for scientists trying to understand what makes a peptide in a peptide-MHCI complex into a strong tumor antigen, the intricacy doesn't stop at how many peptide-MHCI complexes are available to go into the immune synapse, but also depends on the strength of the T cell receptor / peptide-MHCI binding interaction. The strength of these interactions depends on the specific universe of available T cell receptors in any individual, a pool that is broad and contains billions of unique TCRs [41]. This population of circulating CD8+ T cells is sculpted away from self autoantigens in the thymus by a process called central tolerance, and is available to recognize a large universe of potential non-self peptide-MHCI complexes. In addition, an individual's own unique history of previous antigen exposures will control the frequency of circulating activated effector or memory cells and the space

remaining for new activations and effector responses by naïve cells. The chronic viral infection induced by lymphocytic choriomeningitis virus (LCMV) is known to induce a substantial percentage of the entire circulating CD8+ T cell population to target just a few individual viral antigens [42,43]. All new anti-tumor immunity must compete for immunologic space with responses to chronic viruses like LCMV, as well as other prior infections, exposures, and autoimmunity. Therefore, the more frequent, stronger binding, and foreign a tumor antigen appears in a peptide-MHCI complex, the more likely it is for that antigen to become targeted by an effector CD8+ T cell.

Cross-presentation and autophagosome-enriched vaccines

None of the above described tumor recognition and killing can occur unless the CD8+ T cell has been previously activated to become an effector cell. A naïve CD8+ T cell with a T cell receptor that strongly binds a tumor's peptide-MHCI complex is not licensed to kill tumor cells without first being activated to do so by recognizing the same peptide-MHCI complex on an antigen presenting cell (APC) in the context of CD4+ T cell help. Unlike antiviral CD8+ T cell activation, which can occur via direct presentation of peptide-MHCI via viral infection of an antigen presenting cell – anti-tumor CD8+ T cell activation requires a process called cross-presentation for the antigen presenting cell to obtain tumor peptides. During cross-presentation, professional antigen presenting cells acquire external tumor peptides on their surface MHCI molecules [44,45]. These cross-presented peptides are synthesized within tumor cells, later acquired by APCs, and then presented by the APCs as peptide / MHCI complexes to CD8+ T cells for activation [44,45]. Although this can occur directly by acquisition of MHCI from tumor cells or tumor cell fragments via a process called trogocytosis [46] – a direct membrane to membrane transfer of MHCI – this is not

thought to be a major pathway for cross-presentation [44,47,48]. More often, exogenous tumor antigen is thought to be phagocytosed and internally processed for MHCI loading from large tumor cell vesicles, cell fragments, or tumor-antigen / antibody bound immune complexes. This uptake, and subsequent processing for MHCI loading, occurs via one of two major pathways – the phagosome-to-cytosol pathway or the vacuolar pathway [44,45]. The exact uptake mechanism, specific MHCI loading pathway followed, and subsequent signals provided to CD8+ T cells are thought to depend on both the specific antigen presenting cell lineage involved and a surrounding context of toll-like receptor (TLR) ligands [44,45].

In the case of large fragments from necrotic tumor cells – such as autophagosomes with surface C-type lectin receptor (CLEC9A) ligands – these necrotic fragments are acquired by cross-presenting dendritic cells bearing CLEC9A receptors [44,49]. In mice these CLEC9A+ cross-presenting dendritic cells often bear the surface protein CD8α [50], whereas in humans a corresponding population bears the protein CD141 / thrombomodulin / BDCA3 [51]. Although these CLEC9A+ dendritic cells are traditionally thought to be the major subset of cross-presenting dendritic cells, evidence is growing for the importance of dendritic cells which do not bear these markers – including classical dendritic cells and even plasmacytoid dendritic cells [52–54]. These alternative populations of cross-presenting dendritic cells instead are able to utilize IgG antibody-binding Fcγ receptors for sampling of antibody / antigen bound immune complexes from the external environment [54,55]. In this way, cross-presentation to CD8+ T cells can be directly dependent on or enhanced by an antigen-specific context of pre-existing humoral immunity [54]. The exact outcome of the CD8+ T cell interaction following this uptake and processing depends on the specific

dendritic cell subtype, a diversity of Fcγ receptors – each with a different affinity for differing IgG subtypes – and a surrounding signaling context provided by TLR ligands [54,56,57]. Although all of these factors are believed to play an essential role in cross-presentation – in particular for distinguishing whether the antigen's peptide / MHCI complex will be activating or tolerizing to CD8+ T cells – the specific combinations of dendritic cell subtypes, Fcγ receptors, IgG subtypes, and TLR ligands which lead to successful CD8+ T cell immunity are not well understood [54]. This gap in knowledge is compounded by differences between mice and humans in the functions of Fcγ receptors, IgG subtypes, and dendritic cell subtypes. Ligands binding TLR3 – stimulated by viral double-stranded RNA and the vaccine adjuvant polyinosinic : polycytidylic acid (poly I:C) are often reported to enhance cross presentation [58]. In contrast, other pathways such as TLR4 have been reported in differing contexts to either promote or inhibit cross-presentation [54,55,59,60].

After antigen uptake by dendritic cells, ingested proteins destined for cross-presentation must then be processed and loaded onto MHCI molecules. The first of these major pathways is the phagosome-to-cytosol pathway, wherein a fraction of the phagocytosed proteins are transferred to the cytosol and then undergo traditional proteasome digestion, TAP transport, and MHCI loading [44,45]. Exactly how antigens are moved from the phagocytic vesicle into the cytosol is not entirely resolved [44]. In some cases it is thought the phagocytic membrane is disrupted directly, but the mechanism of this destabilization remains unknown. Additional evidence exists for a mechanism analogous to endoplasmic reticulum (ER)-associated degradation (ERAD) - the pathway by which misfolded proteins are removed from the ER. ER-associated machinery such as calreticulin and Sec61 has been found in phagosomes, and silencing of Sec22b – a protein associated

with delivery of ER-associated proteins to phagosomes – severely reduces phagosome-to-cytosol cross-presentation [44,61–63]. ERAD-like systems functioning in phagosomes poly-ubiquitinate ingested proteins before transporting them to the cytosol via transporters such as Sec61, Derlin, or Hrd1 [44,61]. In addition to this incompletely understood phagosome-to-cytosol pathway, cross-presentation can also occur via a vacuolar pathway. In this case, proteins are digested directly in the phagosome by proteases, with further digestion by insulin-regulated aminopeptidase (IRAP), and finally processed for MHCI loading directly in the phagosome [44,45]. MHCI itself can arrive for vacuolar pathway cross-presentation after transport from the ER or via surface-recycling; knockdown of the Rab22a protein that controls MHCI endosome recycling will partially inhibit cross-presentation [64].

As discussed before, two hypothesized classes of tumor-associated proteins –called defective ribosomal products (DRiPs) and short-lived proteins (SLiPs) – are produced in abundance within tumor cells, however are inherently unstable and only expressed transiently under physiologic conditions before being poly-ubiquitinated and degraded by tumor cell proteasomes [65]. These tumor-associated DRiPs/SLiPs, while expressed frequently on tumor MHCI, are inefficiently cross-presented due to many becoming degraded by tumor proteasomes before they reach the antigen presenting cell. Therefore – short-lived antigens might be missed by natural anti-tumor immunity due to a lack of antigen available for cross-presentation. This makes DRiPs/SLiPs a strong pool of candidate antigens for therapeutic intervention, and could form the basis of a novel anti-tumor vaccine.

One proposed way to create such a novel short-lived protein vaccine is via a method of simultaneously blocking proteasomal degradation and manipulating the cellular autophagy pathway – leading to stabilization of DRiPs/SLiPs proteins and formation of autophagosome

microvesicles that contain not only DRiPs/SLiPs, but also other protein products that have been shown to facilitate cross-presentation [66]. These tumor autophagosomes are then harvested by membrane disruption and fractionation to create a DRiPs and SLiPs autophagosome-enriched vaccine (DRibbles). Evidence supporting the utility of this autophagosome-enriched vaccine platform for priming T cell responses was first demonstrated in a series of in vitro experiments with a single dominant OVA antigen [67]. The OVA gene was engineered to produce "short-lived" OVA proteins that would become poly-ubiquitinated and degraded by proteasomes under physiologic conditions [34,67]. Whole cells were treated with bortezomib (Velcade) and ammonium chloride (NH_4Cl), which block proteasome activity and lysosomal digestion of autophagosomes. Then, the treated cells were mechanically disrupted and fractionated by centrifugation to harvest autophagosome-enriched vaccine. Compared to non-treated cells or non-disrupted bortezomib / NH4Cl-treated cells, the short-lived OVA proteins were found to be enriched in this autophagosome-enriched vaccine. Furthermore, autophagosome-enriched vaccine was superior in priming OVA-specific T cells compared to non-treated or non-disrupted cells. These data suggested that such vaccines could be an effective treatment for educating the adaptive immune system against endogenous tumor-associated short-lived proteins. A brief overview of this described vaccine manufacturing process is pictured (Fig 1.2).

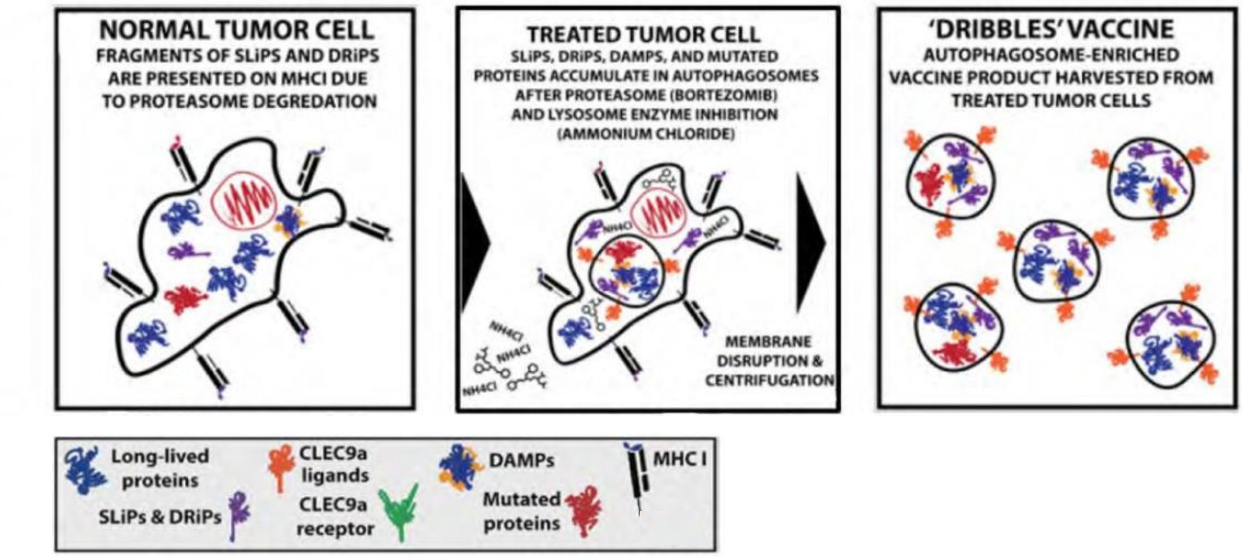

Fig. 1.2 – Overview of DRibbles autophagosome-enriched vaccine. Healthy tumor cells are abundant in long-lived proteins, yet short-lived proteins with higher rates of proteasome turnover are more frequently presented on MHCI molecules. Treating these tumor cells with Velcade (Bortezomib) to block proteasome degradation, and ammonium chloride to block lysosomal digestion, results in increased p62 (Sqstm1) dependent autophagy and an accumulation of poly-ubiquitinated (Ubb) short-lived proteins within autophagosomes. Cells are lysed, and LC3+ autophagosomes enriched in poly-ubiquitinated short-lived proteins are harvested as DRibbles autophagosome-enriched vaccine via centrifugation.

On a theoretical level, such autophagosome-enriched vaccines can either be produced based on an autologous concept (i.e. making the vaccine from a patient's own tumor) or an allogeneic concept (i.e. making an "off-the-shelf" vaccine from one or more tumors to be administered to many patients). An early autologous-concept study using 3LL Lewis lung cancer cell line was shown to delay tumor growth and improve survival in that cancer model [68]. However, it was realized early on that these autophagosome-enriched vaccines would be much more useful if proven effective in an allogeneic setting. To model the allogeneic concept, autophagosome-enriched vaccine was generated from multiple implantable methylcholanthrene (MCA)-induced sarcoma cell lines. The long-standing paradigm was that whole-cell MCA vaccine would be effective only against homologous tumors [69]. However, vaccination with this autophagosome-enriched vaccine derived from unrelated MCA-induced

sarcomas was also effective in slowing tumor growth of other, independently-derived MCA sarcomas [34]. T cells isolated from these mice additionally released interferon gamma (IFNγ) against both homologous and independently derived tumors, suggesting they had been cross-primed to a broader array of antigens present across a variety of sarcomas. This phenomenon was called 'cross-protection,' and was found to depend in part on the function of p62 (Sqstm1), a protein involved in trafficking poly-ubiquitinated proteins to the autophagosome [34]. These results provided evidence that an allogeneic autophagosome-enriched DRibbles vaccine might serve as an "off-the shelf" vaccine in the clinic – a hypothesis which is being investigated in clinical trials [66,70,71]. We realized that if it were possible to determine which tumor antigens were responsible for this cross-protective effect – it might be possible to enrich or isolate them to create an even more powerful generic cancer vaccine. Our attempts to find such antigens are what led to us searching for the coordinated IgG antibody and CD8+ T cell recognition of tumor antigens presented in this document. Further background information on autophagosome-enriched vaccines available to us at the outset of this work included the knowledge that the surfaces of these vaccines contain extracellular filamentous actin or CLEC9A ligands, which have been shown to bind CLEC9A receptor [72] and facilitate antigen uptake by a subset of dendritic cells that play an important role in cross-presentation [73]. Extracellular filamentous actin is associated with debris from catastrophic cell death such as may occur during infection, and is thus not found on the surface of intact whole tumor cell vaccines (Fig. 1.3A). In contrast (Fig. 1.3B), the membrane disruption method of autophagosome-enriched vaccine harvest results in these surface CLEC9A ligands which improves their antigen uptake by CLEC9a expressing APCs (Fig. 1.3C) and cross presentation to T cells (Fig. 1.3D).

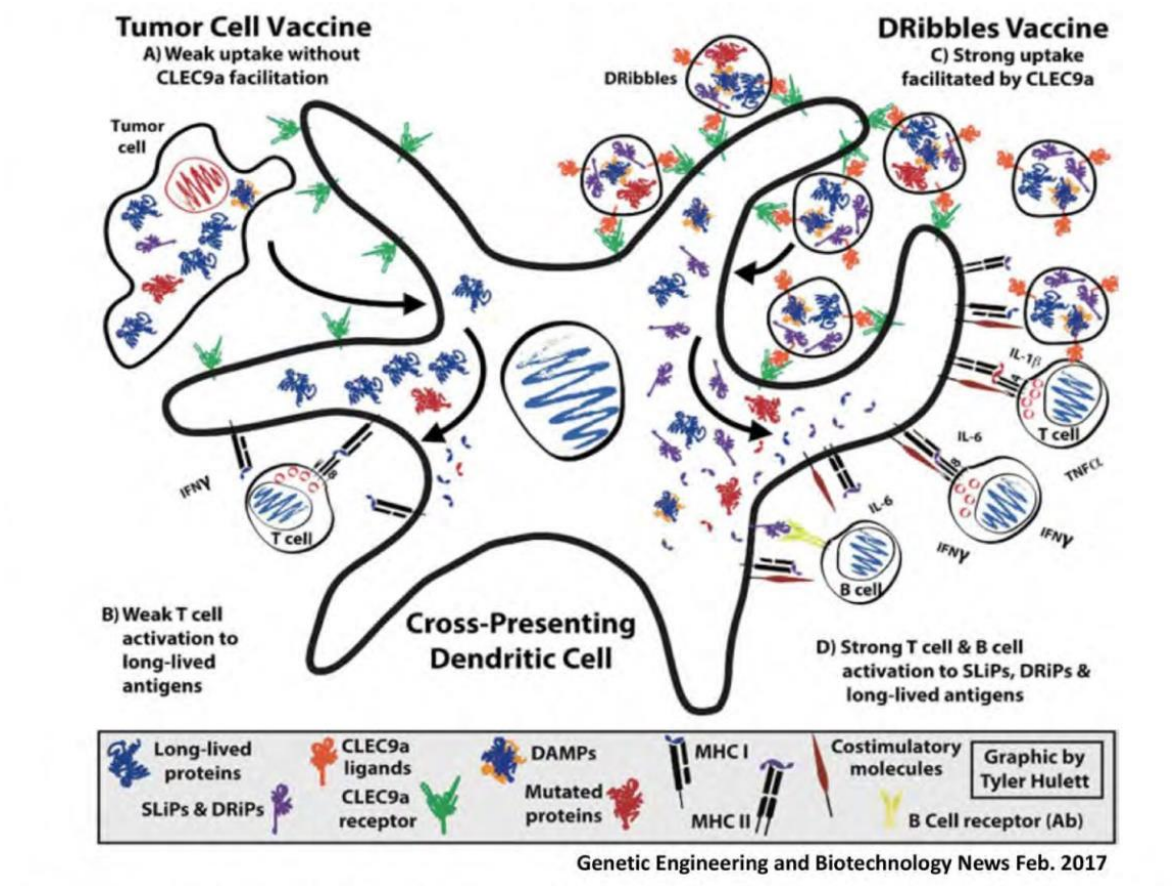

Fig. 1.3 – Comparison of adaptive immunity to whole cell and DRibbles autophagosome-enriched cancer vaccines. Overview of cross-presentation and immune activation by vaccines and an antigen-presenting dendritic cell. Whole tumor cell vaccines (**A**) do not benefit as much from CLEC9a facilitated phagocytosis. The long-lived proteins in whole cells are more available for cross-presentation than the short-lived proteins common on tumor cell MHCI. This leads to (**B**) weak activation of CD8+ T cells specific to the cross presented long-lived antigens. In contrast (**C**), the exterior of DRibbles autophagosome-enriched vaccine is rich in CLEC9a ligands and is easily phagocytosed. The abundant poly-ubiquitinated short-lived proteins in this vaccine more closely mimic the proteins naturally available for MHCI presentation in living tumor cells than the antigens provided by a whole cell vaccine. (**D**) This results in robust activation of CD4+ and CD8+ T cells, as well as B cell activation to membrane proteins captured from the membrane-rich DRibbles vaccine via trogocytosis.

In humans, the autophagosome-enriched DRibbles vaccine was first evaluated as an autologous vaccine manufactured with tumor cells isolated from pleural effusions of patients with non-small cell lung cancer. In this phase I clinical trial, autologous vaccine was found to be safe when combined with docetaxel, a chemotherapy, plus GM-CSF, a cytokine adjuvant [71]. Autologous autophagosome-enriched vaccines, while providing a potential opportunity

to vaccinate against patient-specific antigens, have proven difficult to manufacture consistently. Instead, subsequent trials in malignancies such as prostate adenocarcinoma and non-small cell lung cancer have focused on allogeneic vaccines based upon the cross-protection concept [34]. Not knowing the relevant tumor antigens in such an off-the-shelf clinical vaccine is a gap in knowledge which makes it impossible to determine whether patients are responding optimally to their treatment. This need, combined with preclinical work demonstrating such vaccines are a strong antigen-delivery mechanism, make autophagosome-enriched vaccines a superb and relevant model for studying antigen-specific immune responses to complex tumor antigen populations.

In an ongoing clinical trial, seromic protein arrays are being used to evaluate patient-specific IgG antibody responses based on the hypothesis that some of these antigen-specific responses would prove relevant to vaccine efficacy [70]. The rationale is that the most robust immune responses might be coordinated with concomitant CD4+ T helper cell, CD8+ cytotoxic T cell, and humoral IgG immune responses [74] – and therefore antibody reactivity may serve to identify antigen-specific immune responses associated with therapeutic success. Using the protein array, several of the autophagosome-vaccine patients were found to exhibit robust (i.e. >10-fold increase from baseline) antibody responses to multiple antigens following vaccination [70]. These clinical data provide the rationale behind our desire to directly demonstrate such coordinated cellular and humoral responses in a controlled preclinical mouse model.

IgG antibody and CD8+ T cell activation

No human organ system operates in a vacuum. Even systems once thought to operate with independence are being shown to be more interrelated than was once assumed. For

example, bacterial populations within the gut microbiome have a dramatic impact on the outcome of cancer immunotherapy [75,76]. While the underlying immunologic entanglements behind this are not entirely understood, general bacterial recognition via toll-like receptor (TLR) ligands can induce organism-wide cytokine changes. Additionally, antigen-specific recognition of individual microbial antigens may create cross-reactive immunity which has impact elsewhere in the body. This latter effect could be responsible for another recent report that memory T cells recognizing infectious antigens are common in unexposed individuals [77]. These and many other unique behaviors of the adaptive immune system are simultaneously complex and poorly understood. One of the potential entanglements in need of further investigation is the hypothesis that antigen-specific adaptive immunity might be mirrored across important immunologic systems which are traditionally seen to operate with some degree of independence: effector CD8+ T cells and IgG antibody production by B cells.

An obvious interrelationship between CD8+ T cell and B cell behavior exists via CD4+ T cell help. A productive interaction between helper CD4+ cells is typically required along with antigen recognition for both B cell activation [78] and CD8+ T cell activation [79]. Type 1 CD4+ T helper cells secrete interferon gamma (IFNγ) and the T cell growth factor interleuikin-2 (IL-2) – both associated with cytotoxic effector CD8+ T cell responses. Additionally, IFNγ stimulates expansion of B cells bearing the human IgG subclass IgG_2 [80]. In contrast, Type 2 CD4+ T helper cells (Th2) secrete interleukin-5 (IL-5) and the B cell stimulatory factor interleukin-4 (IL-4), which is associated with the majority of IgG antibody responses – boosting production of the most common IgG subclass IgG1 [81]. For CD8+ T cells, a common understanding of Th1 helped activation occurs as follows: in an

activating environment created by danger signals such as TLR ligands or damage-associated molecular patterns (DAMPs), a cross-presenting dendritic cell will become activated and migrate to a lymph node where it increases expression of surface peptide-MHC complexes and costimulatory molecules. The dendritic cell will increase CD40 expression to provide costimulation to CD40L on any surrounding CD4+ cells who have recognized tumor antigens on dendritic cell MHCII. Pairing with the CD4+ T cell signals the dendritic cell to upregulate chemokines such as CCL3 and CCL4 and induces the Th1 CD4+ cell to secrete IFNγ and IL-2. These chemokines encourage trafficking by CD8+ T cells into the local environment where they sample tumor peptides cross-presented on dendritic cell MHCI. If a strong enough immune synapse is formed between any passing CD8+ T cell and the dendritic cell peptide-MHCI complexes, it will become activated and begin to replicate itself with the aid of local IL-2 via signaling from the Th1 CD4+ T cell [79,82]. In this way, antigen-specific Th1 CD4+ helper T cells can help license CD8+ T cells in a somewhat antigen-linked manner: the same population of tumor antigens available for CD4+ presentation on MHCII are also digested and loaded onto MHCI for cross-presentation to the CD8+ T cell.

B cells do not require MHC signaling for activation, but are instead activated or induced to proliferate when antigens bind to their B cell receptors (BCR) directly via soluble or surface membrane antigens in the context of bystander CD4+ help, TLR ligand stimulation, or an extreme abundance of antigen [78,81,83]. The BCRs of these naïve and newly activated B cells express IgM and some IgD [78,84]. After this initial antigen encounter, activating B cells internalize antigen complexes bound to their BCRs, digest the antigens in MHC class II-loading vesicles, load the fragments onto MHCII, and shuttle peptide-MHCII complexes to the surface for presentation to CD4+ T cells [85].

Simultaneously, the B cells begin expression of costimulatory surface proteins important to T cells such as CD86 and CD80 [85]. These newly-activated B cells may begin to secrete IgM and are now able to present antigen and help prime or restimulate CD4+ T cells through direct cell-to-cell cognate interactions via peptide-MHCII and CD86 / CD80 [85,86]. Stimulated CD4+ T cells are now able to aid the newly activated B cells in an antigen-linked manner by secreting cytokines such as the B cell stimulatory factor IL-4 into the local environment [85–87]. This creates a positive feedback loop of increasing B cell and T cell proliferation.

Later, during a secondary antigen encounter, these previously activated B cells can be restimulated to undergo class switching. This results in the B cell expressing different immunoglobulin isotypes – most often a subtype of IgG [88,89]. This class-switching occurs within a structure known as a germinal center that forms in peripheral lymphoid organs such as the spleen and lymph node [89–91]. Initiation of these germinal centers begins at the center of B cell follicles – lymphoid structures consisting primarily of IgM+IgD+ naïve B cells. At the center of these follicles, follicular dendritic cells serve as an antigen reservoir that awaits activated B cells and the initiation of a germinal center reaction [91–93]. B cells must have been previously activated with the aid of CD4+ helper T cells to enter the germinal center. Once in the germinal center, extremely rapid and error-prone B cell division occurs surrounding the follicular dendritic cell antigen source. This error-prone proliferation results in errors within the immunoglobulin variable region, a process termed somatic hypermutation [91,94]. Although most cells will have similar or inferior affinity for the antigen after this process, a select few will have dramatically higher affinity – and begin to win a Darwinian selection process within the germinal center. The dominant method of

selection in this competition has not been determined, but it is thought to depend on either direct competition for source antigen on follicular dendritic cells or competition for CD4+ follicular T cell help on the periphery via peptide-MHCII presentation [89,91]. The growing colony of dominating high-affinity B cell clones forms a histologically 'dark zone,' surrounded by a 'light zone' of T cells to create the mature germinal center. Other cells, such as CD8+ T cells, can be found in this 'light zone' – but their role is not as well defined as that of CD4+ cells [91,91].

After undergoing development in the germinal center, a mature class-switched B cell may find itself in the same local environment as an activating CD8+ T cell if its BCRs bind local soluble antigen, trogocytosed antigen, or immune complex-bound antigen on the surface of a CD8+ T cell activating dendritic cell. If that B cell has already undergone class-switching to the IgG_2 subclass, it can be stimulated to proliferate by IFNγ secreted any Th1 CD4+ T cells aiding local CD8+ T cell activation in the lymph node [80,95]. This B cell will become further stimulated if the local Th1 CD4+ T cell finds its cognate antigen in a peptide-MHCII complex on the B cell surface [78]. Since IFNγ only supports proliferation of IgG_2 subclass cells and not class-switching to them, this will necessarily represent not activation but a boosting of preexisting B cell immunity [80]. In this way, the observation of a boosted IgG_2 subclass antibody signal might approximately represent the antigen-specificity of an activating effector CD8+ T cell in the local environment. In mice, a similar IFNγ-induced expansion process occurs for B cells bearing IgG2a subclass antibody at the expense of other IgG subclasses [96].

Further rationale for the use of IgG_2 antibody as a surrogate for CD8+ T cell immunity exists in a recent report of natural IgG_2 humoral immunity occurring alongside

concurrent CD8+ and CD4+ T cell immunity to androgen receptor in men with prostate cancer [97]. Interestingly, this IFNγ-driven IgG_2 B cell expansion mechanism occurs at the expense of the more prevalent IgG_1 antibody subclass, with IFNγ directly suppressing IgG_1 B cell proliferation [95]. This means that in some cases an exceptionally strong IFNγ-driven IgG_2 bearing B cell expansion paired with CD8+ T cell activation may present as a misleading decrease in the overall IgG antibody population targeting those antigens. Alternatively, it is also possible for CD8+ T cell activation to be influenced by the more common IgG_1 antibody populations associated with Th2 CD4+ T cell immunity. These IgG_1 antibodies have a dramatically higher affinity for IgG-Fc receptors than IgG_2 [98], meaning they are more likely to scavenge free protein or peptide, create immune complexes, and deliver them to antigen presenting for cross-presentation and thus effector CD8+ T cell activation [99,100]. Since most IgG antibody surveys are global and do not separate differences in IgG_1 and IgG_2 subtype recognition, this has likely confounded or led to conflicting results from some prior searches for CD8+ T cell and IgG antibody correspondence at the antigen level. For the work presented in this document, we also chose to work with global IgG due to constraints of the high-throughput technologies we used to observe antibody responses and the prior success of others using similar methods [74,97,101,102]. However, we believe it is important to remind the reader that in the following pages our measurements and discussion will be of a combined IgG antibody signal composed of different IgG subtypes and that these individual subtypes can be promoted by opposing immunologic environments. Nonetheless, we were impressed by, and are excited to present to you, the results in the following chapters. We believe this document demonstrates a strong argument for future work and applied technologies surrounding the

concept of antigen-specific correspondence between CD8+ T cell and IgG antibody recognition of tumor antigens.

CHAPTER 2

IgG ANTIBODIES IDENTIFY DIVERSE PREEXISTING AND POST-TREATMENT ANTIGEN-SPECIFIC IMMUNITY TO PEPTIDES FROM A NOVEL COMBINATION CANCER IMMUNOTHERAPY

Background: One of today's greatest hurdles for cancer immunotherapy is the absence of information regarding which tumor antigens are already recognized by patients receiving immunotherapies, and whether those therapies then boost or generate an immune response against tumor proteins. Because of this, some immunologists have turned to serum antibodies as an alternative measure of antigen-specific anti-tumor immunity. We sought to thoroughly characterize a novel combination immunotherapy using a cancer vaccine platform currently undergoing human trials, and wished to determine whether we could observe any IgG antibody responses to candidate antigen peptides identified via that characterization.

Methods: We thoroughly profiled an autophagosome-enriched vaccine derived from 4T1 mammary carcinoma by whole exome sequencing and mass spectrometry. We then vaccinated female BALB/c mice with a novel combination of this vaccine along with poly-I:C adjuvant and screened serum for IgG binding to arrays of 15mer peptides containing known mutation-sites in 4T1.

Results: Mass spectrometry analysis demonstrated previously unidentified features of autophagosome-enriched vaccines, while whole exome sequencing confirmed previously reported single nucleotide variant (SNV) mutations in 4T1. Combination vaccinated animals demonstrated improved overall survival and increases in intratumoral CD3+CD8+ infiltrates. Both naïve and treated animals demonstrated a similar background IgG binding to 4T1 mutation-site peptides, with vaccinated animals developing increased IgG signals to some peptides after treatment. In an exemplary group of animals, these vaccine-induced IgG signal increases correlated with the predicted MHCI affinity of the target antigens.

Conclusions: These results demonstrate the efficacy a novel combination immunotherapy: autophagosome vaccine plus poly-I:C adjuvant. Immunohistochemistry assays suggest a role for CD8+ T cells in these improved outcomes, and it was possible to observe IgG antibody signals to antigens from the vaccine in both naïve and vaccinated animals. In an exemplary group of animals, overlap between post-vaccine IgG responses and MHCI affinity suggested coordination between IgG antibodies and CD8+ T cells at the level of individual antigens.

Background:

A large background of autoantibody signals to thousands of normal human proteins is frequently observed in IgG biomarker surveys [103–107]. On average, over 20% of the entire surveyed human proteome is targeted by a unique landscape of these autoantibodies in healthy individuals [103]. Such preexisting or "natural" antibody landscapes are thought to be the result of prior adaptive immunity to similar peptide mimics found in commensal microbes, foods, environmental exposures, infections, and autologous proteins. However, there has not been much investigation into whether this antibody landscape impacts anti-tumor immunity – either via aiding surveillance, or in the recognition and killing of established tumors.

Although the overall benefit of B cell responses to cancer remains controversial [108–110], there is a long history of surveys for antigen-specific anti-tumor antibodies [111,112]. Most of these studies have involved full-length human proteins, with less done at the level of individual peptide antigens. We hypothesized that we could use an autophagosome-enriched vaccine to identify IgG antibody recognition of individual peptide antigens from our vaccine. To identify antigen candidates for our assays, we profiled the vaccine by tandem mass tag

liquid chromatography-tandem mass spectrometry (TMT LC-MS/MS) and performed whole exome sequencing to confirm previously reported tumor-specific single nucleotide variant (SNV) neoantigens. The role of SNV neoantigens in anti-tumor immunity is increasingly recognized [113–117]. These SNV antigens only differ by a single amino acid from their normal wild-type (WT) counterpart autoantigens. We sought to screen for IgG antibodies to peptides centered at previously reported mutation-sites in the 4T1 tumor model in both SNV neoantigen and their WT autoantigen counterpart versions, and determine whether our vaccine could generate immunity to these peptides.

Methods:

Study design

For this work, we chose 4T1, a metastatic murine mammary carcinoma model in BALB/c mice with a limited number of previously described neoantigens, and a autophagosome vaccine model that is known to both work in 4T1 therapeutically and generate cross-reactive immunity to diverse unrelated tumors [118,119]. This vaccine model provided an opportunity to repeatedly interrogate antigen-specific immune responses to specific components of our vaccine in a well-controlled system. Prior to undertaking antigen-specific experiments, we profiled our 4T1 cell line by whole exome sequencing and by quantitative tandem mass tag (TMT) liquid chromatography tandem mass spectrometry (LC-MS/MS). We then utilized these data to create a custom peptide array for profiling IgG antibody responses. These IgG antibody arrays were used to profile serum IgG responses to 4T1 mutation-site peptides by vaccinated and control animals in parallel with prophylactic tumor challenge experiments.

Cell identity confirmation

The 4T1 tumor cell line was a gift of Emmanuel Akporiaye (Earle A. Chiles Research Institute, Portland, OR), from stocks received from Suzanne Ostrand-Rosenberg (UMBC, Baltimore, MD). Cell line identity was confirmed identical to ATCC 4T1 and free from *Mycoplasma* and other common eukaryotic contaminants via microsatellite profiling (IDEXX RADIL).

4T1 autophagosome vaccine production

Tumor cells were thawed directly from the confirmed bank and passaged less than 4 times before use. Cells were cultured in complete media consisting of RPMI-1640 (Lonza) with 1% L-Glutamine (Lonza), 1% Sodium Pyruvate (Lonza), 1% Non-essential Amino Acids (Lonza), 0.1% Beta Mercaptoethanol, 50 mg/L Gentamicin Sulfate, and 10% fetal bovine serum (Atlas Biologicals Lot # 1070612). Production of three 4T1 autophagosome-enriched vaccine lots was performed as previously described [118,120]. In brief, tumor cells were seeded into T225 flasks, grown to ~70% confluence, and treated with 20 mM ammonium chloride and 100 nM Bortezomib (Velcade) to induce autophagosome formation. Treated 4T1 cells were harvested and sonicated to release autophagasomes. Suspended autophagasomes were harvested with centrifugation at 12,000 G. Protein content was measured by a BCA assay using bovine serum albumin as a standard, and harvested 4T1 autophagosome-enriched vaccine was diluted to a protein concentration of 1 mg/mL in hetastarch vehicle and frozen at -80 °C until use. Quality and similarity of autophagosome vaccine lot preparations was confirmed by flow cytometry analysis; vaccine microvesicles

were stained and analyzed for LC3+, a widely used marker for autophagasomes microvesicles.

TMT LC-MS/MS of 4T1 cells and autophagosome-enriched vaccine

Quantitative tandem mass tag (TMT) liquid chromatography tandem mass spectrometry (LC-MS/MS) was performed by the Proteomics Shared Resource at Oregon Health & Science University on three 4T1 autophagosome-enriched vaccine lots and three paired samples of untreated whole 4T1 cells. Samples were lysed using a probe sonicator and protein concentration was estimated using BCA assay. Forty μg of protein per sample was trypsin digested in solution. In brief, samples were dried, dissolved in 10 μL of 4X buffer (8 M urea,1 M Tris (pH 8.5), 8 mM $CaCl_2$, 0.2 M methylamine), reduced, alkylated, diluted to a final 2M urea concentration and digested by addition of 1.6 μg of sequencing grade trypsin overnight (ProMega) Completion of the digestion was confirmed by 1-D gel analysis. Twenty-five μg of each digested sample was then solid phase extracted using Oasis HLB 1cc cartridges (Waters Corporation), and peptides dried by vacuum centrifugation. Samples were labeled with 10-plex TMT reagents (Thermo Scientific), pooled together, and on-line two dimensional reverse phase / reverse phase (RP-RP) liquid chromatography used to separate into 9 fractions at high pH, and each fraction further separated at low pH. Peptides were analyzed using an Orbitrap Fusion Mass Spectrometer (Thermo Scientific) with a synchronous precursor selection MS3 TMT method [121]. Twenty μL samples (32.9 μg) were injected onto a NanoEase 5 μM XBridge BEH130 C18 300 μM x 50 mm column (Waters) at 3 μL/min in a mobile phase containing 10 mM ammonium formate (pH 10). Peptides were eluted by sequential injection of 20 μL volumes of 14, 20, 22, 24, 26, 28, 30,

40, and 90% acetonitrile (ACN) in 10 mM ammonium formate (pH 10) at a 3 μL/min flow rate. Eluted peptides were diluted with mobile phase containing 0.1% formic acid at a 24 μL/min flow rate and delivered to an Acclaim PepMap 100 μM x 2 cm NanoViper C18, 5 μM trap (Thermo Scientific) on a switching valve. After 10 min of loading, the trap column was switched on-line to a PepMap RSLC C18, 2 μM, 75 μM x 25 cm EasySpray column (Thermo Scientific). Peptides were then separated at low pH in the 2nd dimension using a 7.5–30% ACN gradient in mobile phase containing 0.1% formic acid at 300 nL/min flow rate. Each 2nd dimension LC run required 2 hours for separation and re-equilibration, so the entire LC/MS method required 18 hours for completion. Survey scans were performed in the Orbitrap mass analyzer (resolution = 120,000), and data-dependent MS2 scans performed in the linear ion trap using collision-induced dissociation (normalized collision energy = 35) following isolation with the instrument's quadrupole. Reporter ion detection was performed in the Orbitrap mass analyzer (resolution = 60000) using MS3 scans following synchronous precursor isolation of the 10 most intense ions in the linear ion trap, and higher-energy collisional dissociation in the ion-routing multipole (normalized collision energy = 65).

Mass spectrometry data was processed against the UniProt Swiss-Prot canonical mouse protein database (v. 2014_05, 16669 sequences) with SEQUEST HT in Proteome Discoverer v1.4 (Thermo Scientific). Search settings were: monoisotopic parent ion mass tolerance of 1.25 Da, monoisotopic fragment ion tolerance of 1.0 Da, tryptic cleavage with up to 2 missed cleavages, variable modification of oxidized methionine, and static modifications for TMT reagents (peptide N-term and lysines) and alkylated cysteines. Peptide sequence assignments were validated using Percolator [122] q-values (less than 0.05) and 20 ppm delta mass agreement between measured and theoretical peptide masses.

TMT reporter ion intensities of individual peptides were exported as text files and processed with in-house scripts. A median reporter ion intensity cutoff of 1500 was used to reject low quality peptides, and all reporter ion intensities for unique peptides matched to each respective protein were summed to create total protein intensities. A minimum of 2 peptides contributing to the protein total was required for each identification to improve data quality. Protein identification, quantitative information, and additional UniProt annotations were tabulated for all proteins. A total of 4416 proteins were identified and quantification was done on 4196 proteins (excluding contaminants).

4T1 whole exome sequencing and variant detection

DNA was then isolated from our 4T1 cell line bank using a Qiagen DNeasy kit and sent to a contractor for whole-exome sequencing (Otogenetics) at a target 50x coverage depth. Using CLC Genomics Workbench v7.04, the resulting Illumina FASTQ files were aligned to the mm10 reference genome using CLC NGS core tools, a BWS algorithm, to preserve annotations. Known SNVs and indels in BALB/cJ versus mm10 were subtracted using a variant file downloaded from the Sanger mouse genome project (www.sanger.ac.uk/science/data/mouse-genomes-project). Heterozygous non-synonymous protein-coding variants detected >10 times were determined to be 4T1-specific SNV mutation candidates.

Mitochondrial protein comparison

The Mouse MitoCarta2.0 database [123], a list of 1158 nuclear and mtDNA genes encoding proteins with strong support for mitochondrial localization, was downloaded from the Broad Institute and compared to proteins identified by TMT LC-MS/MS .

Tumor challenge assays

Age-matched 14-20 week old female BALB/c mice (Jackson Laboratories) were vaccinated in both inguinal nodes with a total of 10 μg 4T1 autophagosome-enriched vaccine plus 3 μg of Vaccigrade poly-I:C (Sigma-Aldrich) in 20 μL hetastarch carrier, vaccine and carrier alone, poly-I:C adjuvant and carrier alone, or left untreated. Animals were boosted after two weeks with a single subcutaneous injection of the same total dose in the left flank. After another two weeks serum was harvested for analysis or mice were challenged with 5000 live 4T1 cells in the left mammary fat pad. Tumor growth in challenged mice was measured thrice weekly for 30 days until immunohistochemistry and tumor-bearing serum experiments, or until a maximal area of 150 mm^2, which was the determinant for death in overall survival experiments.

Multispectral IHC

Day 30 4T1 tumors were pretreated for 24 hours in a zinc solution, placed in 70% ethanol, and then paraffin embedded until staining as previously described [124]. Five μm sections were cut and fluorescently stained with DAPI and specific antibodies to CD8a (53-6.7, BD Pharmingen), F4/80 (Cl:A3-1, Bio Rad), CD3 (SP7, Spring Bioscience), FOXP3 (FJK-16s, eBioscience), and CD4 (RM4-5, BD Biosciences) via tyramide signal amplification. Multispectral fields were imaged with a multispectral microscope (PerkinElmer, Vectra) and 15 representative 20x fields per sample were quantified with vendor software (PerkinElmer, Inform).

4T1 15mer mutation-site peptide arrays

Mutation-site candidates identified from our sequencing were compared to a list of heterozygous non-synonymous protein coding 4T1 SNVs identified in prior publications [125,126]. One of these studies reported immunologic response data to 17 4T1 neoantigens [125], and we included all of these previously reported immunogenic 4T1 mutation-sites on the arrays. As space allowed in the array design, we additionally included 66 of the 81 total mutation-sites identified by both our independent sequencing and confirmed by at least one of the other reports. The Mouse ENSMBL protein database was downloaded from BioMart (www.ensembl.org/biomart) [127], and 15mer wild-type peptide sequences were extracted centered at the 75 selected coordinates. The 15mer wild-type sequences were then altered to the identified SNV versions for a total of 150 WT and SNV peptides. These 150 peptides were printed in triplicate in replicate arrays along with the known 4T1 retroviral antigen AH1 [128] and anti-mouse IgG control spots by JPT Peptides (Berlin, Germany). Whole mouse sera were pooled from 2-3 animals per experimental group, diluted 1:200, and incubated on the peptide arrays for one hour at 30 °C. IgG signals were detected with a fluorescent anti-mouse IgG secondary. All samples reacted to anti-mouse IgG control spots. Each array spot was imaged with a high resolution fluorescence scanner and its intensity quantified with GenePix spot-recognition software (Molecular Devices). Resulting IgG fluorescence intensity values were averaged across each of the three replicate spots for further analysis. In this initial study, the average intensity values from all 20 arrays were normalized simultaneously using an interquartile range transformation performed using BRB-ArrayTools v4.5.0 developed by Dr. Richard Simon and the BRB-Array Tools Development Team (brb.nci.nih.gov/BRB-ArrayTools).

MHCI binding predictions of mutation-sites

NetMHCpan v2.8 Server was used to calculate predicted H2-Kd, H2-Dd, and H2-Ld MHCI binding scores for all possible WT and SNV 8mers, 9mers, 10mers, and 11mers that include the mutation-site [129]. Out of all outputs, the highest score was selected for plotting.

MHCII binding predictions of mutation-sites

NetMHCII v2.2 Server was used to calculate predicted H2-IAd MHCII binding scores for all possible WT and SNV 15mers that include the SNV site [130,131]. The highest score was selected for plotting.

Statistical analyses

Analyses were performed on either summary data or individualized experiments, and this information is placed alongside the specific type of test performed and p-value (P) within the figure legends. All statistical tests were considered significant at the $P<0.05$ level and were performed with Prism 7 (GraphPad). In general, parametric comparisons were either two sample t-tests or paired t-tests, and non-parametric tests were Wilcoxon matched-pairs signed rank tests. Significance of all correlations was determined by linear regression and Pearson correlation coefficient.

Results:

We have previously demonstrated the benefits of our tumor cell-derived autophagosome-enriched vaccine model [118–120,132], a vaccine that has demonstrated both prophylactic and therapeutic efficacy against both syngeneic and unrelated tumors. This vaccine platform is currently in clinical trials, and has demonstrated increased therapeutic efficacy when combined with anti-OX40 for the treatment of established 4T1 [119], a metastatic mammary carcinoma model with established sequencing and neoantigen immunity data [125,126,133]. In order to develop robust assays for measuring antigen-specific immunity to this vaccine, it was first necessary to create controlled production lots of the vaccine and analyze them thoroughly. A master cell bank was created from existing stocks used in our previous studies [119], and aliquots from this 4T1 cell bank were demonstrated to be free of mycoplasma, other mouse tumor cell lines, and non-murine eukaryotic contaminants by a third party vendor. Cells from this bank were then used to harvest DNA for whole exome sequencing, and used to create three independent 4T1 autophagosome vaccine lots paired with normal 4T1 cells for use in both future immunologic assays and tandem mass tag (TMT) liquid chromatography tandem mass spectrometry (LC-MS/MS) analysis (Fig. 2.1 A). These vaccine lots were demonstrated by flow cytometry to be enriched in autophagasomes, with >80% of the vaccine microvesicles being positive for LC3+, a widely used marker of autophagasomes (Fig. 2.1 B,C). Enrichment for autophagasomes is a feature associated with biologic activity for the DRibbles vaccine platform [120], and gave us confidence in the quality and consistency of our 4T1 autophagosome vaccine lots. Since there was no published proteomic profile of either preclinical or clinical autophagosome vaccines, we sought to better understand antigen

candidates in 4T1 vaccine by quantitative tandem mass tag (TMT) liquid chromatography tandem mass spectrometry (LC-MS/MS). TMT LC-MS/MS provided an opportunity to identify and relatively quantify thousands of proteins in our vaccine. TMT LC-MS/MS is unique suited to analyzing autophagosome vaccines over RNAseq because the production method for these vaccines involves creating an altered proteomic profile via blocking proteasome digestion and lysosome fusion with autophagasomes. The TMT LC-MS/MS analysis was performed by our collaborators on the three pairs of 4T1 autophagosome vaccine lots and whole cells already presented (Fig. 2.1). This analysis identified fragments from 4416 unique proteins and provided quantitative data to a depth of 4196 proteins.

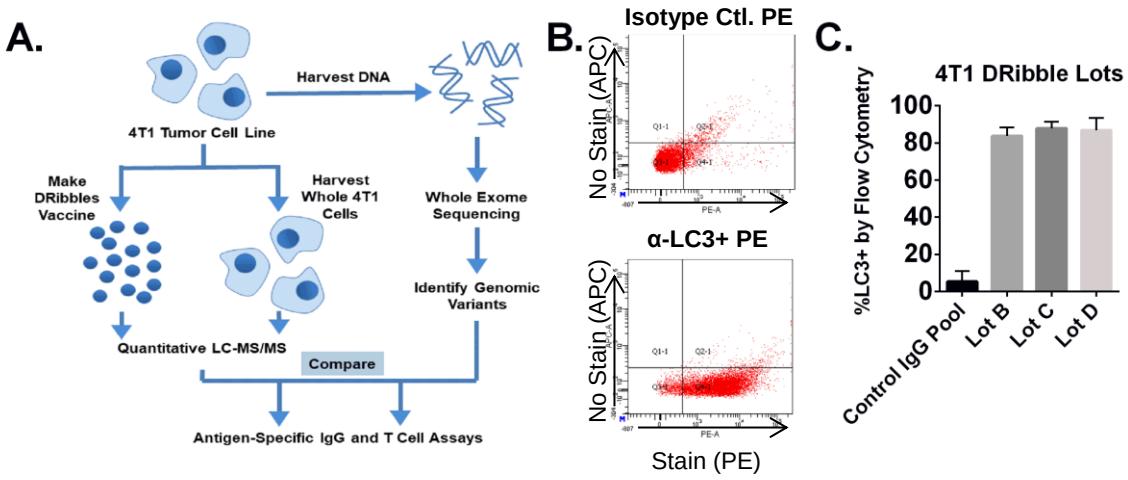

Figure 2.1 – Overview of 4T1 autophagosome vaccine characterization. (**A**) DNA was harvested from a prepared 4T1 cell bank for cell identity confirmation and whole exome sequencing. For each of three independent vaccine lots, 4T1 DRibbles autophagosome-enriched vaccine was prepared from whole 4T1 cells, or whole 4T1 cells were harvested without treatment. Protein amounts were quantified in each lot, and samples were analyzed simultaneously by quantitative tandem mass tag (TMT) liquid chromatography tandem mass spectrometry (LC-MS/MS). Data from TMT LC-MS/MS and genomic sequencing were integrated to select antigen candidates for immunologic analyses. (**B**) Representative flow cytometry plot from 4T1 autophagosome vaccine microvesicles stained for LC3 autophagosome marker or IgG isotype control. (**C**) Average percentage of LC3+ microvesicles in each of the three independent autophagosome vaccine lots plotted from n=2 independent flow cytometry experiments with SEM.

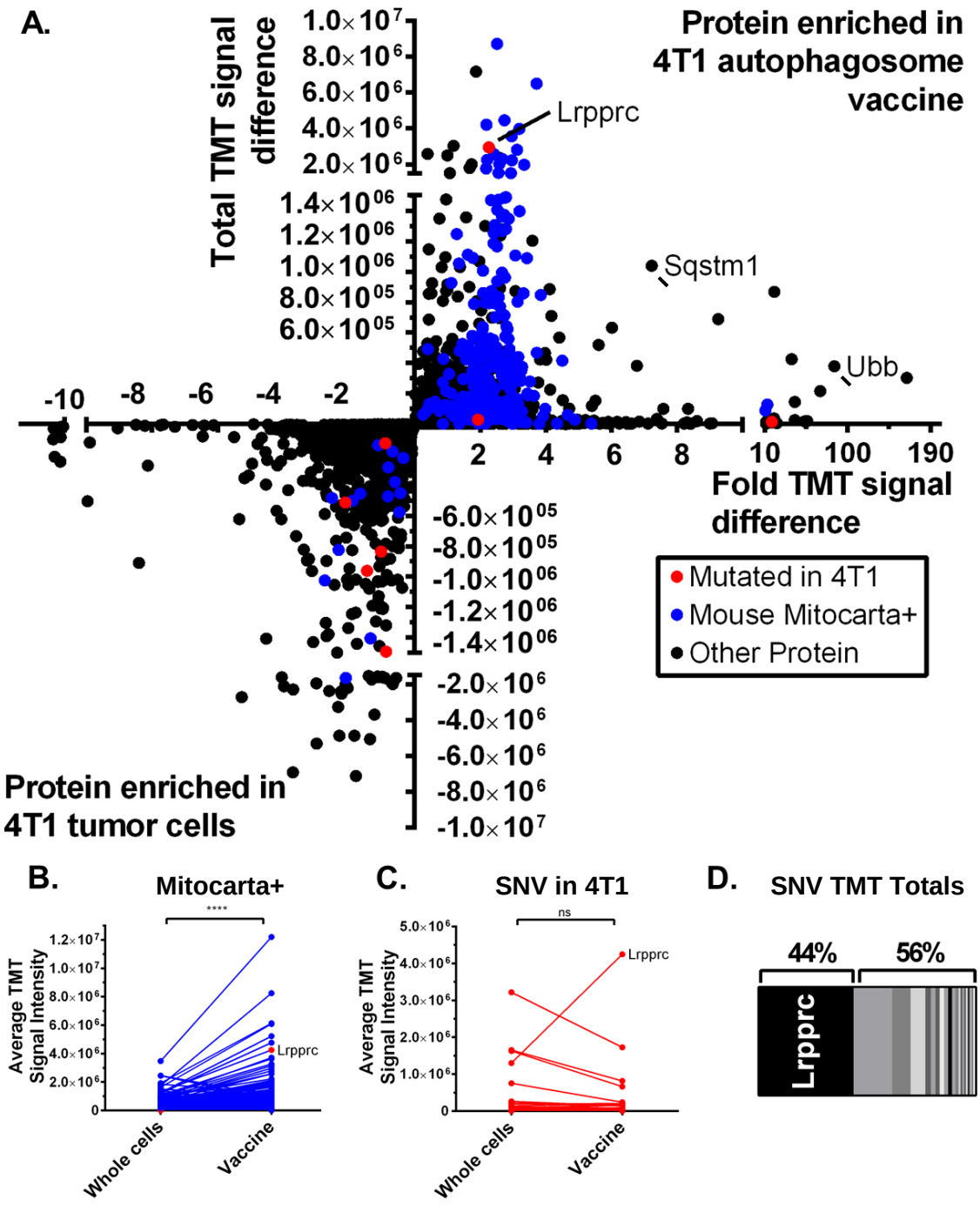

Figure 2.2 – Quantitative tandem mass tag liquid chromatography tandem mass spectrometry demonstrates that 4T1 autophagosome vaccines are enriched in mitochondria. Average data from three 4T1 whole cell lots versus three paired autophagosome vaccine lots. (**A**) Each of the 4196 quantified proteins are plotted according to their normalized difference in TMT LC-MS/MS signal for vaccine lots versus whole cells for both fold enrichment and total signal enrichment. Fragments from proteins identified as carrying an SNV in 4T1 plotted in red, fragments matching proteins in the Mouse Mitocarta2.0 database plotted in blue, and other proteins plotted in black. (**B**) Higher average TMT LC-MS/MS signal intensity in 4T1 autophagosome vaccine lots for mitochondrial proteins from the Mouse Mitocarta2.0 database (P<.0001) by Wilcoxon matched-pairs signed rank test. (**C**) No average difference in TMT LC-MS/MS signal intensity for proteins with SNV mutations identified in 4T1 by whole exome sequencing (P=.59) by Wilcoxon matched-pairs signed rank test. (**D**) The mitochondrial protein Lrpprc is the most common SNV mutated protein in 4T1 autophagosome vaccine, responsible for 44% of the total TMT LC-MS/MS signal intensity from proteins containing a known SNV.

Normalized average differences between 4T1 vaccine and whole cells are plotted by both fold-enrichment and overall signal enrichment (Fig. 2.2 A). These results demonstrated that p62 (Sqstm1) and poly-ubiquitin (Ubb) are highly enriched in 4T1 autophagosome vaccines versus whole 4T1 cells, a feature shared with autophagosome vaccines made from different cell lines [118,120]. This gave us further confidence in the quality of our vaccine preparations. We next sought to determine whether any other features differentiated 4T1 vaccine from whole cells, and noticed many of the enriched proteins seemed to be localized to mitochondria. To quantify this, we downloaded the Mouse MitoCarta2.0 database [123] and compared it to our list of quantified proteins. We observed that the average TMT signal intensity for proteins in the Mouse MitoCarta2.0 database was much higher in 4T1 autophagosome vaccine than whole 4T1 cells (Fig. 2.2 B). Additionally, we overlaid our prior variant analysis data and determined that the average TMT signal intensity was not enriched for proteins with a SNV mutation in 4T1 (Fig. 2.2C). This demonstrates that on average, SNV mutations in 4T1 are not severe enough to alter protein turnover and become enriched in the vaccine. If severe mutations were in fact degraded more often in normal 4T1 cells, we would expect them to become enriched in 4T1 autophagosome vaccine. However, the mitochondrial-localized protein Lrpprc is both mutated in 4T1 and highly enriched in the vaccine, accounting for nearly half the total TMT signal from identified proteins with a known SNV (Fig. 2.2D).

Now that we had a more thorough understanding of the antigenic profile of our vaccine, we sought to simultaneously confirm the vaccine efficacy and to save serum samples for future antigen-specific IgG assays. Animals received the 4T1 autophagosome-enriched vaccine + poly-I:C adjuvant injected into the inguinal lymph nodes of naïve female

BALB/c mice. A single booster vaccination was given subcutaneously at 2 weeks, and, at 4 weeks, animals were killed for sera harvests or challenged with live 4T1 tumor cells (Fig. 2.3A). Challenged animals that had received prophylactic 4T1 autophagosome-enriched vaccine + poly-I:C, but not either alone, benefitted from a significant delay in tumor growth (Fig. 2.3B), results similar to our prior publications [118,119]. Additionally, the only group that demonstrated a statistically significant increase in long-term survival was the combination treatment (Fig. 2.3C). It should be noted that while the level of protection is

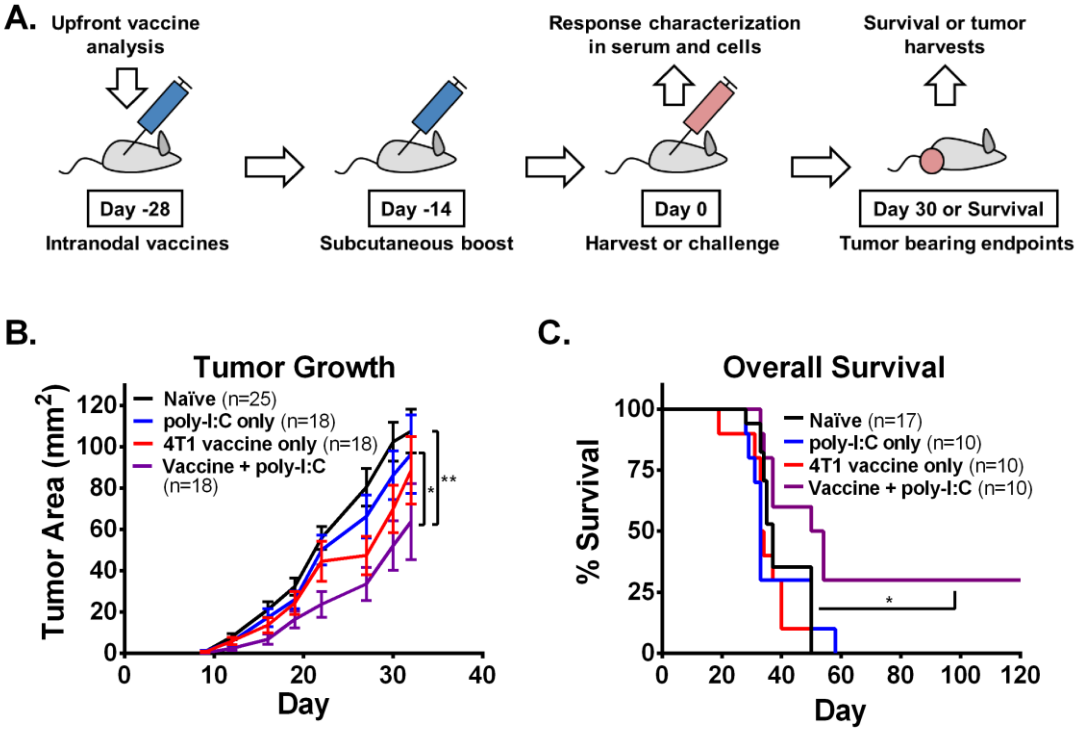

Figure 2.3 – Prophylactic autophagosome vaccination delayed 4T1 tumor growth and improved overall survival. (**A**) Mice were vaccinated in both inguinal lymph nodes with 4T1 autophagosome-enriched vaccine plus poly-I:C, vaccine alone, adjuvant alone, or left untreated. Animals were boosted subcutaneously after two weeks. After another two weeks, sera or spleens were harvested at Day 0 for in vitro antibody and T cell assays or animals were challenged with live 4T1 tumor cells for survival endpoints, tumor-bearing sera, and immunohistochemistry. (**B**) Upon challenge, reduced average tumor growth was observed in combination vaccine + poly-I:C pretreated animals with maximum separation occurring at Day 22 versus poly-I:C alone (P=0.04) and Day 27 versus naïve animals (P=0.002) by Dunnett's multiple comparisons test. Data were pooled from five independent experiments with error bars plotted as the standard error of the mean. (**C**) Overall survival was improved in combination treatment versus all other groups (P=0.02) by Gehan-Breslow-Wilcoxon test. Data were pooled from three independent experiments.

small, 4T1 is considered to be a poorly immunogenic tumor as vaccination with irradiated 4T1 tumor cells fails to protect any animals from a tumor challenge [134].

We next applied immunohistochemistry in order to determine whether these tumors had any differences in intratumoral T cell infiltrates. We hypothesized this might help explain the treatment benefit because numerous studies [135] have linked increased T cell infiltrate with improved outcomes following original work by Galon and colleagues [136]. Similar associations have also been observed in preclinical mouse models [137]. We stained sections from day 30 4T1 tumors as previously reported [124] for CD3, CD4, CD8, FOXP3, and F4/80 and quantified the infiltrates. Versus all other groups, including adjuvant-only controls, combination vaccinated animals demonstrated an increase in CD3+CD8+ infiltrates (Fig. 2.4A,B). Versus adjuvant-only controls, these same tumors demonstrated no difference in CD3+CD4+FOXP3- or CD3+CD4+FOXP3+ infiltrates (Fig 2.4C,D). These results demonstrate that our combination autophagosome-enriched vaccine creates increased frequencies of CD8+ T cells that were capable of trafficking to 4T1 tumors in vivo. These results correlate with delayed in vivo tumor growth similar to previous clinical reports [136].

We next sought to determine whether antigen-specific IgG antibodies might occur in concert with these treatment-induced CD8+ T cell infiltrates. If so, we hoped such antibodies might help provide a window into the antigens recognized by vaccine-induced CD8+ T cells. We were led to this by our own experience and others who have observed links between IgG antibody and T cell responses to human tumor antigens [138,139]. We utilized whole-exome sequencing on our 4T1 cell bank, and used the sequencing data to identify heterozygous single nucleotide variants by comparison to a female BALB/cJ reference sequence –

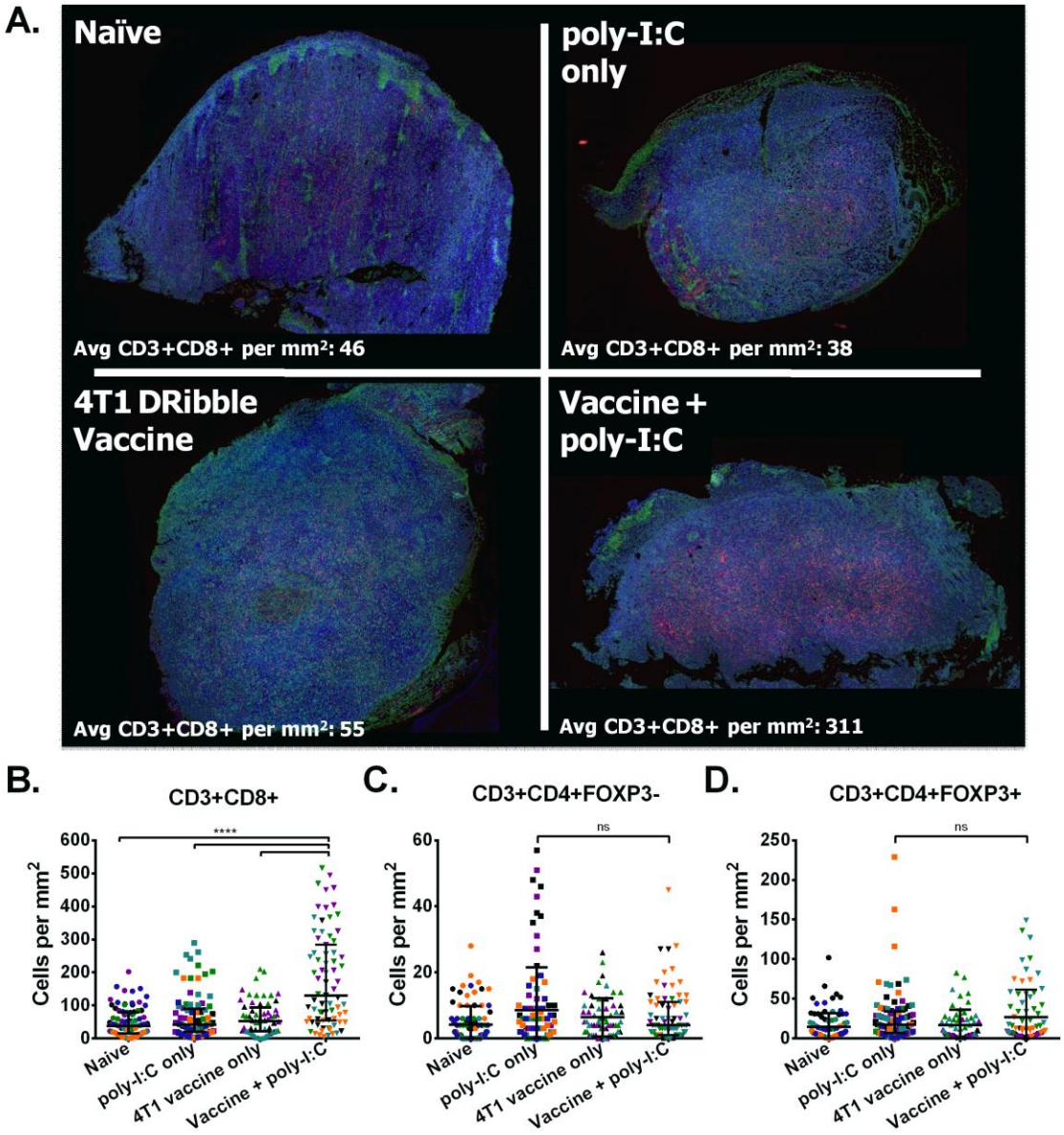

Figure 2.4 – Prophylactic autophagosome vaccination results in increased intratumoral CD3+CD8+ infiltration. Mice were vaccinated in both inguinal lymph nodes with 4T1 autophagosome-enriched vaccine plus poly-I:C, vaccine alone, adjuvant alone, or left untreated. Animals were boosted subcutaneously after two weeks. After another two weeks, animals were challenged with live 4T1 tumor cells for immunohistochemistry. Zinc and alcohol fixed day 30 4T1 tumors were stained for six color immunohistochemistry with tyramide signal amplification. (**A**) Three color representative image from each group showing CD8+ (red), F4/80 (green), and DAPI (blue). (**B-D**) Fifteen 20x fields were imaged for each of 4 to 6 tumors per group and quantified for labeled cells per mm^2. Lines plotted are the median and interquartile range, and fields from individual tumors are colored separately. (**B**) Higher numbers of CD3+CD8+ infiltrates were seen in the fields from vaccine + poly-I:C pretreated tumors versus all other groups ($P<0.0001$) by t-test. There is no significant difference for combination vaccine group (**C**) CD3+CD4+FOXP3- infiltrates versus poly-I:C only ($P=0.29$) by t-test or in (**D**) CD3+CD4+FOXP3+ infiltrates versus poly-I:C only ($P=.94$) by t-test.

subsequently referred to as SNVs. We used SNVs that were both identified in previous reports [125,126,133] and confirmed by our sequencing to design a custom 15mer peptide array for 75 SNV neoantigens and 75 alternate allele wild type (WT) autoantigens centered at 4T1 mutation-sites, as well as the known retroviral antigen AH1 [128]. An overview of the design layout of these peptide arrays is shown (Fig. 2.5), and the specific printed sequences are also available (Table 2.1). A number of these mutation-sites have been previously reported as immunogenic to murine CD4+ or CD8+ T cells [125]. Each array contained all peptides printed in triplicate along with anti-mouse IgG controls. We ran IgG arrays with

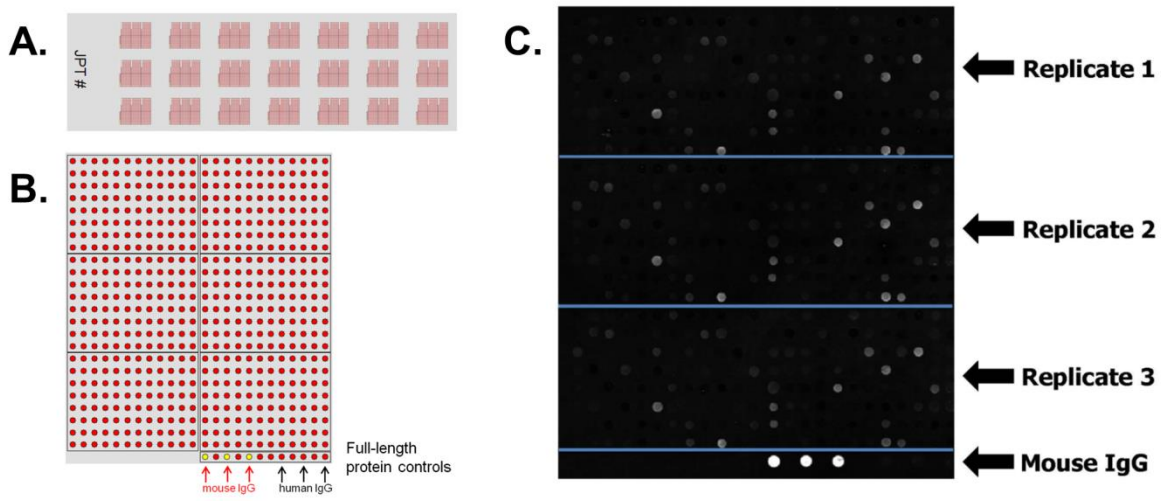

Figure 2.5 – Overview of custom 4T1 mutation-site peptide array. Twenty arrays were printed by JPT peptides on a single slide with individual wells for each sample. Twenty arrays were used for the first study with IgG only, and forty for the follow-up experiments paired with T cell assays presented in Chapter 3 (**A**). These arrays consisted of AH1 plus 75 WT and 75 SNV 15mer peptides centered at 4T1 mutation-sites. Peptides were printed in triplicate on each array along with anti-mouse IgG control spots (**B**). Whole mouse sera were pooled from three animals per experimental group, diluted 1:200, incubated on the arrays for one hour at 30 °C, and developed with an anti-mouse IgG secondary. All samples reacted to anti-mouse IgG control spots. Each spot was imaged with a high-resolution fluorescence scanner and quantified with spot-recognition software. Example image provided showing fluorescence from one of the arrays printed for this experiment (**C**). Resulting values for each replicate were averaged across each of the three replicate spots.

				WT	SNV
Gene	Variant Coordinate	MS+	Selected for Cellular T Cell Assays	Mutation-Site 15mer	Mutation-Site 15mer
AH1	gp70 423-431	N/A	TRUE	SPSYVYHQF	N/A
Dpp9	G633E	TRUE	TRUE	KPHTLQPGRKHPTVL	KPHTLQPERKHPTVL
Gen1	K707N	TRUE	TRUE	RVAVKTTKNLVMKNS	RVAVKTTNNLVMKNS
Ilkap	I127S	TRUE	TRUE	EMQDAHVILNDITQE	EMQDAHVSLNDITQE
Lrpprc	L1347M	TRUE	TRUE	EYLTAKNLKLDDLFL	EYLTAKNMKLDDLFL
Man2b2	V210I	TRUE	TRUE	QQEIFTHVMDHYSYC	QQEIFTHIMDHYSYC
Polr2a	M1102I	TRUE	TRUE	LGEPATQMTLNTFHY	LGEPATQITLNTFHY
Wdr11	T340I	TRUE	TRUE	LDPVQELTYDLRSQC	LDPVQELIYDLRSQC
Wdr33	H13Y	TRUE	TRUE	GSPPRFFHMPRFQHQ	GSPPRFFYMPRFQHQ
Zfr	K411T	TRUE	TRUE	AKHQKVVKLHTKLGK	AKHQKVVTLHTKLGK
Abcc4	I1140K		TRUE	DPRTDELIQQKIREK	DPRTDELKQQKIREK
Cyp26a1	L316I		TRUE	ATSLITYLGLYPHVL	ATSLITYIGLYPHVL
Gzmc	P33S		TRUE	EISPHSRPYMAYYEF	EISPHSRSYMAYYEF
Olfr618	A290T		TRUE	LYVVVPPALNPIIYG	LYVVVPPTLNPIIYG
Qars	E530D		TRUE	RRRGFPPEAINNFCA	RRRGFPPDAINNFCA
St8sia3	L235F		TRUE	RNNFFLSLKKLDGAI	RNNFFLSFKKLDGAI
Dusp1	C24R	TRUE		LREGAAQCLLLDCRS	LREGAAQRLLLDCRS
Flnb	L500Q	TRUE		GPKGLEELVKQKGFL	GPKGLEEQVKQKGFL
Gli2	N980K	TRUE		FHSTHNMNPGSLPPC	FHSTHNMKPGSLPPC
Gprc5a	F119L	TRUE		SCLLAHAFNLIKLVR	SCLLAHALNLIKLVR
Itprip	A15G	TRUE		VCLVVVTAIINHPLL	VCLVVVTGIINHPLL
Mrpl22	A98V	TRUE		MSIDQALAQLEFNDK	MSIDQALVQLEFNDK
Myh14	R1415P	TRUE		LEAGEEARRRAAREA	LEAGEEAPRRAAREA
Scrn1	C89G	TRUE		GANEHGVCIANEAIN	GANEHGVGIANEAIN
Vars	G821S	TRUE		PGTLLETGHDILFFW	PGTLLETSHDILFFW
Abca13	Q4266H			LLRKFRDQDPVCADA	LLRKFRDHDPVCADA
Actn2	N68K			NIEEDFRNGLKLMLL	NIEEDFRKGLKLMLL
Adam24	A730P			KKSREAAASQPAEER	KKSREAAPSQPAEER
Adamts9	I623L			GFSSFQKIRLDLTSM	GFSSFQKLRLDLTSM
B3galnt1	D267V			VKPIKFEDVYVGICL	VKPIKFEVVYVGICL
Bmp4	H51Y			GRRSGQSHELLRDFE	GRRSGQSYELLRDFE
Cep120	H68N			DRKVLHQHRLQRTPI	DRKVLHQNRLQRTPI
Chd2	D1357G			NKAPRLKDEHGLEPA	NKAPRLKGEHGLEPA
Cpxm1	L625I			VRDKDTELGIADAVI	VRDKDTEIGIADAVI
Ctsg	S133T			PVALPQASKKLQPGD	PVALPQATKKLQPGD
Cyp2c39	S99G			EEFSDRGSIPMVEKI	EEFSDRGGIPMVEKI
Dmrta2	R73G			TPKCARCRNHGVVSA	TPKCARCGNHGVVSA
Enho	L10I			AAISQGALIAIVCNG	AAISQGAIIAIVCNG
Fmo2	F69L			TSKEMSCFSDFPMPE	TSKEMSCLSDFPMPE
Ggt7	W222R			EEALQRSWDTKPGLL	EEALQRSRDTKPGLL
Glycam1	T45I			PAAQSTPTSYTSEES	PAAQSTPISYTSEES
Hpcal4	A61V			KFFPYGDASKFAQHA	KFFPYGDVSKFAQHA
Isoc1	V205L			IPGVRSVVLFGVETH	IPGVRSVLLFGVETH
Kbtbd2	T91R			MIIAYAYTGNLAVND	MIIAYAYRGNLAVND
Kif2b	G454R			DLAGNERGADTAKAT	DLAGNERRADTAKAT
Lhx4	A31S			MQQIPQCAGCNQHIL	MQQIPQCSGCNQHIL
Lyst	S850F			DIQQELPSLSVGPSL	DIQQELPFLSVGPSL
Malt1	T534A			LLEDKKITVLLDEVA	LLEDKKIAVLLDEVA
Mc3r	A214G			YIHMFLFARLHVQRI	YIHMFLFGRLHVQRI
Mrgprd	S28T			LVTWIYFSVTFLAMA	LVTWIYFTVTFLAMA
Nlrp14	S155R			EQVLSKPSSLLFIID	EQVLSKPRSLLFIID
Olfr1057	N307S			ALKEFLKNPCKRFNL	ALKEFLKSPCKRFNL
Olfr1216	K20R			LGLSQNPKIEKILFV	LGLSQNPRIEKILFV
Olfr1278	M208V			ANSGFISMGTFLLLI	ANSGFISVGTFLLLI
Olfr50	M146V			SLCVLLVMVSWAFSS	SLCVLLVVVSWAFSS
Olfr635	Q65H			RTEPSLHQPMYLFLS	RTEPSLHHPMYLFLS
Olfr77	A300S			RNKDVKGALVRLLRR	RNKDVKGSLVRLLRR
Olfr862	F161V			MNSLVHYFIVSQLKF	MNSLVHYVIVSQLKF
Olfr881	C101Y			NIISHAECMTQLFFF	NIISHAEYMTQLFFF
Olfr938	N42K			YLVTVVGNLGMIVLI	YLVTVVGKLGMIVLI
Olfr979	T75K			DMWFSTVTVPKMLMT	DMWFSTVKVPKMLMT
Pzp	G1199E			SLHWQRPGDVQKVKA	SLHWQRPEDVQKVKA
Rragd	L268P			HQTSAPSLKALAHNG	HQTSAPSPKALAHNG
Slc19a3	F185L			LACVSVAFFFSLFLP	LACVSVALFFSLFLP
Slc6a2	V307E			YRLKEATVWIDAATQ	YRLKEATEWIDAATQ
Sostdc1	N112K			LPLPVLPNWIGGGYG	LPLPVLPKWIGGGYG
Spam1	I144S			DKLGLAIIDWEEWRP	DKLGLAISDWEEWRP
Sult2a1	Q262H			KNHFTVAQAEAFDKV	KNHFTVAHAEAFDKV
Sva	T41P			HNEPRNYTLTLNMKI	HNEPRNYPLTLNMKI
Taf4b	P561H			TPVNAVMPTSKFPPS	TPVNAVMHTSKFPPS
Tcf3	S255N			PLPLAPGSSSVGSGT	PLPLAPGNSSVGSGT
Tmtc2	V201I			AVSAVYDVFVFHRLK	AVSAVYDIFVFHRLK
Usp43	R621W			NMAPHVARRSTNSKA	NMAPHVAWRSTNSKA
Vmn1r9	V126D			LKKYMVCVFLCIWSF	LKKYMVCDFLCIWSF
Zmynd12	R13C			PLAVPKGRRLSCEVC	PLAVPKGCRLSCEVC
Zzz3	K311N			FKKLKKQKLQQMQAE	FKKLKKQNLQQMQAE

Table 2.1 – Individual peptides printed on the 4T1 mutation-site peptide arrays. Listed are the individual sequences for AH1 and the 75 WT and 75 SNV 15mer peptides printed in triplicate on arrays for serum IgG antibody analysis of naïve and treated animals.

sera harvested from animals used in the tumor challenge experiments already presented (Fig. 2.3, Fig. 2.4). All arrays presented positive anti-mouse IgG controls. Prior to analysis, triplicate spots were averaged and data from all arrays were simultaneously normalized via an interquartile range transformation. Serum from naïve animals contains preexisting background IgG signals to WT (Fig. 2.6A) and SNV (Fig. 2.6B) versions of the mutation-sites peptides. The largest of these IgG signals are against Wdr33:H13Y mutation-site peptides. We next analyzed serum IgG array fluorescence intensity data from 4T1 autophagosome-enriched vaccine + poly-I:C vaccinated animals versus poly-I:C only controls. An increase in normalized IgG signals was observed to the known 4T1 retroviral antigen AH1 in all four experiments. There was no significant preference for increased antibody signals to WT or SNV forms of the peptides (Fig. 2.7A), or to peptides from proteins previously confirmed present in the vaccine by mass spectrometry (Fig. 2.7B). We next performed MHCI and MHCII peptide predictions using NetMHCpan and NetMHCII for both WT and SNV forms of each mutation-site on the array [129–131] to assess for antibody / MHC relationships similar to previous reports (13,18). On average, there was a vaccine-dependent increase in normalized IgG signals to both WT and SNV 4T1 peptides from a higher-affinity MHCI binding mutation-site (Fig. 2.7C). This was not true for higher-affinity MHCII binding sites (Fig. 2.7D).

This observed association between MHCI affinity and antibodies after vaccination was very interesting because it suggested some underlying link or cross-talk between antibody and T cell responses at the level of individual peptide antigens. In the normalized antibody data, a trend between IgG and MHCI was observed in 3 of 4 experimental groups –

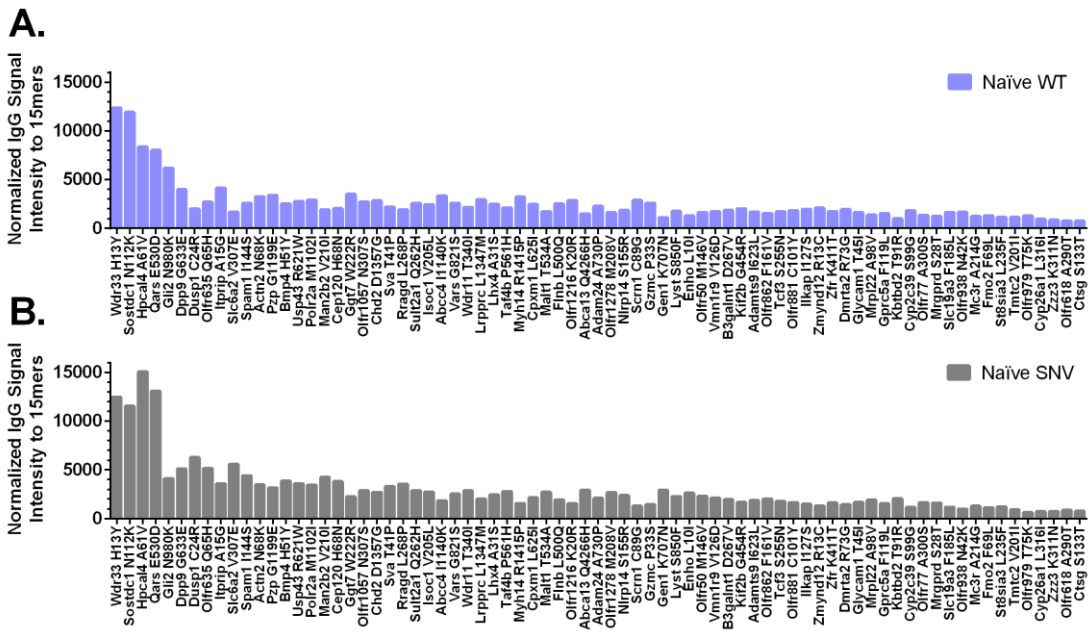

Figure 2.6 – Background IgG antibodies in naïve serum bind 4T1 mutation-site 15mer peptides. Data are from initial IgG arrays and are not paired with T cell data. Normalized average naïve serum IgG fluorescence signal intensity versus 15mer peptides centered at WT (**A**) and SNV (**B**) versions of 4T1 mutation-sites. Data are averages of two independent experimental arrays each with 3 replicate spots per peptide, and sorted by increasing combined average WT and SNV signal intensity.

but we observed that one group appeared much stronger than the others. We revisited the raw IgG array data without normalization, and found that in one group of animals the result was so strong that a direct correlation between IgG and MHCI could be observed in the raw values (Fig. 2.8C). Although it is not clear what conditions caused the effect in this case, we were not surprised by the variability. Our laboratory has long understood that cancer vaccine experiments can be highly variable from experiment to experiment, even with the same production lot of vaccine. Diversity in the antigen- specificity of response was also observed independent of MHCI affinity. A circos [141] plot of all the naïve and post-vaccine antibody

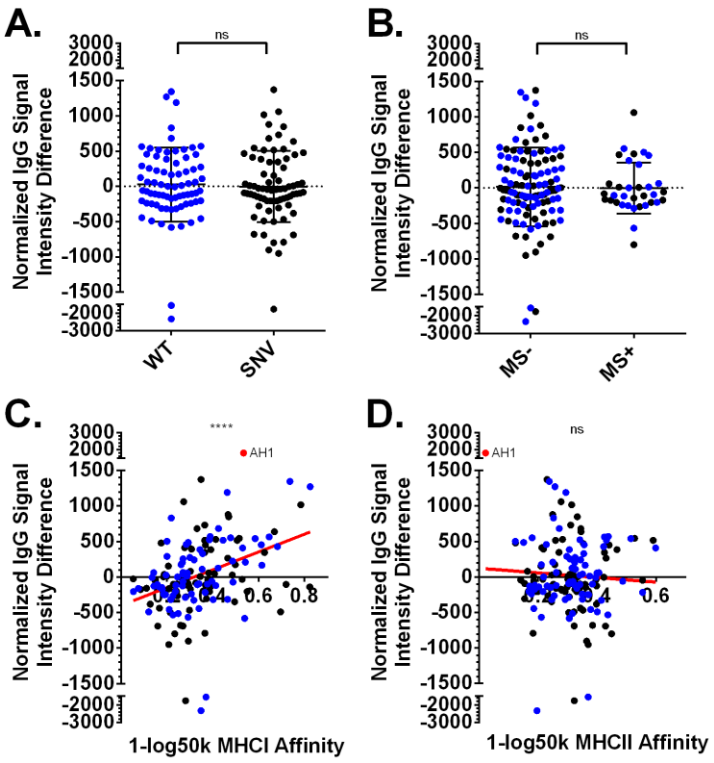

Figure 2.7- Increased IgG antibody signals in post-vaccine sera correlate with MHCI binding affinity. All data are the average normalized serum IgG signal differences between four independent 4T1 autophagosome vaccine + poly-I:C experimental arrays versus four paired poly-I:C only control experimental arrays. Each array contained 3 replicate spots per peptide. Positive values are increased in groups receiving vaccine. (**A**-**D**) SNV versions of mutation-sites are plotted in black, and WT versions in blue. (**A**) IgG signal differences in vaccine groups show no preference for WT or SNV versions of mutation-site peptides (P=0.62) by paired t-test. (**B**) No association between signal intensity differences and LC-MS/MS mass spectrometry confirmed parent proteins in the vaccine (Data File S1) (P=0.53) by unpaired t-test. (**C**) A strong average normalized association between higher observed IgG signals in vaccine groups and stronger top-predicted 9-11mer H2-Dd,Kd,Ld MHCI binding score for that mutation-site (P<0.0001) by Pearson correlation coefficient. (**D**) No association between observed IgG signal differences in vaccine groups and stronger top-predicted 15mer H2-IAd MHCII binding score for that mutation-site (P=0.47) by Pearson correlation coefficient.

array data (Fig. 2.9) demonstrates that although most IgG antibodies similarly target WT and SNV versions of the 4T1 mutation-site peptides, these new responses are stochastic with some strong responses only occurring once across the 4 experiments. However, even with these new antibody responses, the bulk of the antibody profile was similar across both naïve and combination vaccinated animals.

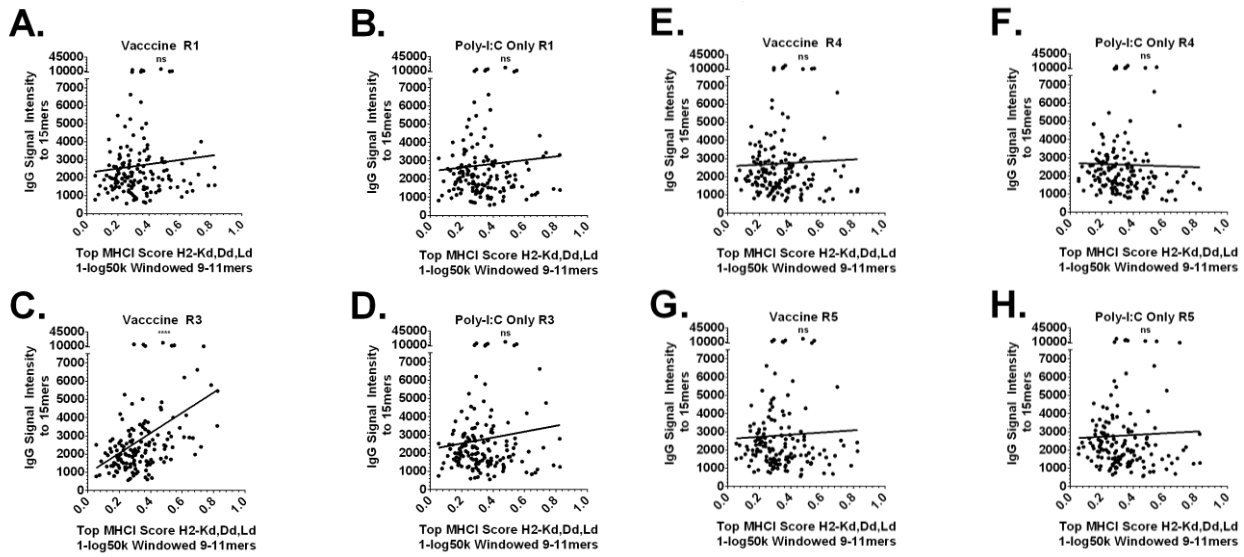

Figure 2.8 – Raw IgG antibody signals in post-vaccine sera correlated with increased MHCI binding affinity in an exceptional single experiment. (**A-H)** All data are the raw serum IgG signals for four independent 4T1 autophagosome vaccine + poly-I:C experimental arrays versus four paired poly-I:C only control experimental arrays. Each array contained 3 replicate spots per peptide. In an exceptional experiment (**C**) there is a correlation between the MHCI affinity of 4T1 mutation-sites and the raw IgG signal intensity against those site after vaccination (P<.0001) by Pearson correlation coefficient.

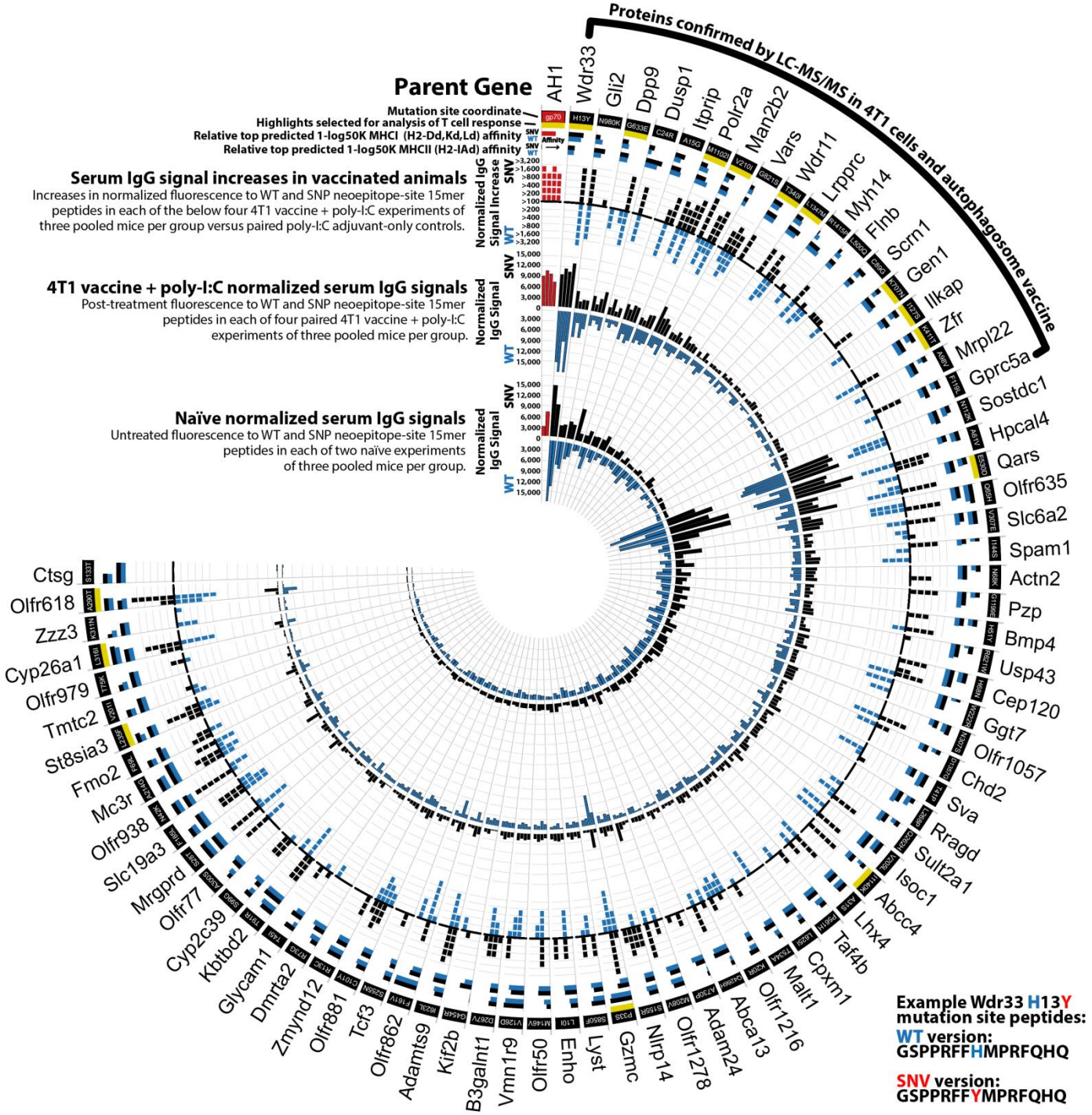

Figure 2.9 – Diversity of preexisting serum IgG landscape and new responses to 4T1 mutation-site 15mer peptides. Circos plot of normalized IgG fluorescence intensity in individual experiments. From interior out, plot shows total normalized fluorescence intensity to WT and SNV for individual naïve serum pool experiments (n=2), combination vaccine experiments (n=4), and normalized IgG fluorescence signal increases in combination vaccine experiments over paired adjuvant-only controls (n=4). Mutation-sites are arranged by total normalized WT and SNV signal intensity in naive groups, with proteins confirmed by mass spectrometry in 4T1 vaccine and cells presented separately. In all plots, black graphs pointing outward represent IgG fluorescence signals against SNV 15mers and blue graphs pointing inward the corresponding WT 15mer. Yellow outer highlights are used to recognize sites selected for further T cell assays. Relative top-predicted MHCI affinity for both SNV and WT versions of the mutation-site is plotted along with relative top-predicted MHCII affinity in the outer rings.

Discussion:

The efficacy of autophagosome-enriched cancer vaccines have been previously reported as depending on p62 (Sqstm1) dependent trafficking of poly-ubiquitinated proteins to autophagosome microvesicles [118]. This poly-ubiquitinated protein compartment is thought to be enriched in the high-turnover proteins more commonly presented on MHCI, and thus provide a more relevant antigen compartment for cross-presentation than vaccines based on whole tumor cells [32,33]. However, this study is the first report to thoroughly characterize the proteome of autophagosome-enriched vaccines and attempt identification of antigen-specific responses. The TMT LC-MS/MS results reported here identify a strong enrichment for mitochondrial proteins, suggesting a potential role for mitophagy – another p62 dependent process involving trafficking of mitochondria to autophagosomes [142] – in the function of these vaccines. Both mutated and normal mitochondrial proteins could be a source of the p62-dependent cross-protective immunity observed in previous studies with autophagosome vaccines [118,120], and should be investigated further. Additionally, though the efficacy of autophagosome vaccines in the 4T1 tumor model has been previously reported – this was in combination with OX40 T cell agonist [119]. This model reports poly-I:C as an effective adjuvant for 4T1 autophagosome vaccines, and additionally demonstrates via immunohistochemistry that these vaccines create a CD3+CD8+ T cell response capable of trafficking to these tumors in vivo.

With this working and thoroughly characterized vaccine model, we used whole exome sequencing to demonstrate that our 4T1 vaccine contained the same SNV neoantigens previously reported by others [125,126], and used them to design an array of 15mer peptides

for measuring IgG antibody responses. Interestingly, we found that even naïve animals demonstrated strong background binding to a handful of the peptides prior to treatment. This is similar to work with human protein arrays which has demonstrated IgG autoantibodies targeting normal proteins are common [103]. However, although we observed increased antibody signals in vaccine groups, there was no preference for SNV over WT peptides and these new IgG signals targeted both versions of the peptides simultaneously. This suggests a cross-reactive response for these antibodies which is not as selective as many neoantigen T cell responses reported in the literature. This lack of specificity could be due to the fact that we only administered two vaccines – leaving less opportunity for affinity maturation toward a more neoantigen-specific response. Alternatively, it could be a sign that the observed IgG antibody responses are boosted antibodies based on prior immunity to microbes and other antigenic exposures in these animals, and are simply boosted more non-specifically in response to the vaccine. This would be consistent with our vaccine creating an IFNγ driven expansion of IgG2a bearing B cells [143].

Also interesting is the diversity of the new antibody responses observed. Since our earliest experiments with autophagosome cancer vaccines, it has been observed that some experiments can work dramatically better than others. Similar results were observed here. Many strong IgG responses to both SNV and WT versions of a peptide were only observed in a single vaccine experiment, an effect which could be due to the rarity of each antigen in comparison with the B cell and T cell repertoire of those specific animals. Additionally, a strong correlation between peptide MHCI affinity and new IgG responses was observed best in a single exceptional group of animals, a result which hints at an underlying

correspondence between IgG antibody and CD8+ T cells that demands further investigation. This will be interrogated directly in the following chapter.

CHAPTER 3

COORDINATED RESPONSES TO INDIVIDUAL TUMOR ANTIGENS BY IgG ANTIBODY AND CD8+ T CELLS FOLLOWING CANCER VACCINATION

Background: Our previous work in Chapter 2 suggested coordination might occur between IgG antibody and CD8+ T cell responses, and additionally provided antigen targets for follow-up experiments. Using antibody-based assays to evaluate immune response repertoires and focus T cell antigen exploration could afford substantial advantages for discovering and monitoring the anti-cancer immune responses of patients enrolled on clinical trials. This is important because for CD8+ T cells in particular, patient-specific immune recognition and responses at the level of individual tumor antigens are rarely characterized. In this work, we sought to simultaneously interrogate serum IgG antibody and CD8+ T cell recognition of individual tumor antigens to determine whether antigen-specific serum IgG antibodies provide a window into the behavior of antigen-specific CD8+ T cell responses.

Methods: As before, we vaccinated female BALB/c mice with a combination of an autophagosome-enriched vaccine derived from 4T1 mammary carcinoma along with poly-I:C adjuvant, then screened serum for IgG binding to arrays of 15mer peptides containing known mutation-sites in 4T1. In these additional experiments, we simultaneously primed CD8+ T cell cultures from these animals with peptides targeting the same antigens featured on the IgG arrays. These primed T cells were then stimulated to measure recognition of the peptides or live 4T1 cells by IFNγ release.

Results: Vaccinated animals demonstrated increases in antigen-specific CD8+ T cell recognition of 4T1 tumor cells and peptides. For proteins confirmed in 4T1 cells and vaccine by mass spectrometry, there is a correlation between this increased CD8+ T cell IFNγ release and serum IgG binding to individual peptide antigens.

Conclusions: These results suggest it is possible to observe some features of a patient's antigen-specific T cell repertoire via an antibody surrogate, which has implications for tumor antigen discovery and clinical monitoring of antigen-specific anti-tumor immunity.

Background:

In spite of the frequency of autoantibodies observed in humans, and the similarity between many types of tumor antigens and autologous targets, it is not known whether these serum antibodies or changes in their abundance might also hint at the antigen-specific behavior of an individual's T cell repertoire. Others have used antibody as a surrogate measure of antigen-specific anti-tumor immunity [106,107,138], and we hypothesized that IgG antibody signals would be more likely to overlap with features of antigen-specific CD8+ T cell recognition than expected by chance. Potential mechanisms for such a relationship could occur via overlap with the underlying CD4+ T cell repertoire necessary for activating both CD8+ T cells and B cells, or from antibody-aided T cell activation via Fc receptor targeting of antigens to antigen presenting cells. Improved understanding of the antigen-specific relationships between antibody and T cell responses to tumor antigens could lead to improved immune monitoring for cancer patients and a deeper understanding of what features define clinically-relevant tumor antigens.

Based on published literature and our own work presented in Chapter 2, we hypothesized that some vaccine-induced patterns in these antibody profiles would relate to vaccine-induced T cell recognition of those same antigens. In viral immunity, there are documented examples of IgG antibody responses mirroring CD4+ responses at the level of individual antigens [140,144,145]. Similar to the viral literature, potential links have been

observed between anti-tumor antibodies and T cell responses to specific tumor antigens [139,146]. Additionally, increased antigen-specific antibody responses have been observed in association with improved outcomes following immunotherapy treatments typically understood to depend on T cells [106,138,147].

Methods:

Study Design

After profiling our 4T1 vaccine and identifying features of overlap between IgG antibody and T cell responses to peptide antigens, we next sought to determine whether we could observe simultaneous antigen-specific recognition by T cells and IgG antibody from the same groups of animals. Using the same vaccine lots, antibody array batches, and cell lines profiled previously, we repeated our initial experiments and added to them antigen-specific T cell assays. These assays involved either 8-11mer MHCI binding peptides or 15mer peptides matching the IgG arrays. The experiments were performed both with whole T cell populations and CD8+ enriched T cell populations. Tumor recognition by CD8+ T cells was confirmed using live 4T1 cells in vitro. Finally, all these data were integrated into combined analysis which included IFNγ T cell recognition, serum IgG array recognition, 4T1 variant profiling, and vaccine TMT LC-MS/MS profiling.

4T1 15mer mutation-site peptide arrays

An additional set of 15mer peptide array data was generated using the same lot and batch of IgG peptide arrays created for the first experiments (Chapter 2). 40 new samples were run on 40 arrays. In these follow-up studies, arrays were used to analyze pooled serum IgG from groups of animals paired with T cell assays utilizing pooled splenocytes from these

same groups. As before, 2-3 mice were used in each group, and the array design and measurement methods remained unchanged. Array data were not normalized in this case, and all plots and correlations involve direct comparisons of raw IgG signal intensity data.

Peptide selection for T cell assays

Antigens selected for additional profiling via IFNγ T cell assays were selected based on a profile of the preliminary peptide array data. We selected thirty-one antigen targetsIL-2 that spanned a range of properties determined in Chapter 2: sites with a strong preexisting IgG background signal, sites with a post-vaccine IgG signal increase across multiple experiments, sites with high and low predicted MHCI affinity, and mutation-sites without any of these distinctions but previously reported as immunogenic [125]. These were additionally divided among mutation-sites from proteins either confirmed or below the threshold of detection by mass spectrometry in both 4T1 cells and the autophagosome-enriched vaccine.

8-11mer in vitro T Cell IFNγ release peptide recognition assays

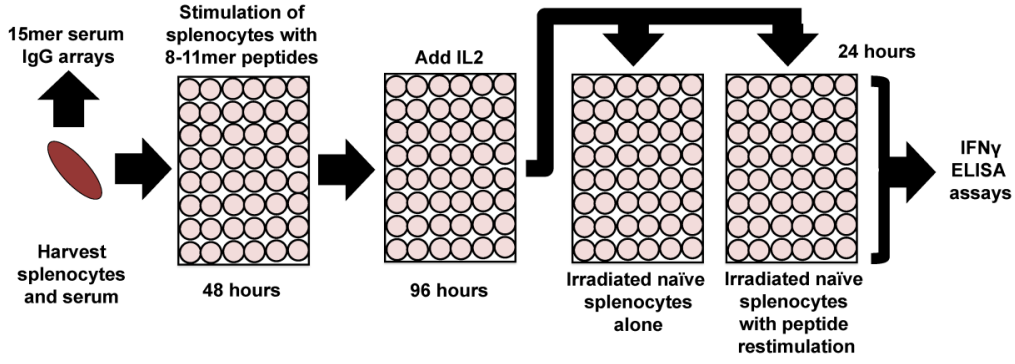

All experiments were performed using pooled splenocytes from 2-3 individual female BALB/c mice. These were either naïve animals or vaccinated animals two weeks after their second vaccination, a schedule identical to previously presented IgG array and tumor

challenge experiments (Chapter 2). After ACK lysis of red blood cells, $1x10^6$ splenocytes were plated into each well of 96 well round-bottom tissue culture plates and given primary stimulation in complete media with 10% FBS and 5 μM of either WT or SNV versions of mutation-site peptides manufactured by A&A Labs (San Diego, California). 8-11mer minimal peptides designs were based on predicted ability to bind MHCI. Both WT and SNV 8-11mer peptides were based on the length and frame of the top predicted MHCI binding minimal 8-11mer SNV peptide identified using NetMHCpan v2.8 Server. NetMHCpan, which was used to calculate predicted H2-Kd, H2-Dd, and H2-Ld MHCI binding scores for all possible WT and SNV 8mers, 9mers, 10mers, and 11mers that include the mutation-site [129]. After 48 hours of primary peptide stimulation with WT or SNV peptide, IL-2 was added at 10 Cetus units/mL. After an additional 96 hours, contents of each well were washed and split onto either WT or SNV 2° peptide restimulation with $5x10^5$ irradiated splenocytes or irradiated splenocytes alone. Supernatants were harvested after an additional 20 hours, frozen at -80 °C, and later analyzed for IFNγ by ELISA.

15mer in vitro T Cell IFNγ release peptide recognition assays

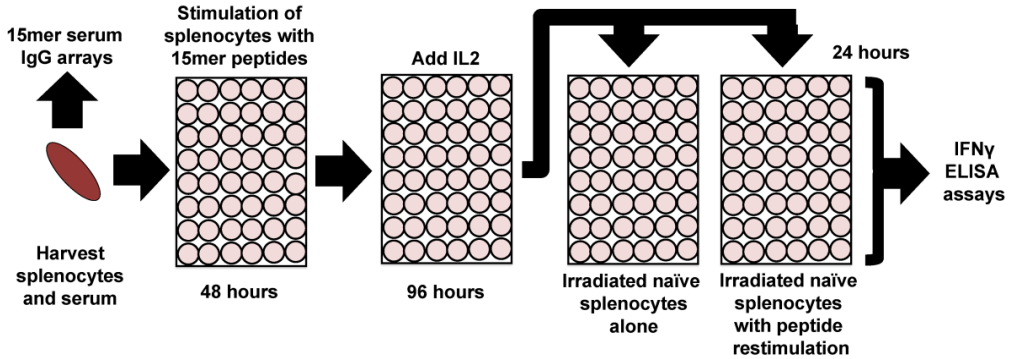

All experiments were performed using pooled splenocytes from 2-3 individual female BALB/c mice. These were either naïve animals or vaccinated animals two weeks after their

second vaccination, a schedule identical to previously presented IgG array and tumor challenge experiments (Chapter 2). After ACK lysis of red blood cells, $1x10^6$ splenocytes were plated into each well of 96 well round-bottom tissue culture plates and given primary stimulation in complete media with 10% FBS and 5 μM of either WT or SNV versions of mutation-site peptides manufactured by A&A Labs (San Diego, California). 15mer peptides were identical in design to the 15mer peptides printed on the IgG peptide arrays. After 48 hours of primary peptide stimulation with WT or SNV peptide, IL2 was added at 10 Cetus units/mL. After an additional 96 hours, contents of each well were washed and split onto either WT or SNV 2° peptide restimulation with $5x10^5$ irradiated splenocytes or irradiated splenocytes alone. Supernatants were harvested after an additional 20 hours, frozen at -80 °C, and later analyzed for IFNγ by ELISA.

8-11mer in vitro CD8+ T Cell IFNγ release peptide recognition assays

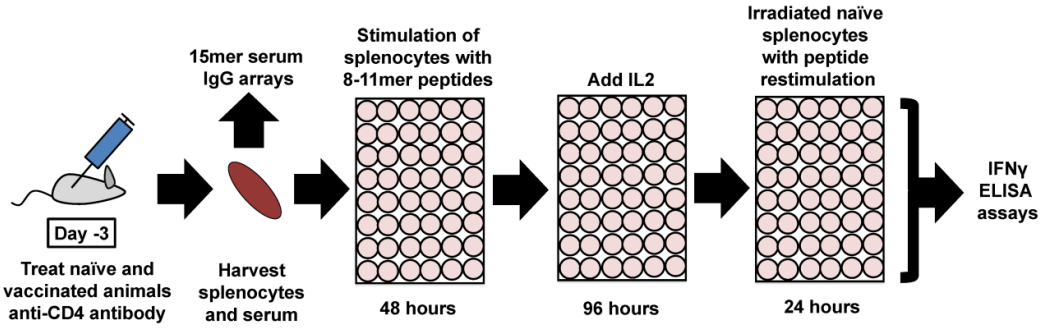

All experiments were performed using pooled splenocytes from 2-3 individual female BALB/c mice. These were either from naïve animals or vaccinated animals two weeks after their second vaccination, a schedule identical to previously presented IgG array and tumor challenge experiments (Chapter 2). In this case of CD8+ enriched experiments, CD4+ cells were depleted in vivo three days prior to spleen harvest using 200 μg of GK1.5 anti-CD4

antibody administered IP. CD4 depletion was confirmed by flow cytometry. After ACK lysis of red blood cells, $1x10^6$ splenocytes were plated into each well of 96 well round-bottom tissue culture plates and given primary stimulation in complete media with 10% FBS and 5 μM of either WT or SNV versions of mutation-site peptides manufactured by A&A Labs (San Diego, California). 8-11mer minimal peptides used were the same 31 peptides used in the previous 8-11mer peptide assays without CD4-depletion. After 48 hours of primary peptide stimulation with WT or SNV peptide, IL-2 was added at 10 Cetus units/mL. After an additional 96 hours, contents of each well were washed and split onto either WT or SNV 2° peptide restimulation with $5x10^5$ irradiated splenocytes. Supernatants were harvested after an additional 20 hours, frozen at -80 °C, and later analyzed for IFNγ by ELISA.

8-11mer in vitro CD8+ T Cell IFNγ release 4T1 tumor recognition assays

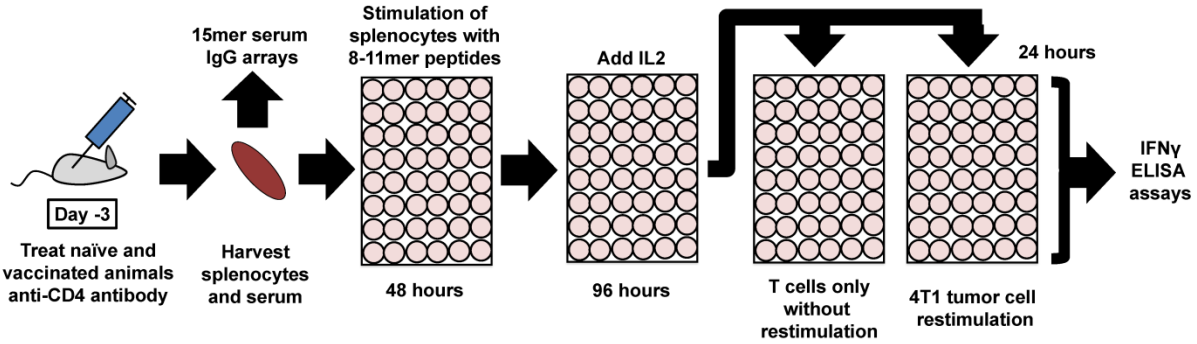

All experiments were performed using pooled splenocytes from 2-3 individual female BALB/c mice. These from vaccinated animals two weeks after their second vaccination, a schedule identical to previously presented IgG array and tumor challenge experiments (Chapter 2). In this case of CD8+ enriched experiments, CD4+ cells were depleted in vivo three days prior to spleen harvest using 200 μg of GK1.5 anti-CD4 antibody administered IP.

CD4 depletion was confirmed by flow cytometry. After ACK lysis of red blood cells, $1x10^6$ splenocytes were plated into each well of 96 well round-bottom tissue culture plates and given primary stimulation in complete media with 10% FBS and 5 μM of either SNV or WT versions of mutation-site peptides manufactured by A&A Labs (San Diego, California). 8-11mer minimal peptides used were the same 31 peptides used in the previous 8-11mer peptide assays with and without CD4-depletion. After 48 hours of primary peptide stimulation, IL-2 was added at 10 Cetus units/mL. After an additional 96 hours, contents of each well were washed and split onto either 2° restimulation with $1x10^5$ live 4T1 cells, or empty wells with media only.

TMT LC-MS/MS of 4T1 cells and autophagosome-enriched vaccine

Methods for quantitative tandem mass tag (TMT) liquid chromatography tandem mass spectrometry (LC-MS/MS) on the vaccine lots used in these experiments was previously reported (Chapter 2). In summary, a total of 4416 proteins were identified as being present in both 4T1 tumor and vaccine, and quantification was done on 4196 proteins (excluding contaminants). This discovery confirmation, and not quantitative abundance, was used to separate experimental groups by LC-MS/MS identification status in Figs. 3.7, 3.8, 3.9, and 3.10.

Adoptive Transfer

In both experiments, splenocytes were harvested from 3 individual female BALB/c mice two weeks after their 2nd 4T1 autophagosome vaccine as described in the initial IFNγ release T cell assays above without CD4-depletion. After ACK lysis, these were seeded into 24 well plates with $6x10^6$ cells seeded per well and given primary stimulation in complete

media with 10% FBS and 5 μM of either SNV or WT versions of 8-11mer mutation-site peptides manufactured by A&A Labs (San Diego, California). After 48 hours of primary peptide stimulation, IL-2 was added at 10 Cetus units/mL. After an additional 96 hours, contents of each well were washed, counted, resuspended in HBSS, and administered to female BALB/c mice that had just been irradiated with 500 rads. These mice had been intravenously seeded with $2x10^5$ live 4T1 tumor cells three days previously. In the first experiment, all harvested cells were adoptively transferred regardless of counts, and in the second experiment $40x10^6$ cells were administered to each animal. Mice were additionally given doses of IL-2 at the time of administration, and at twice daily intervals afterwards. In the first experiment this was five total doses of 15,000 Cetus units IL-2, and in the second nine total doses of 50,000 Cetus units IL-2. On day 13, animals were killed, lungs stained with India ink, fixed, and counted for lung metastases.

Statistical Analyses

Analyses were performed on either summary data or individualized experiments, and this information is placed alongside the specific type of test performed and p-value (P) within the figure legends. All statistical tests were considered significant at the $P<0.05$ level and were performed with Prism 7 (GraphPad). In general, parametric comparisons were either two sample t-tests or paired t-tests, and non-parametric tests were Wilcoxon matched-pairs signed rank tests. Significance of all correlations was determined by linear regression and Pearson correlation coefficient.

Results:

The results presented in Chapter 2 demonstrate that 4T1 autophagosome vaccine is able to improve outcomes in the context of increased intratumoral CD3+CD8+ infiltrates, suggesting a CD8+ T cell dependent effect. This, combined with our peptide array results demonstrating that there can be a strong link between IgG antibody and MHCI binding in those same experiments, led us to a new series of experiments with the goal of directly measuring antigen-specific overlap between IgG antibody and T cell responses to 4T1 autophagosome vaccines. We used data from those earlier experiments to select a smaller set of antigens for investigation in parallel T cell assays. These selected antigens spanned a range of previously determined features: peptides with a strong preexisting IgG background signal in naïve animals, peptides with a post-vaccine IgG signal increase across multiple experiments, peptides with high and low predicted MHCI affinity, and peptides from mutation-sites without any of these distinctions but previously reported as immunogenic [125]. These were additionally divided among mutation-sites from proteins either confirmed

				WT	SNV	WT	SNV
Gene	Variant Coordinate	MS+	Selected for Cellular T Cell Assays	Mutation-Site 15mer	Mutation-Site 15mer	Predicted MHCI Binding 8-11mer	Predicted MHCI Binding 8-11mer
AH1	gp70 423-431	N/A	TRUE	N/A	N/A	SPSYVYHQF	N/A
Dpp9	G633E	TRUE	TRUE	KPHTLQPGRKHPTVL	KPHTLQPERKHPTVL	QPGRKHPTVLF	QPERKHPTVLF
Gen1	K707N	TRUE	TRUE	RVAVKTTKNLVMKNS	RVAVKTTNNLVMKNS	RVAVKTTKNL	RVAVKTTNNL
Ilkap	I127S	TRUE	TRUE	EMQDAHVILNDITQE	EMQDAHVSLNDITQE	AHVILNDI	AHVSLNDI
Lrpprc	L1347M	TRUE	TRUE	EYLTAKNLKLDDLFL	EYLTAKNMKLDDLFL	EYLTAKNLKL	EYLTAKNMKL
Man2b2	V210I	TRUE	TRUE	QQEIFTHVMDHYSYC	QQEIFTHIMDHYSYC	SGQQEIFTHY	SGQQEIFTHI
Polr2a	M1102I	TRUE	TRUE	LGEPATQMTLNTFHY	LGEPATQITLNTFHY	TQMTLNTF	TQITLNTF
Wdr11	T340I	TRUE	TRUE	LDPVQELTYDLRSQC	LDPVQELIYDLRSQC	TYDLRSQCDAI	IYDLRSQCDAI
Wdr33	H13Y	TRUE	TRUE	GSPPRFFHMPRFQHQ	GSPPRFFYMPRFQHQ	SPPRFFHM	SPPRFFYM
Zfr	K411T	TRUE	TRUE	AKHQKVVKLHTKLGK	AKHQKVVTLHTKLGK	KHQKVVKL	KHQKVVTL
Abcc4	I1140K		TRUE	DPRTDELIQQKIREK	DPRTDELKQQKIREK	IQQKIREKF	KQQKIREKF
Cyp26a1	L316I		TRUE	ATSLITYLGLYPHVL	ATSLITYIGLYPHVL	TYLGLYPHVL	TYIGLYPHVL
Gzmc	P33S		TRUE	EISPHSRPYMAYYEF	EISPHSRSYMAYYEF	PYMAYYEFL	SYMAYYEFL
Olfr618	A290T		TRUE	LYVVVPPALNPIIYG	LYVVVPPTLNPIIYG	LYVVVPPAL	LYVVVPPTL
Qars	E530D		TRUE	RRRGFPPEAINNFCA	RRRGFPPDAINNFCA	RGFPPEAI	RGFPPDAI
St8sia3	L235F		TRUE	RNNFFLSLKKLDGAI	RNNFFLSFKKLDGAI	SLKKLDGAI	SFKKLDGAI

Table 3.1– Individual peptides printed for T cell assays. Listed are the individual sequences for AH1 and the 15 WT and 15 SNV mutation-site peptides chosen for paired IgG and T cell assays. Each peptide was printed as both a 15mer identical to the sequence used in the IgG arrays, and as the best-predicted MHCI binding 8-11mer peptide including the mutation-site.

or below the threshold of detection by mass spectrometry in both 4T1 cells and the autophagosome-enriched vaccine. These peptides were printed as both MHCI binding minimal 8-11mer peptides and full-length 15mers matching the IgG array. A full list of the peptides chosen for investigation in T cell assays is presented (Table 3.1).

A total of five independent experiments were performed which resulted in paired T cell and antibody data. The serum from these experiments was saved as before, and run on an additional set of IgG antibody arrays from the same batch of arrays as the experiments presented in Chapter 2. In this case, the data were not normalized, but always directly compared as raw signal intensity values. These array data demonstrate IgG binding signals against 4T1 peptides from both naïve and vaccinated animal sera, with increased average IgG signals in vaccine groups against many individual WT autoantigen 15mer peptides (Fig. 3.1A), and SNV neoantigen 15mer peptides (Fig. 3.1B). The IgG signals to both WT and SNV 4T1 peptides were significantly higher in sera from vaccinated animals (Fig. 3.1C), but these increased IgG signals after vaccination did not significantly favor SNV neoantigen over WT autoantigen peptides (Fig. 3.1D). However, there were stronger overall IgG signals against SNV peptides in serum from both naïve (Fig. 3.1E) and vaccinated (Fig. 3.1F) animals, suggesting a background landscape of preexisting serum antibodies that favors neoantigens over autoantigens. Interestingly, we did not again observe an experiment with a positive correlation between increased IgG signal intensity and predicted MHCI affinity (Fig. 3.2), but instead observed a few inverse trends which did not reach statistical significance.

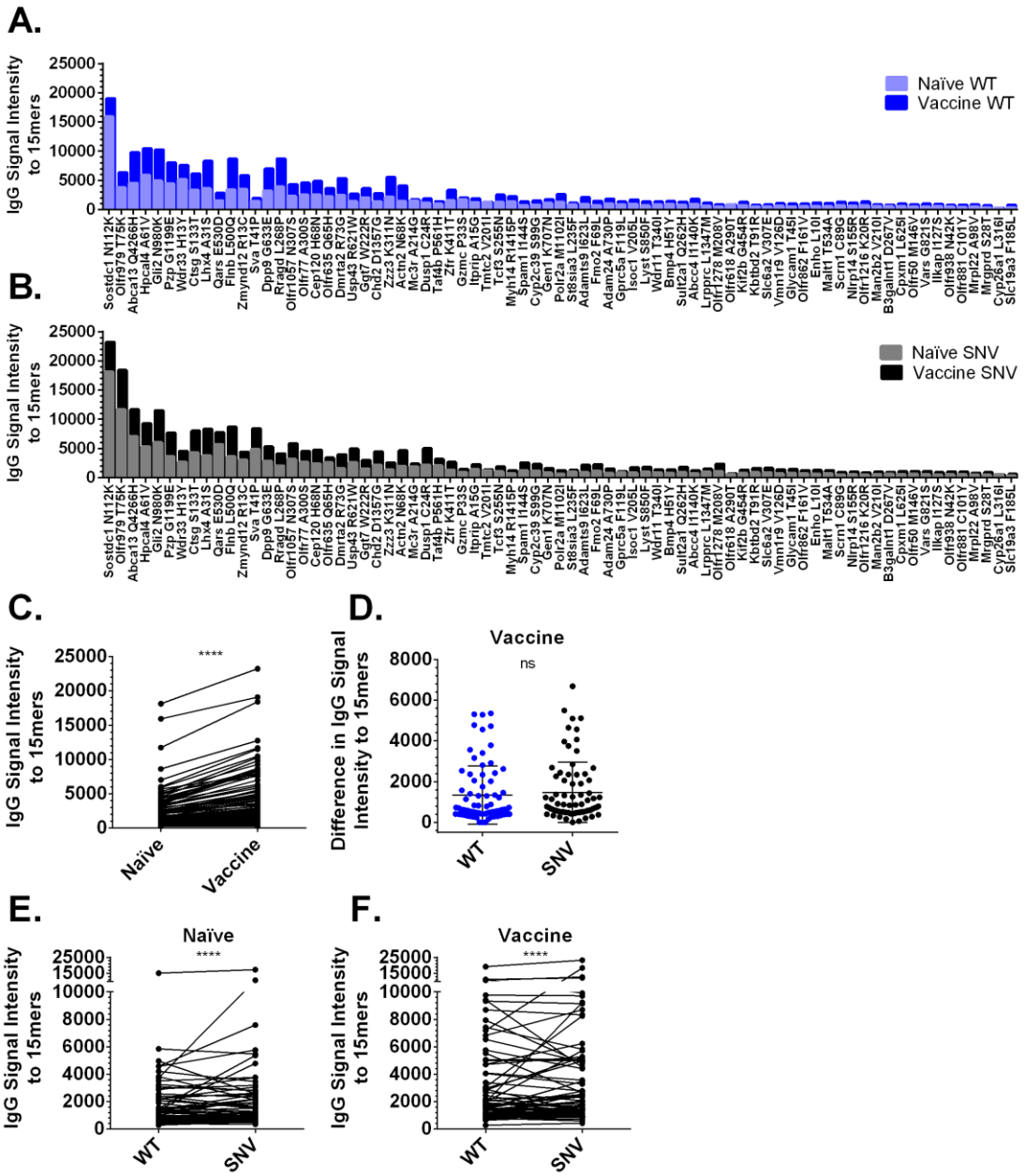

Figure 3.1 – Sera of vaccinated animals had increased IgG antibodies to WT and SNV 15mer peptides centered at mutation-sites in 4T1. (**A-F**) Data are from five independent pairs of IgG arrays reacted with pooled naïve or vaccinated mouse serum. Each array consists of 151 15mer peptides printed in triplicate and centered at WT autoantigen and SNV neoantigen mutation-sites in 4T1. (**A**) Average serum IgG fluorescence signal intensity versus 15mer peptides centered at WT versions of listed 4T1 mutation-sites in naïve and vaccinated animals sorted by the combined WT and SNV IgG signals observed in naïve animals. (**B**) Average serum IgG fluorescence signal intensity versus 15mer peptides centered at SNV versions of listed 4T1 mutation-sites in naïve and vaccinated animals sorted by the combined WT and SNV IgG signal observed in naïve animals. (**C-D**) Data are plotted as average values, but statistics are computed from all individualized pairs of experimental values. (**C**) Vaccinated animals demonstrated increased serum IgG signal intensity to a WT and SNV 15mer peptides ($P<0.0001$) by Wilcoxon matched-pairs signed rank test, (**D**) but these observed increases in IgG signal intensity from vaccine groups were not significantly higher for SNV peptides than WT peptides ($P=0.26$) by Wilcoxon matched-pairs signed rank test. However, there are stronger IgG signal intensities for SNV neoantigens than paired WT autoantigens in serum from both (**E**) naïve animals ($P<0.0001$), and (**F**) vaccinated animals ($P<0.0001$) by Wilcoxon matched-pairs signed rank test.

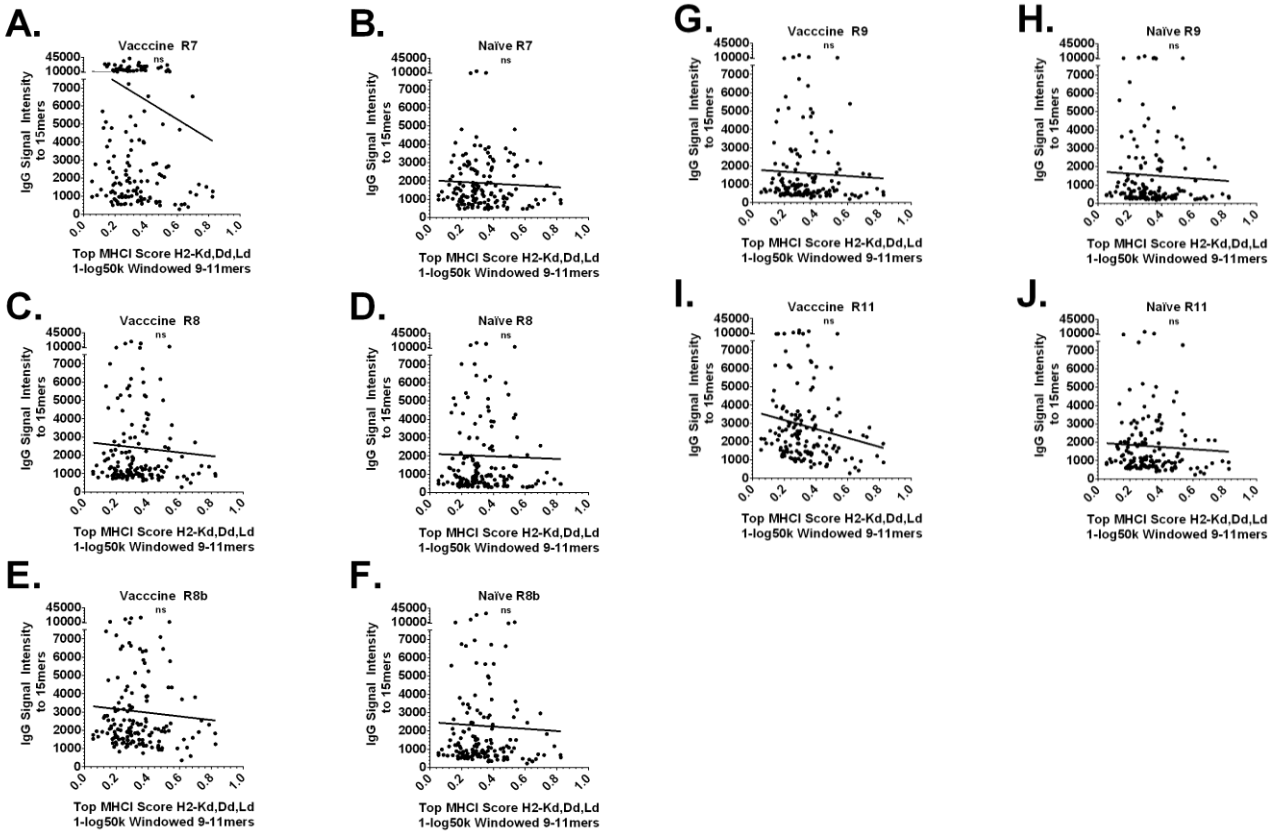

Figure 3.2 – Raw IgG antibody signals in post-vaccine sera do not correlate with increased MHCI binding affinity. (**A-J)** All data are the raw serum IgG signals for five independent 4T1 autophagosome vaccine + poly-I:C experimental arrays versus four paired naïve control experimental arrays. Each array contained 3 replicate spots per peptide. There was no significant correlation between the MHCI affinity of 4T1 mutation-sites and the raw IgG signal intensity against those mutation-sites after vaccination by Pearson correlation coefficient in any of the experiments. Observed trends were negative.

In the initial set of experiments with paired IgG and cellular assays, T cells from vaccinated animals had increased recognition of both WT and SNV 8-11mer 4T1 peptides (Fig. 3.3A-B), and serum from these vaccinated animals also demonstrates increased IgG binding to 15mer peptides containing this same group of mutation-sites (Fig. 3.3C-D). For several of these 4T1 antigens, we observed simultaneous increases in IgG 15mer signal intensity and T cell recognition of 8-11mer peptides for specific antigens in vaccinated animals (Fig. 3.3E). A similar result was observed for splenocyte assays involving WT

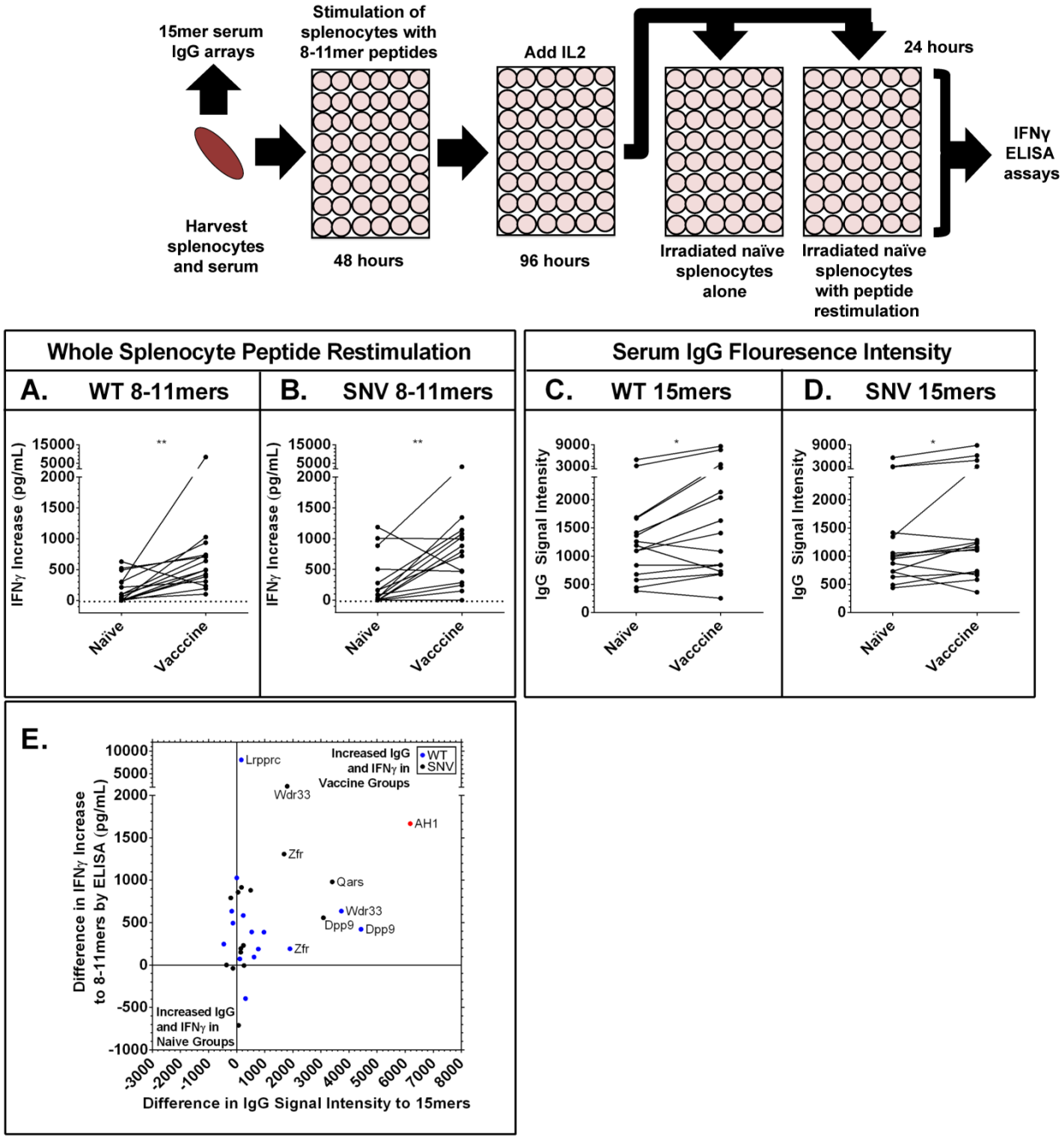

Figure 3.3 – Vaccinated animals displayed simultaneous increases in serum IgG signals to 15mers and splenocyte IFNγ recognition of individual 8-11mer 4T1 antigens. Serum and splenocytes were harvested from naïve and 4T1 autophagosome-enriched vaccine + poly-I:C vaccinated animals. Serum was run on the 15mer arrays presented previously (Fig. 3.1). Splenocytes were stimulated with WT and SNV versions of top predicted MHCI binding 8-11mer mutation-site peptides for 48 hours, then expanded on IL2 for an additional 96 hours before wells were split and restimulated with either naïve splenocytes or naïve splenocytes pulsed with a second stimulation of peptide. Graphs are of the average increase in IFNγ secretion by ELISA in wells with peptide restimulation over splenocytes alone for n=3 experiments with vaccine groups and n=2 experiments with naïve groups. (**A,B**) Increase in average IFNγ secretion in vaccine groups upon secondary exposure to n=15 different WT (P=0.002) (**A**) and n=15 different SNV (P=0.005) peptides (**B**) by Wilcoxon matched-pairs signed rank test. (**C,D**) Simultaneous serum IgG array recognition data for 15mer peptides centered at these same mutation-sites from the same n=3 vaccine groups and n=2 naïve groups used in splenocyte assays. Increase in average IgG signal intensity to n=15 different WT (P=0.01) (**C**) and n=15 different SNV (P=0.02) (**D**) peptides by Wilcoxon matched-pairs signed rank test. (**E**) Combined data previously presented in (**A-D**) plots average differences in IgG and IFNγ recognition for each of the n=15 WT and n=15 SNV mutation-sites along with AH1. Positive values represent increased signals in vaccine groups and negative values represent increased signals in naïve groups. Values in upper-right quadrant demonstrated simultaneous increases in IgG and splenocyte IFNγ recognition of individual 4T1 mutation-site antigens in vaccine groups. However, there was no significant overall correlation of these increases in recognition (P=0.6) by Pearson correlation coefficient.

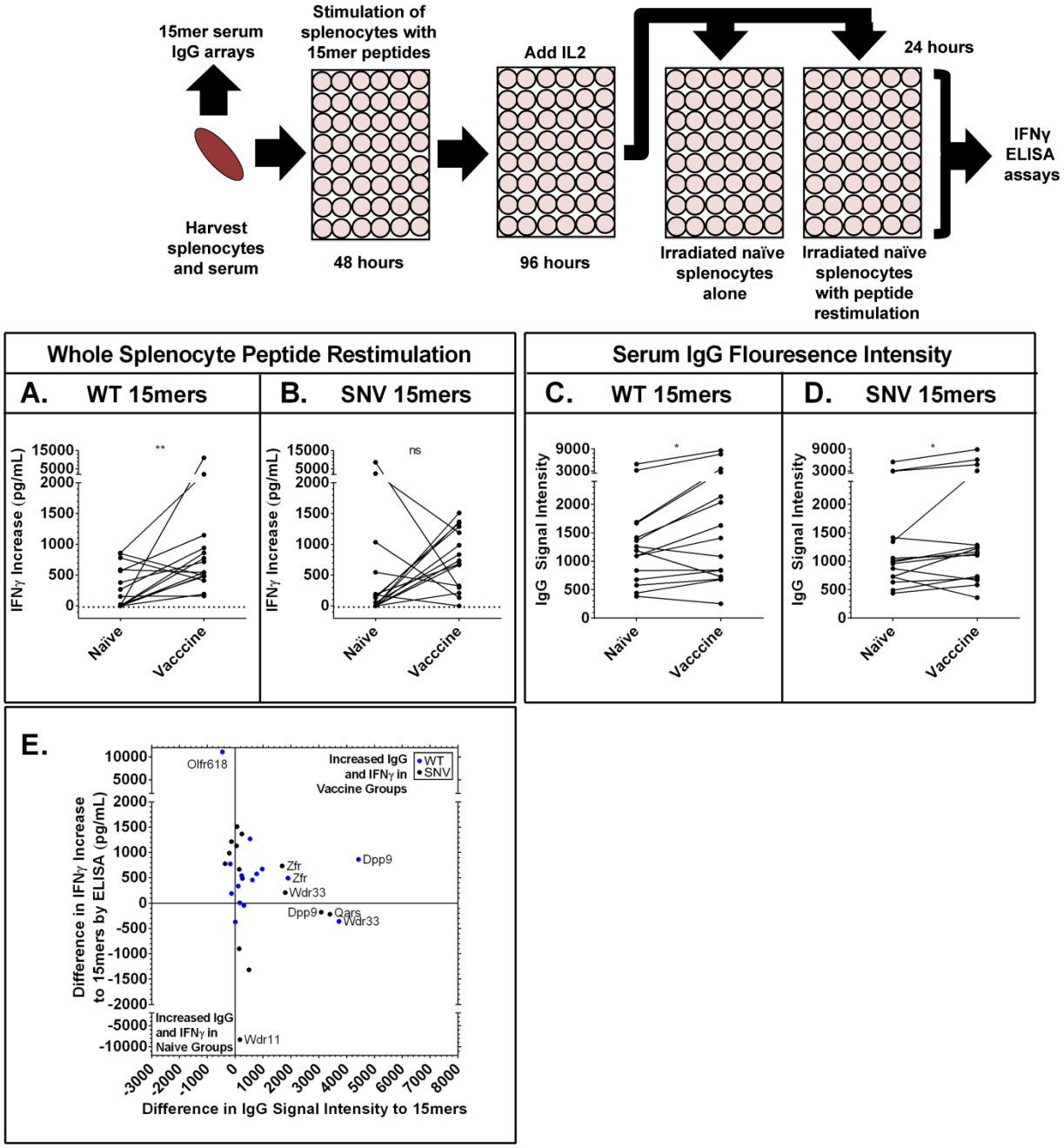

Figure 3.4 – Vaccinated animals displayed increased serum IgG signals to 15mers and splenocyte IFNγ recognition of individual 15mer 4T1 antigens. Serum and splenocytes were harvested from naïve and 4T1 autophagosome vaccine + poly-I:C vaccinated animals. Serum was run on the 15mer arrays presented previously (Fig. 2). Splenocytes were stimulated with WT and SNV versions of 15mer mutation-site peptides matching serum arrays for 48 hours, then expanded on IL2 for an additional 96 hours before wells were split and restimulated with either naïve splenocytes or naïve splenocytes pulsed with a second stimulation of peptide. Graphs are of the average increase in IFNγ secretion by ELISA in wells with peptide restimulation over splenocytes alone for n=3 experiments with vaccine groups and n=2 experiments with naïve groups. (**A,B**) Increase in average IFNγ secretion in vaccine groups upon secondary exposure to n=15 different WT (P=0.005) (**A**) but not n=15 different SNV peptides (P=0.25) (**B**) by Wilcoxon matched-pairs signed rank test. (**C,D**) Simultaneous serum IgG array recognition data for the same 15mer peptides from the same n=3 vaccine groups and n=2 naïve groups used in splenocyte assays. Increase in average IgG signal intensity to n=15 different WT (P=0.01) (**C**) and n=15 different SNV (P=0.02) (**D**) peptides by Wilcoxon matched-pairs signed rank test. (**E**) Combined data previously presented in (**A-D**) plots average differences in IgG and IFNγ recognition for each of the n=15 WT and n=15 SNV mutation-sites. Positive values represent increased signals in vaccine groups and negative values represent increased signals in naïve groups. Values in upper-right quadrant demonstrated simultaneous increases in IgG and splenocyte IFNγ recognition of individual 4T1 mutation-site antigens in vaccine groups. However, there was no significant overall correlation of these increases in recognition (P=0.5) by Pearson correlation coefficient.

15mer peptides (Fig. 3.4A-E), except that naïve splenocyte from some animals were additionally able to recognize SNV 15mer peptides after our culture process (Fig. 3.4B). This observation was perhaps from an in vitro induction of preexisting neoantigen-specific precursor cells in the naïve mice by these longer peptides; a similar priming of neoantigen-specific T cells has been observed using peripheral blood cells from healthy human donors cultured with tumor neoantigen mini-genes [148]. Because of this poorer separation between vaccine and naïve groups we did no further experiments with 15mer peptides.

Since we observed increased recognition of 8-11mer 4T1 peptides by T cells from vaccinated animals, and initial immunohistochemistry experiments suggested a greater role for CD3+CD8+ cells than CD3+CD4+ cells for tumor control in this model (Fig. 2.4A-D), we next sought to confirm the role of CD8+ T cells with an enriched population of CD8+ T cells. Experiments were performed as before except with the addition of a CD4-depleting antibody in vivo prior to spleen harvest. Compared to naïve animals, vaccinated animals demonstrated stronger CD8+ T cell IFNγ recognition of both WT autoantigen and SNV neoantigen 8-11mer peptides from 4T1 (Fig. 3.5A,B). Interestingly, serum from these vaccinated animals also demonstrated a significantly ($p<0.0001$) increased IgG binding to 15mer WT peptides as well as 15mer SNV peptides containing these mutation-sites (Fig. 3.5C,D), and there was a significant ($p=0.0039$) correlation between increased IgG binding to 15mer peptides after vaccination and increased IFNγ recognition of both the WT and SNV 8-11mer peptides by CD8+ T cells (Fig. 3.5E). This suggests that at least in some cases, vaccination with an autophagosome vaccine leads to the development of CD8+ T cell antigen recognition in tandem with increased IgG antibody recognition of those same tumor peptides.

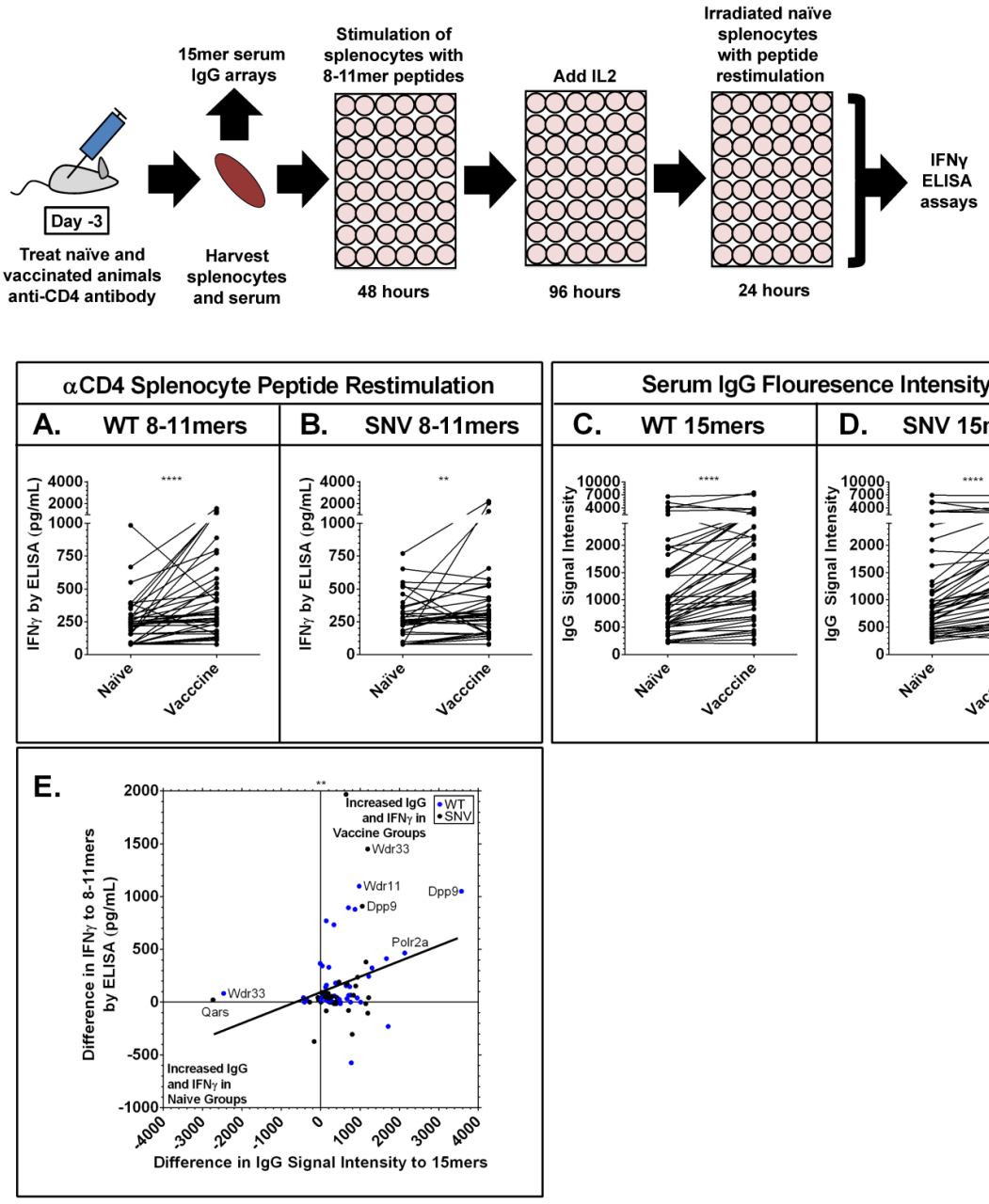

Figure 3.5 – Vaccinated animals displayed simultaneous increases in serum IgG signals to 15mers and CD8+ T cell IFNγ recognition of individual 8-11mer 4T1 antigens. Serum and CD4-depleted splenocytes were harvested from naïve and 4T1 autophagosome-enriched vaccine + poly-I:C vaccinated animals. Serum was run on the 15mer arrays presented previously (Fig. 3.1). CD4-depleted splenocytes were stimulated with WT and SNV versions of top predicted MHCI binding 8-11mer mutation-site peptides for 48 hours, then expanded on IL2 for an additional 96 hours before wells were split and restimulated with naïve splenocytes pulsed with a second stimulation of peptide. Graphs are of the IFNγ secretion for each individual paired experiment from n=3 paired replicates with vaccine and naïve groups, each involving n=15 different WT and n=15 SNV peptide experiments. (**A,B**) Increase in IFNγ secretion in vaccine groups upon secondary exposure to n=45 paired experiments with WT peptides (P<0.0001) (**A**) and n=45 paired experiments with SNV (P=0.005) peptides (**B**) by Wilcoxon matched-pairs signed rank test. (**C,D**) Simultaneous serum IgG array recognition data for 15mer peptides centered at these same mutation-sites from the same n=3 vaccinated animal groups and n=3 naïve groups used in splenocyte assays. Increase in average IgG signal intensity to n=45 paired WT peptide experiments (P<0.0001) (**C**) and n=45 SNV peptide experiments (P<0.0001) (**D**) by Wilcoxon matched-pairs signed rank test. (**E**) Combined data previously presented in (**A-D**) plots average differences in IgG and IFNγ recognition for each of the n=45 WT experiments and n=45 SNV experiments. Positive values represent increased signals in vaccine groups and negative values represent increased signals in naïve groups. Values in upper-right quadrant demonstrated simultaneous increases in IgG and splenocyte IFNγ recognition of individual 4T1 mutation-site antigens in vaccine groups. There was a significant overall correlation of these increases in IgG and CD8+ IFNγ recognition (P=0.0039) by Pearson correlation coefficient.

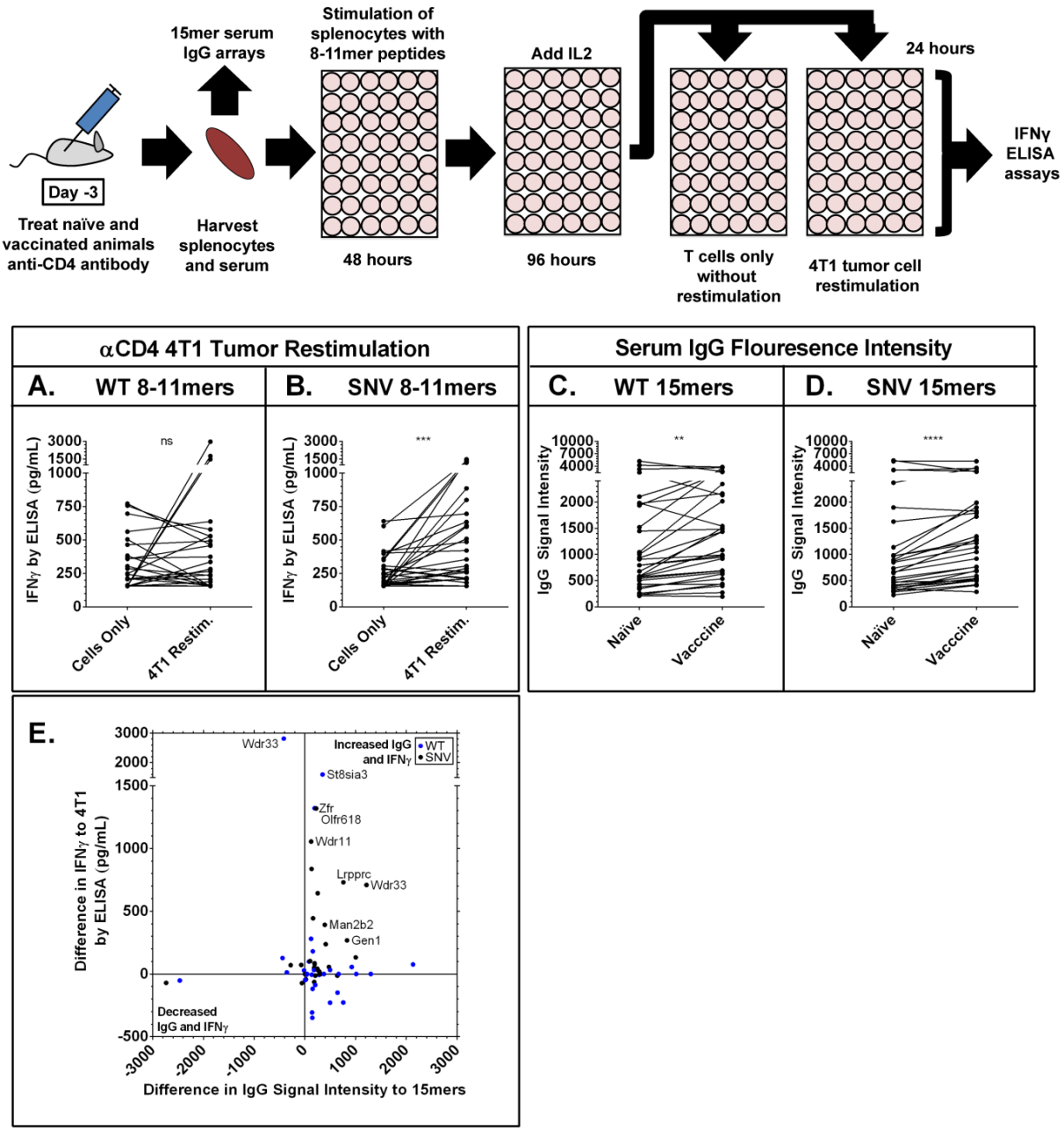

Figure 3.6 – Simultaneous increases in IgG signals to 15mers and improvements in CD8+ IFNγ recognition of tumor. Serum and CD4-depleted splenocytes were harvested from 4T1 autophagosome-enriched vaccine + poly-I:C vaccinated animals. Serum was run on the 15mer arrays presented previously (Fig. 3.1). CD4-depleted splenocytes were stimulated as presented previously (Fig. 3.5), then placed in empty wells or restimulated with 4T1 tumor cells. Graphs are of the IFNγ secretion for each individual paired experiment from n=2 paired replicates with CD8+ T cells only or CD8+ T cells plus live 4T1 cells, each pair initially stimulated with one of n=15 WT or n=15 SNV peptides. (**A,B**) IFNγ secretion in 4T1 tumor restimulated groups demonstrated outliers, but no overall increased 4T1 recognition after primary exposure to n=30 paired experiments with WT peptides (P=0.65) (**A**), but did show overall increased 4T1 recognition after primary exposure to n=30 paired experiments with SNV peptides (P=0.0002) (**B**) by Wilcoxon matched-pairs signed rank test. (**C,D**) Simultaneous serum IgG array recognition data for 15mer peptides centered at these same mutation-sites from the same n=2 vaccinated animal groups used in splenocyte assays and n=2 naïve group controls. Increase in average IgG signal intensity to n=30 paired WT peptide experiments (P<0.0022) (**C**) and n=30 SNV peptide experiments (P<0.0001) (**D**) by Wilcoxon matched-pairs signed rank test. (**E**) Combined data previously presented in (**A-D**) plots average differences in IgG and IFNγ recognition for each of the n=30 WT experiments and n=30 SNV experiments. Positive values represent increased IgG signals versus naïve controls and increased IFNγ recognition of 4T1 tumor over T cells only. Values in upper-right quadrant demonstrated increases in serum IgG recognition of that antigen, and a simultaneous ability for that antigen to improve CD8+ T cell IFNγ recognition of live 4T1 cells. However, there was no significant direct correlation of these increases in IgG and CD8+ IFNγ recognition (P=0.95) by Pearson correlation coefficient.

In order to determine the relevance of these results to tumor recognition, we performed two of the CD4-depleted experiments with additional restimulation groups of live 4T1 tumor cells. In vitro priming of CD8+ T cells from vaccinated animals with 8-11mer WT autoantigen peptides produced tumor recognition in three cases, but not as an overall group (Fig. 3.6A). In contrast, a larger fraction of CD8+ T cells from vaccinated animals stimulated with 8-11mer SNV neoantigen peptides demonstrated improved 4T1 tumor recognition (Fig. 3.6B). It is interesting to note that when evaluating the development of strong IFNγ responses, arbitrarily set at 1000pg, WT peptides induced 3 strong responses and the SNV peptides induced 4 strong responses. Similar to previous results, this coincided with increased IgG antibody to both WT and SNV 15mer versions of these mutation-sites (Fig. 3.6C,D), which often resulted in simultaneous improvements in IgG and tumor recognition related to specific 4T1 SNV neoantigens (Fig. 3.6E). Although not directly correlative for the whole group of candidate 4T1 antigens, there were several post-vaccine IgG signal increases which matched the antigens that improved CD8+ T cell responses against 4T1 tumor.

To confirm that we had observed stronger immune responses to proteins from our 4T1 vaccine, we next integrated these results with quantitative tandem mass tag (TMT) liquid chromatography tandem mass spectrometry (LC-MS/MS) data previously captured using the same 4T1 autophagosome-enriched vaccine lots used in these studies. A number of the antigens studied in the T cell and IgG assays were confirmed as being found by TMT LC-MS/MS at a depth of 4416 confirmed tumor proteins. Interestingly, there appeared to be a

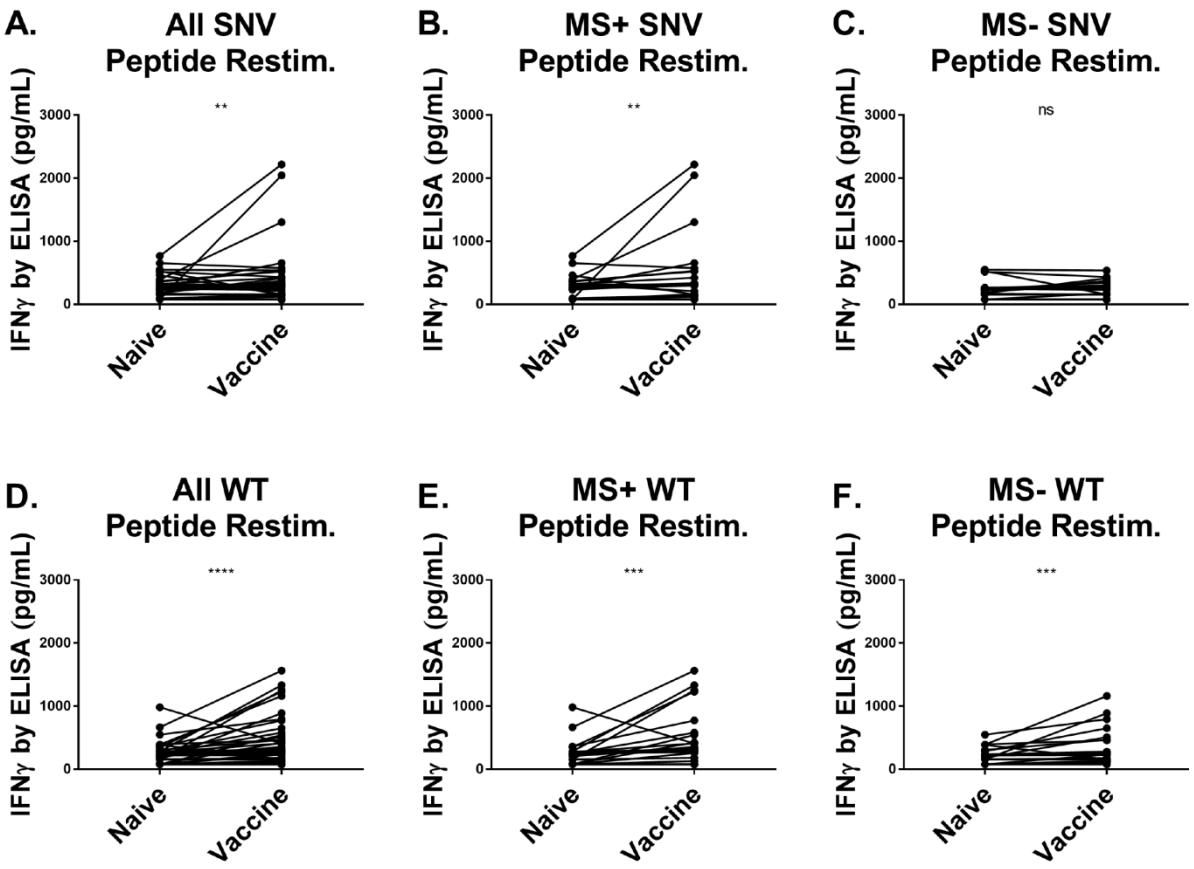

Figure 3.7 – Increased post-vaccination CD8+ T cell IFNγ secretion in response to 4T1 mutation-site peptides. Individualized data from all three sets of paired experiments with breakdown by mass spectrometry identification status presented (Fig. 3.5). CD4 depleted splenocytes from naïve and 4T1 autophagosome-enriched vaccine + poly-I:C vaccinated animals were stimulated with WT and SNV versions of top predicted MHCI binding 8-11mer mutation-site peptides, then expanded on IL-2, before being washed, split, and restimulated with naïve irradiated splenocytes and peptides. (**A**) Increased IFNγ secretion in vaccine groups upon secondary exposure to n=15 SNV peptides regardless of LC-MS/MS confirmation (P=0.0015). (**B**) Increased IFNγ secretion in vaccine groups upon secondary exposure to n=9 different SNV peptides from LC-MS/MS confirmed proteins (P=0.0031). (**C**) No difference in IFNγ secretion was observed in vaccine groups upon secondary exposure to n=6 different SNV peptides from LC-MS/MS unconfirmed proteins (P=0.22). (**D**) Increase in IFNγ secretion in vaccine groups observed upon secondary exposure to n=15 WT peptides regardless of LC-MS/MS confirmation (P<0.0001). (**E**) Increase in IFNγ secretion in vaccine groups observed upon secondary exposure to n=9 different WT peptides from LC-MS/MS confirmed proteins (P<0.0001). (**F**) Increased IFNγ secretion in vaccine groups observed upon secondary exposure to n=6 different WT peptides from LC-MS/MS unconfirmed proteins (P=0.0010). All statistics by Wilcoxon matched-pairs signed rank test.

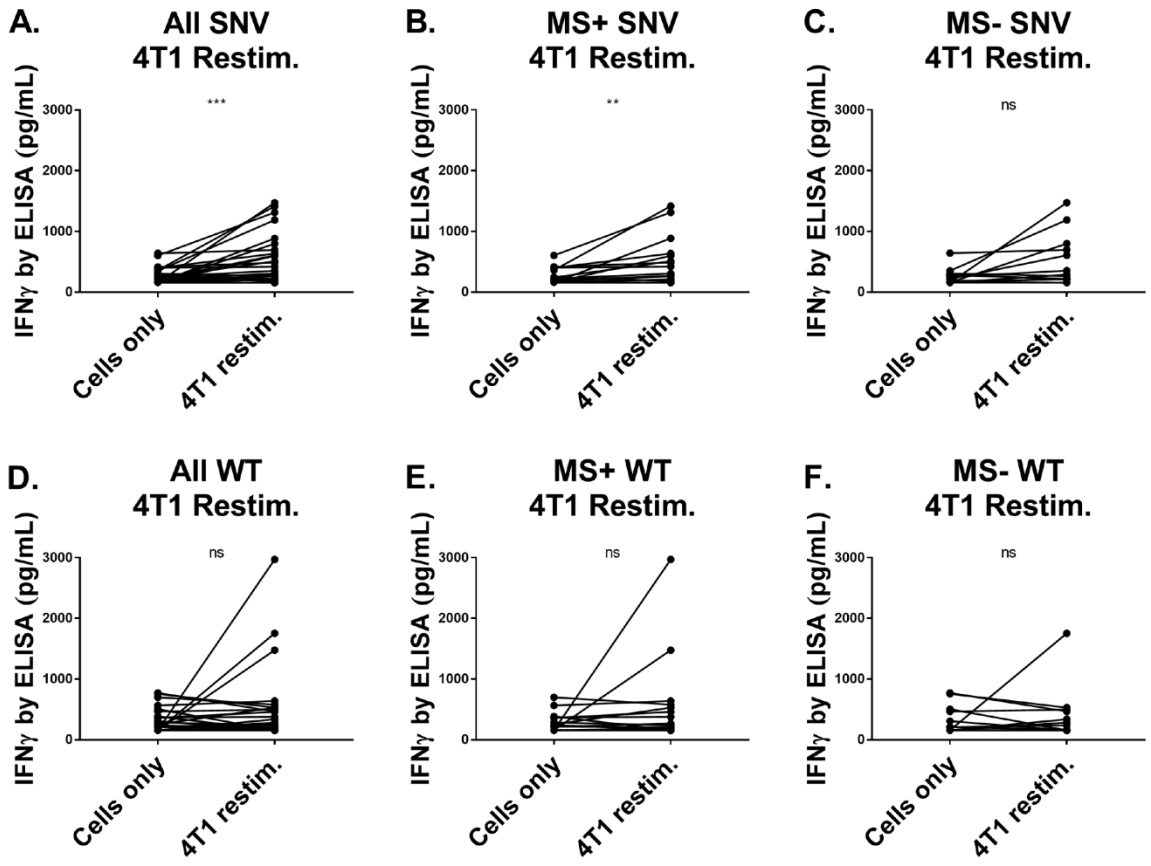

Figure 3.8 – Increased post-vaccination CD8+ T cell IFNγ secretion upon restimulation with 4T1 tumor cells. Individualized data from both sets of paired experiments presented with breakdown by mass spectrometry identification status (Fig. 3.6). CD4 depleted splenocytes from naïve and 4T1 autophagosome-enriched vaccine + poly-I:C vaccinated animals were stimulated with WT and SNV versions of top predicted MHCI binding 8-11mer mutation-site peptides, then expanded on IL-2, before being washed, split, and restimulated with live 4T1 cells or placed into empty wells with media alone. (**A**) Increase in IFNγ secretion in vaccine groups observed upon secondary exposure to 4T1 after primary exposure with n=15 SNV peptides regardless of LC-MS/MS confirmation (P=0.0002). (**B**) Increase in IFNγ secretion in vaccine groups observed upon secondary exposure to 4T1 after primary exposure with n=9 different SNV peptides from LC-MS/MS confirmed proteins (P=0.0004). (**C**) No difference was observed in IFNγ secretion in vaccine groups upon secondary exposure to 4T1 after primary exposure with n=6 different SNV peptides from LC-MS/MS unconfirmed proteins (P=0.148). (**D**) No difference in IFNγ secretion in vaccine groups was observed upon secondary exposure to 4T1 after primary exposure with n=15 WT peptides regardless of LC-MS/MS confirmation (P=0.65). (**E**) No difference in IFNγ secretion in vaccine groups upon secondary exposure to 4T1 was observed after primary exposure with n=9 different WT peptides from LC-MS/MS confirmed proteins (P=0.597). (**F**) Increase in IFNγ secretion was seen in vaccine groups upon secondary exposure to 4T1 after primary exposure with n=6 different WT peptides from LC-MS/MS unconfirmed proteins (P=0.99). All statistics by Wilcoxon matched-pairs signed rank test.

separation of the peptide restimulation data after filtering groups for mass spectrometry confirmed proteins. For CD8+ peptide recognition data already presented (Fig. 3.5A,B), significant SNV peptide recognition was found to depend on the group of mass-spectrometry confirmed proteins, and not the peptides from proteins unconfirmed by mass spectrometry (Fig. 3.7A-C). This suggests a neoantigen-specific priming event induced by the vaccine. In contrast, mass spectrometry recognition status did not alter CD8+ T cell recognition of WT peptides (Fig. 3.7D-F), suggesting a more general boosting effect of preexisting autoreactive cells. A similar result was observed in the tumor recognition data (Fig. 3.8A-F). Although increased recognition of 4T1 occurred with peptides from all groups, the only group to demonstrate a statistically significant increase in IFNγ release was induced by the group of mass spectrometry confirmed neoantigen peptides (Fig. 3.8B). These results give us confidence that our vaccine does not merely boost the overall population of IFNγ secreting CD8+ T cells, but can prime new neoantigen reactive T cells with vaccine-specific antigens.

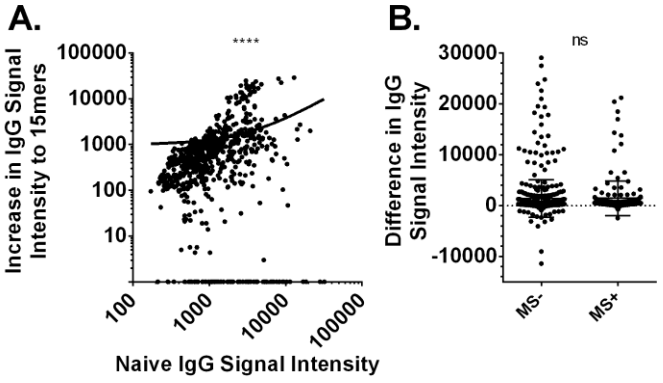

Figure 3.9 Increased IgG signal intensity to 4T1 15mers correlated with IgG signals in naïve animals and not mass spectrometry identification status. Data are from five independent pairs of IgG arrays presented previously (Fig. 3.1). These arrays were constructed with 15mer peptides matching 75 WT autoantigens paired with 75 SNV neoantigen mutation-sites in 4T1 plus AH1, and were reacted with pooled serum from naïve and autophagosome-enriched vaccine + poly-I:C treated mice. (**A**) Data compare the positive increase in IgG signal intensity after vaccination to the IgG signal intensity in naïve animals for each of n=755 paired points, and are plotted in $\log_{10}$ scale. There was a significant overall correlation (P<0.0001) by Pearson correlation coefficient. (**B**) Data compare the difference in IgG signal intensity for 15mer proteins either confirmed, or not confirmed, in the vaccine by mass spectrometry. There was no significant increase in signal intensity to 15mer peptides from proteins confirmed in 4T1 vaccine by mass spectrometry (P=0.61) by Mann Whitney test.

In contrast to this observed dependence of T cell responses to SNV peptides on mass spectrometry identification, we observed that larger IgG signals after vaccination depended more on a preexisting IgG signal to that peptide in naïve animals (Fig. 3.9A) than mass spectrometry identification status (Fig. 3.9B). This suggested that many of our observed IgG response are systemic boosts of preexisting responses, such as we might expect with an IgG2a-centric IFNγ boosted antibody response, and not necessarily specific to antigens from the vaccine. These same principles also held through to the specific pool of antigens investigated in both assays; IgG recognition after vaccination did not depend on mass spectrometry identification for the 30 antigens investigated in T cell assays (Fig. 3.10A). However, there was an overall increase in CD8+ T cell recognition of WT and SNV 8-11mer peptides from proteins confirmed in the vaccine by TMT LC-MS/MS (Fig. 3.10B).

These results translated to the correlation between IgG and CD8+ T cell data presented previously (Fig. 3.5E), where the positive correlation between increased IgG signals and IFNγ release after vaccination occurred only in the mass spectrometry positive fraction of the assays (Fig. 3.10C,D). Finally, we filtered the 4T1 tumor recognition data presented (Fig. 3.6A-E) for mass spectrometry identification, and observed a relationship between serum IgG signals against an antigen, and that antigen's ability to improve recognition of 4T1 tumor (Fig. 3.10E). Interestingly, this same pattern of increased 4T1 recognition was also associated with the predicted MHCI affinity of the stimulating peptide (Fig. 3.10F); an observation possibly caused in part by 4T1 cells presenting more high-affinity peptides than low-affinity peptides on MHCI. Taken together, these results demonstrate a set of overlapping relationships between antigen-specific IgG recognition, antigen-specific CD8+ T cell recognition, and MHCI affinity across multiple independent

antigens and multiple independent experimental groups – building upon data presented in Chapter 2 (Fig. 2.7C) – and demonstrating coordinated IgG antibody and CD8+ T cell recognition of tumor antigens.

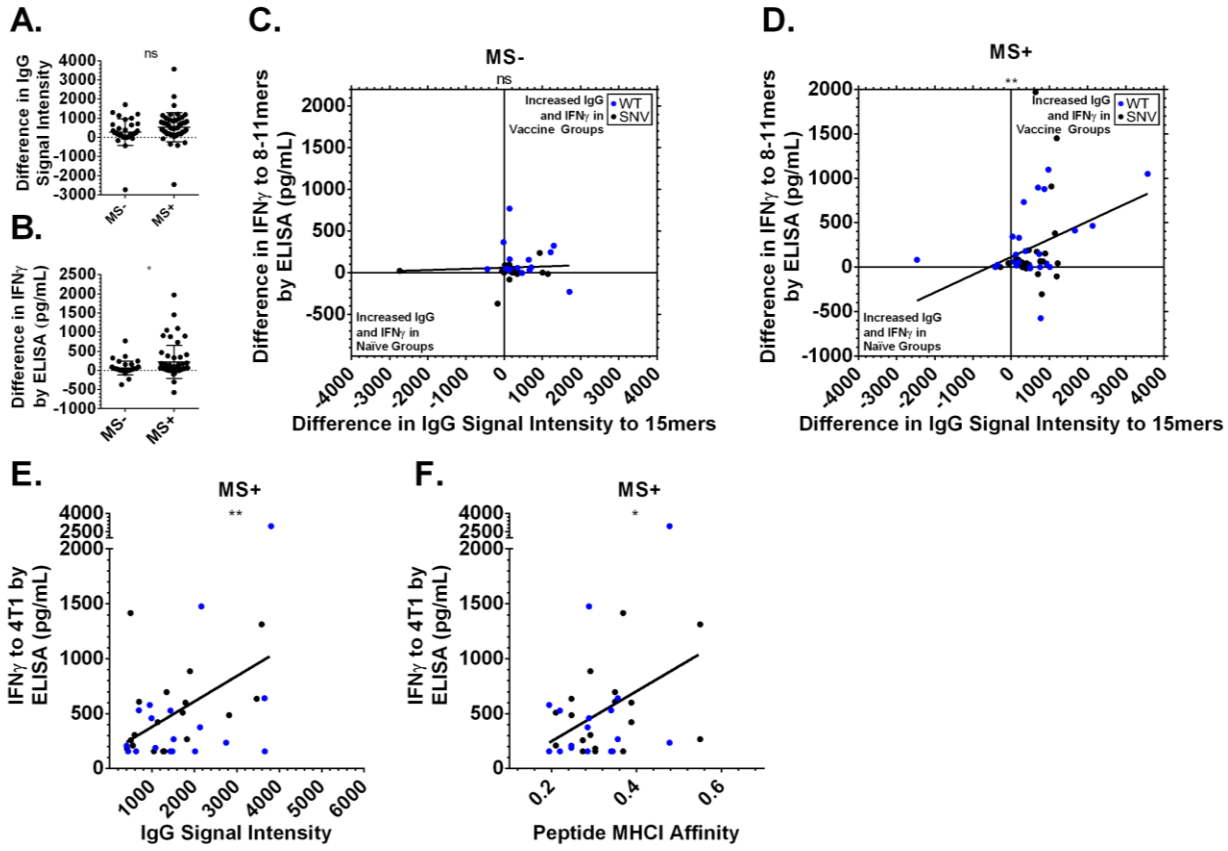

Figure 3.10 – Simultaneous vaccine-induced IgG and CD8+ IFNγ recognition of 4T1 tumor and peptides confirmed by LC-MS/MS. LC-MS/MS was performed to determine whether proteins containing the 4T1 peptides were present in live 4T1 cells and 4T1 autophagosome-enriched vaccine. Of the 15 4T1 WT and SNV pairs additionally analyzed in T cell assays, there were n=9 WT and SNV antigen pairs from proteins confirmed in 4T1 by mass spectrometry and n=6 WT and SNV antigen pairs not confirmed by mass spectrometry. (**A-D**) Data shown are from experiments previously presented (Fig. 3.5). Vaccinated animals demonstrated increased serum IgG to the peptides analyzed in T cell assays; however, there was no improved IgG response (**A**) to the WT and SNV peptides confirmed by mass spectrometry over unconfirmed proteins (P=0.1) by unpaired t-test. However, confirmed presence of the antigenic protein in the vaccine by mass spectrometry (**B**) resulted in improved IFNγ secretion in vaccine groups upon secondary exposure to WT and SNV 4T1 8-11mer peptides (P=0.04) by unpaired t-test. There was no significant overall correlation of these increases in IgG and CD8+ IFNγ peptide recognition (**C**) for peptides unconfirmed by mass spectrometry (P=0.75), but there was a significant correlation between improvements in IgG and CD8+ IFNγ peptide recognition (**D**) for mass spectrometry confirmed proteins (P=0.01) by Pearson correlation coefficient. For 4T1 tumor recognition data previously presented (Fig. 3.6), WT and SNV antigens from proteins confirmed in 4T1 cells and vaccine by mass spectrometry (**E**) produced greater CD8+ IFNγ recognition of 4T1 cells if serum from those animals also had higher IgG recognition of those antigens. A similar relationship (**F**) was observed between this same 4T1 recognition data and the predicted MHCI affinity of the original stimulating peptides (P=0.025) by Pearson correlation coefficient).

We sought to further confirm these results in vivo with adoptive transfer experiments using T cells cultured with specific minimal 4T1 SNV peptides and transferred into irradiated mice seeded with 4T1 tumors. The purpose was to demonstrate that beyond simply recognizing 4T1 cells in culture, these CD8+ T cells could prevent metastases in vivo. Unfortunately, in our first experiment the number of cells transferred was small. As hypothesized, the best performing animals were observed in experimental groups. However, there was no statistically significant difference from control animals (Fig. 3.11A,B). Encouraged by this result, we attempted a second experiment with a larger cell transfer – but the initial 4T1 seeding in this case proved so variable that it is impossible to draw any conclusions (Fig. 3.11C,D). Repeat experiments would be necessary to determine whether our culture processes can create effector T cells capable of influencing outcomes in vivo.

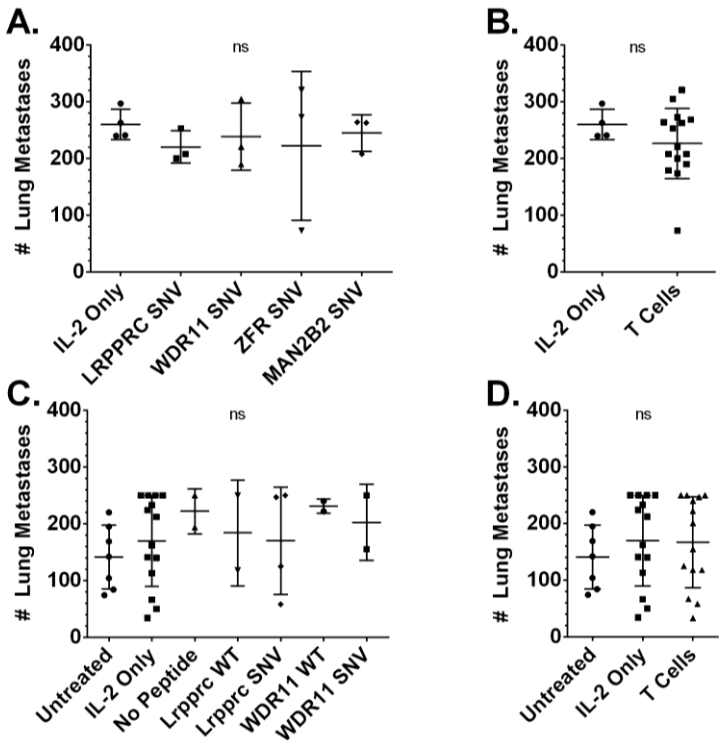

Figure 3.11 – Adoptive transfer of T cells primed with 4T1 peptides are unable to affect tumor growth in vivo. A selection of WT and SNV 4T1 mutation-site 8-11mers were chosen for adoptive transfer assays. In vitro cultures of cells from vaccinated animals were similar to previous experiments without CD4 depletion (Fig. 3.3). Splenocytes from 4T1 autophagosome-enriched vaccine + poly-I:C vaccinated animals were stimulated with WT and SNV versions of top predicted MHCI binding 8-11mer mutation-site peptides, then expanded on IL-2, before being washed, split, counted, and adoptively transferred into irradiated mice previously seeded with live 4T1 cells. Animals were administered IL-2 after transfer. On day 13 after T cell transfer, lungs were harvested, stained, and counted for metastases. (**A**) No significant difference between individual peptide primed adoptive transfer groups or IL-2 alone by one-way ANOVA (P=0.92), or between (**B**) all pooled T cell transfer groups versus IL-2 alone by t-test (P=0.31). In an additional experiment, (**C**) no significant difference was observed between individual peptide primed adoptive transfer groups, IL-2 alone, or untreated animals by one-way ANOVA (P=0.7), or between (**D**) all pooled T cell transfer groups versus IL-2 alone and untreated animals (P=0.7) by one-way ANOVA.

Discussion:

In this series of experiments, we again observed IgG antibodies binding 4T1 peptides in naïve female BALB/c mice, and this population of antibodies demonstrated stronger recognition of neoantigen peptides than autoantigen counterpart peptides. This result suggests a bias for the recognition of certain tumor antigens prior to tumor exposure, perhaps caused by an individual's unique history of tolerance to autoantigens or prior exposure to cross-reactive foreign antigens. Recent work has demonstrated a dramatic dependence of checkpoint blockade immunotherapies on specific microflora [149,150], an effect typically ascribed to system-wide cytokine changes, but perhaps also due in part to bacterial antigen cross-reactivity with tumor antigens. For example, germ-free animals lacking such immunologic history do not respond well to cancer therapy [151]. The correlations between vaccine-induced T cell responses and antigen-specific IgG antibody signals observed in this study suggest that IgG may be one biomarker to observe such relationships between prior immunologic history and future or ongoing anti-tumor immunity. And beyond the potential role of antibody as a biomarker, antibody may be directly involved in transferring prior immunologic knowledge to help prime or boost T cell populations.

Antigen-specific antibody can increase T cell activation through improved antigen uptake and cross-presentation by antigen presenting cells in mice [152], and a similar Fc receptor dependent effect has also been observed in humans: some patients receiving monoclonal antibodies to EGFR (Cetuximab) generate elevated circulating $EGFR_{853–861}$– specific CD8+ T cells [153]. Therefore, preexisting antibodies that happen to bind a tumor peptide or protein – such as those observed in this work – could provide a mechanism for improved CD8+ T cell responses to those same antigens via increased cross-presentation

efficiency. Such a hypothesis would be consistent with a Th2 driven IgG1 response, although a Th1 / IFNγ driven IgG2a subtype boost perhaps provides a more-direct link to CD8+ T cell activation [143]. In reality, both processes are likely ongoing simultaneously with some varying degree of dominance being won by either Th2 / IgG1 or Th1 / IgG2a across experiments. Such an IgG1 / IgG2a imbalance perhaps accounts for our diverse results regarding IgG signals and peptide-MHCI affinity observed across Chapters 2 and 3.

In addition to the overall trends we observed between IgG and CD8+ responses, we were struck that minimal peptides from Wdr33:H13Y – a mutation-site with strong preexisting IgG signals in naïve animals – were recognized regularly in vaccinated animals by IgG and produced large increases in CD8+ T cell recognition of both 4T1 tumor and Wdr33:H13Y peptides. This exemplary case builds on our overall hypothesis that some antigen-specific CD8+ T cell responses to our vaccine are additionally favored by B cell and / or CD4+ recognition of similar peptides. While the mechanism is still uncertain, the observations reported here warrant further investigation into the roles of IgG and other antibody isotypes on future anti-tumor responses. Future work should focus on isotype-specific relationships and include data from clinical samples; this will be essential to determine these nuances of antibody and T cell interrelationships.

In the viral literature, the dependence of future responses on past ones to similar antigens is well documented [154–157], and there are recent reports suggesting that preexisting immunity not only occurs, but is common; many healthy adults have memory T cells reactive to peptides from viruses they have never encountered [158]. Perhaps such T cell repertoires relate to the observed universe of preexisting IgG autoantibodies common in

humans [103]. If true, these IgG antibodies may help point to the types of antigens targeted by – or that evade – cancer immune surveillance. We may find that some patients require not just a release of tolerance by checkpoint blockade or boosting of the natural priming environment by costimulatory agonists or cytokines, but perhaps vaccines and therapies directed toward those antigens inadvertently avoided by their own unique history of antigen exposure. In the future, it may be possible to determine this antigenic history and correct gaps in immune surveillance with either personalized cancer vaccines or generalized complex vaccines like the autophagosome-enriched vaccine studied here.

CHAPTER 4

CONCLUDING REMARKS

Many of today's most heralded advances in cancer immunotherapy function via manipulating systemic immunologic processes with little or no knowledge of the underlying antigen-specific immunity involved. Such non-specific systemic treatments date to the days of William Coley, whose crude intratumoral injections of bacterial 'Coley's toxins' provide the first intentional evidence of cancer immunotherapy [159]. Similar treatments based on microbes and their analogues are in clinics today in the form of injectable intratumoral viruses and toll-like receptor (TLR) agonists [160–165]. While we have a deeper understanding of why these treatments sometimes work today – we often remain as blind as Coley to most of the symphony of adaptive immunity that these treatments create. Even current checkpoint blockade treatments such as anti-PD-1 (e.g. Nivolumab) and anti-CTLA-4 (e.g. Ipilimumab) [14], as well as next generation checkpoint blockade and costimulatory agonist therapies targeting ICOS, VISTA, and OX40 are administered equally blind to the antigen-specific adaptive immune environment [25,166–169]. T cell receptor (TCR) sequencing is a recent advance that provides the opportunity to watch specific clonal T cell populations grow and expand during these treatments [170], but without considerable additional effort this method also remains antigen blind. Future advances in computational immunology and TCR sequencing may eventually allow for peptide-MHC antigen predictions from these TCR sequences [171], but these methods should remain unreliable in the immediate future. Until such computational specificity analysis improves, direct measurement of antigen-specific immunity will be required; the easiest method to accomplish this will be though humoral immunity.

This document has advanced the field of tumor immunology by demonstrating that antigen-specific correspondence can occur between IgG antibody and CD8+ T cell responses to cancer vaccines – a result that has important implications for high-throughput discovery and monitoring of antigen-specific anti-tumor immunity. But how will this observation be directly applied? Custom patient-specific antibody arrays analogous to the 15mer peptide arrays used in our preclinical work may prove immediately useful to groups developing anti-tumor patient-specific neoantigen vaccines [172] because these groups have an immediate need for determining whether their vaccines augment immunity to patient-specific targets. Nevertheless, until cheap automated analysis methods are developed, creating custom neoantigen arrays will not be practical for the average oncology clinic. The requirement for individualized genomic analysis and array design presented in this document are simply too expensive and time intensive to become broadly applied in the near future.

In contrast to customized patient-specific assays, we propose that generalized neoantigen peptide arrays may provide a more immediate opportunity to apply our observations. Although the bulk of mutations in any individual cancer are unique to that tumor and to that patient – a handful of neoantigens are shared surprisingly often between them. For melanoma patients, it has long been recognized that only a handful of specific missense mutations are responsible for most errors in tumor protein P53 (TP53) [173]. And in recent years, The Cancer Genome Atlas (TCGA) and similar collaborative sequencing initiatives have revealed that there are many other 'hotspot' mutations that are shared across tumor oncogenes [173–176]. These neoantigen hotspots provide novel opportunities for generalized immune monitoring and cancer vaccine design. For example: the specific single

letter amino acid change R132H in the gene IDH is strongly associated with glioblastoma [175], and cancer vaccines targeting this mutation are under development [177]. Also, T cells naturally recognizing hotspots and other neoantigens have already been found in patient tumor infiltrating lymphocyte samples [178–181]. These observations suggest that generic yet mutation-specific immune monitoring methods might be useful for surveying some of this neoantigen immunity in patients with cancer. If our preclinical work demonstrating antibody / T cell correspondence has an analogue in humans, future studies may discover that antibodies targeting certain oncogene mutations are associated with successful immunosurveillance and a lifetime free of cancer, or that patients who develop new hotspot-specific antibodies after therapy are more likely to respond successfully to their treatments.

It is now possible to turn to publically available tumor sequencing databases to determine just how broadly shared these neoantigen hotspots are. As a demonstration, we have downloaded data from a recent sequencing study performed at the Memorial Sloan-Kettering Cancer Center: the MSK-IMPACT cohort [182]. These data are publically available for download at the cBioPortal for Cancer Genomics (http://www.cbioportal.org/), and include 10,945 primary and metastatic tumors from 143 different primary tissue sites and represent over 10,000 individual cancer patients. Though there is exceptional diversity amongst the passenger mutations carried by these patients, many share hotspot mutations in their oncogenes. We found that a remarkable 37.8% of all samples in this study carried at least one of just 50 hotspot amino acid changes (Fig. 4.1A). For example, around 1 in 14 of the patients in this diverse cohort will carry either the KRAS G12D or PIK3CA E545K mutation. The reason for this remarkable overlap of hotspot neoantigens is because these

A.

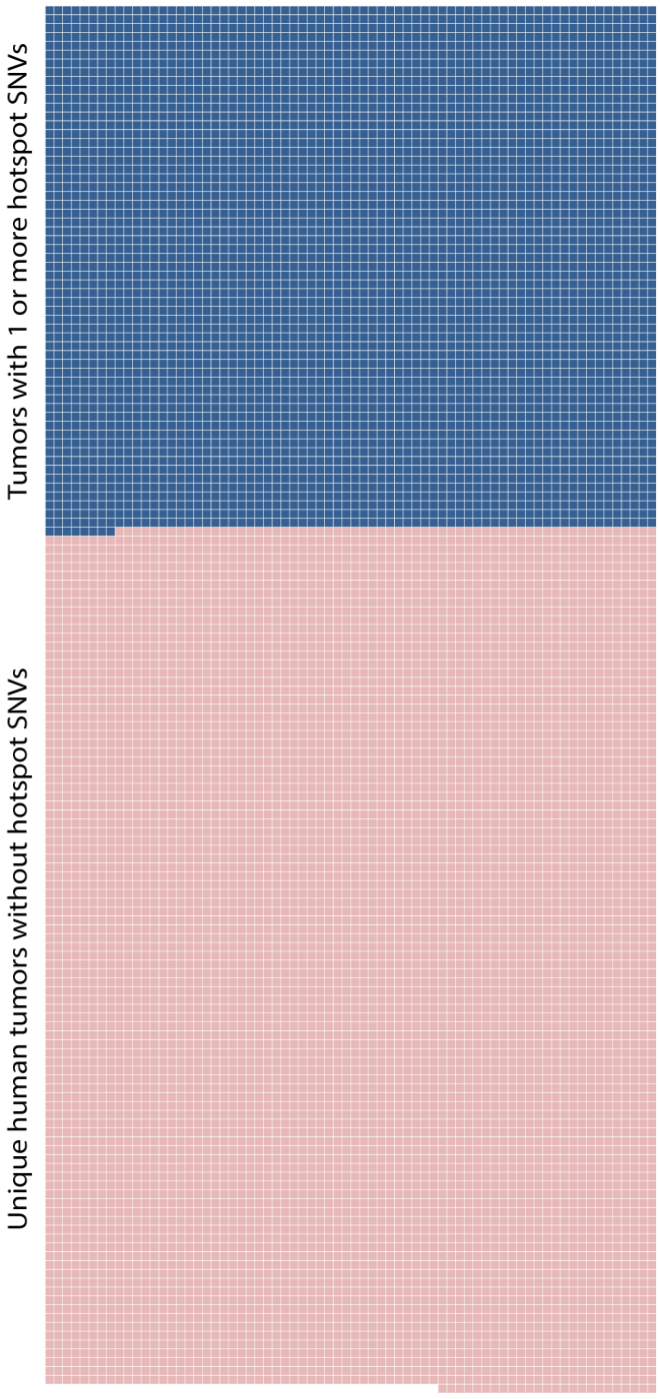

B.

Unique Site	Mutant 15mer Peptide	Frequency
KRAS G12D	KLVVVGADGVGKSAL	443
KRAS G12V	KLVVVGAVGVGKSAL	368
PIK3CA E545K	DPLSEITKQEKDFLW	304
PIK3CA H1047R	MKQMNDARHGGWTTK	301
BRAF V600E	GDFGLATEKSRWSGS	295
KRAS G12C	KLVVVGACGVGKSAL	257
PIK3CA E542K	STRDPLSKITEQEKD	216
TP53 R175H	HMTEVVRHCPHHERC	209
IDH1 R132H	VKPIIIGHHAYGDQY	169
TP53 R248Q	SCMGGMNQRPILTII	152
TP53 R273H	GRNSFEVHVCACPGR	135
KRAS G13D	LVVVGAGDVGKSALT	133
EGFR L858R	VKITDFGRAKLLGAE	131
TP53 R273C	GRNSFEVCVCACPGR	125
TP53 R248W	SCMGGMNWRPILTII	113
TP53 R282W	CACPGRDWRTEEENL	96
KRAS G12A	KLVVVGAAGVGKSAL	89
NOTCH2NL S67P	EDCQYSTPHPCFVSR	81
NRAS Q61R	DILDTAGREEYSAMR	79
HLA-B E100V	AQAQTDRVSLRNLRG	77
FGFR3 S249C	TLDVLERCPHRPILQ	76
TP53 G245S	CNSSCMGSMNRRPIL	75
KRAS G12R	KLVVVGARGVGKSAL	72
IDH1 R132C	VKPIIIGCHAYGDQY	69
EGFR T790M	TSTVQLIMQLMPFGC	57
NRAS Q61K	DILDTAGKEEYSAMR	56
KRAS Q61H	DILDTAGHEEYSAMR	54
HLA-B N104K	TDRESLRKLRGYYNQ	52
TP53 Y220C	RHSVVVPCEPPEVGS	49
ERBB2 S310F	YLSTDVGFCTLVCPL	48
GNAS R201H	DQDLLRCHVLTSGIF	48
ESR1 D538G	KNVVPLYGLLLEMLD	46
U2AF1 S34F	CRHGDRCFRLHNKPT	45
KRAS G12S	KLVVVGASGVGKSAL	41
PIK3CA H1047L	MKQMNDALHGGWTTK	41
PIK3CA N345K	ILCATYVKVNIRDID	41
HLA-C V36M	MRYFDTAMSRPGRGE	40
GNAS R201C	DQDLLRCCVLTSGIF	39
SMAD4 R361H	VDPSGGDHFCLGQLS	39
TP53 E285K	PGRDRRTKEENLRKK	39
KRAS A146T	IPFIETSTKTRQRVE	38
PTEN R130Q	HCKAGKGQTGVMICA	33
CDKN2A H83Y	ATLTRPVYDAAREGF	32
FBXW7 R465H	YGHTSTVHCMHLHEK	32
CDKN2Ap14ARF H83Y	ATLTRPVYDAAREGF	31
CDKN2Ap16INK4A H83Y	ATLTRPVYDAAREGF	31
PIK3CA R88Q	EFFDETRQLCDLRLF	31
TP53 V157F	TPPPGTRFRAMAIYK	31
CTNNB1 S37F	YLDSGIHFGATTTAP	30
PIK3CA C420R	KGAKEEHRPLAWGNI	30

Fig. 4.1 – Hotspot neoantigens in the MSK-IMPACT cohort. Whole genome sequencing data was downloaded for 10,945 samples from 143 different primary tissues. Data were filtered for hotspots of common SNV amino acid changes shared across patients. (**A**) A total of 4138 samples shared at least one of the top 50 hotspot SNV amino acid changes. (**B**) The top 50 hotspot SNV amino acid changes are listed, with surrounding peptide context and frequency within this sample set.

mutations are in protein-coding oncogenes directly involved in creating the tumors they are found in. This means that even a simple neoantigen peptide array composed of 50 targets could monitor antigen-specific humoral immunity to at least one tumor-specific mutation in a large percentage of the clinical population. The full list of top hotspot mutations, along with their observed frequency in this cohort, is shown alongside 15mer peptide sequences for a proposed antibody array (Fig. 4.1B).

In addition to immune monitoring, there is an additional opportunity to use these hotspot neoantigens as part of a generalized cancer vaccine. Although vaccines to simple peptide tumor antigens have failed to add benefit in otherwise successful immunotherapy trials [183], this does not mean hotspot neoantigen vaccines could not work with an improved formulation or in the prophylactic setting. Improved formulations could involve different adjuvants, delivery mechanisms, or antigen delivery as whole-protein or DNA vaccines in longer sequences beyond the short peptides shown (Fig. 4.1B). Future work might strengthen this hypothesis by surveying immunity in older individuals who never develop cancer or patients who have successfully gone into remission after therapy. Such antigen-specific surveys of high-risk tumor-free individuals could demonstrate whether immunosurveilance against these neoantigen targets occurs, and if so – whether it correlates to differences in disease incidence or outcome. If such correlations exist, they would support the idea of hotspot neoantigen prevention vaccines. Support for this concept already exists in the observation that certain cancers linked to specific oncogene hotspots are less prevalent in patients with specific MHC genotypes and more frequent in others [184–186]. Such MHC-associated differences in cancer incidence suggest that these oncogenes likely create an

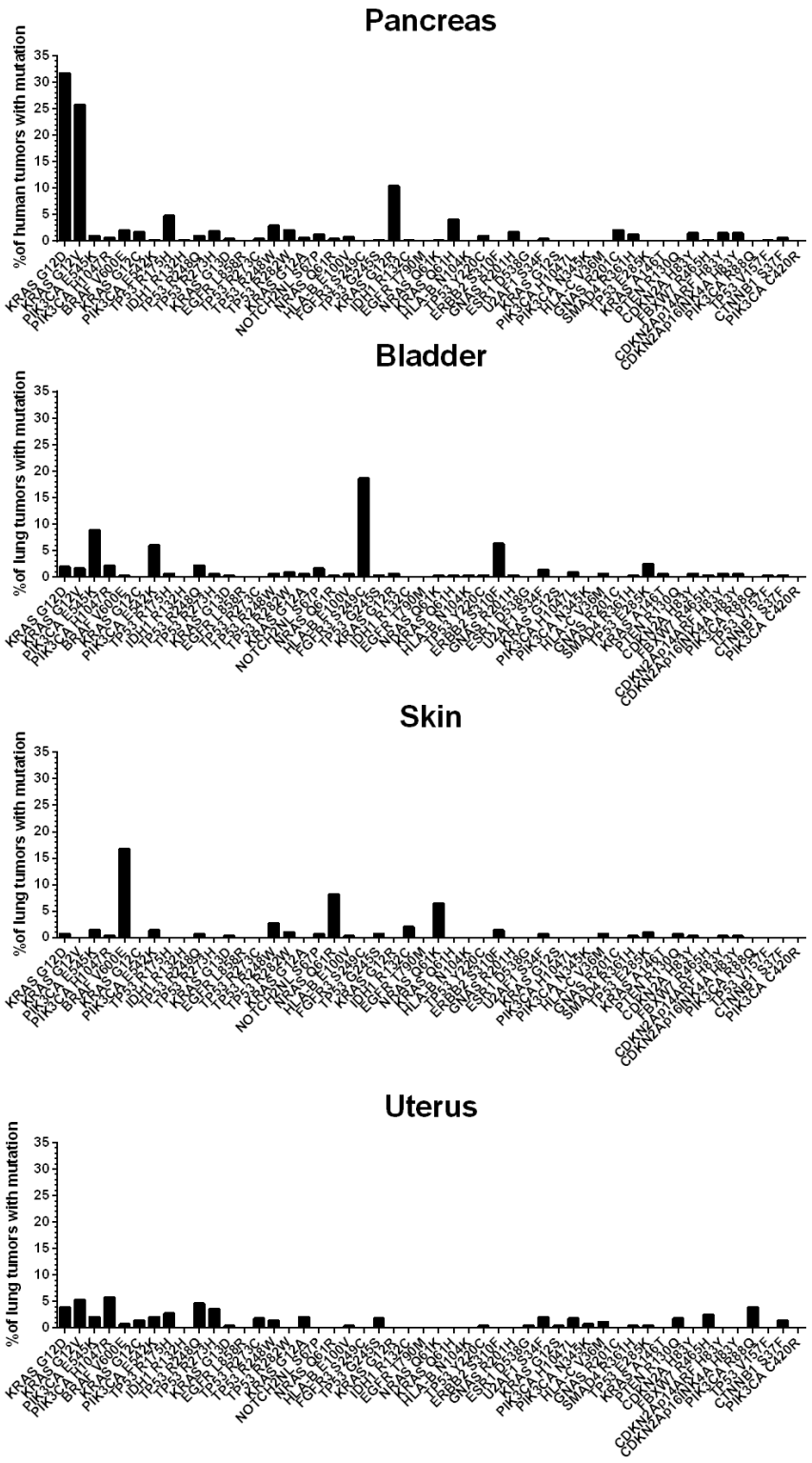
Pancreas
%of human tumors with mutation
Bladder
%of lung tumors with mutation
Skin
%of lung tumors with mutation
Uterus
%of lung tumors with mutation

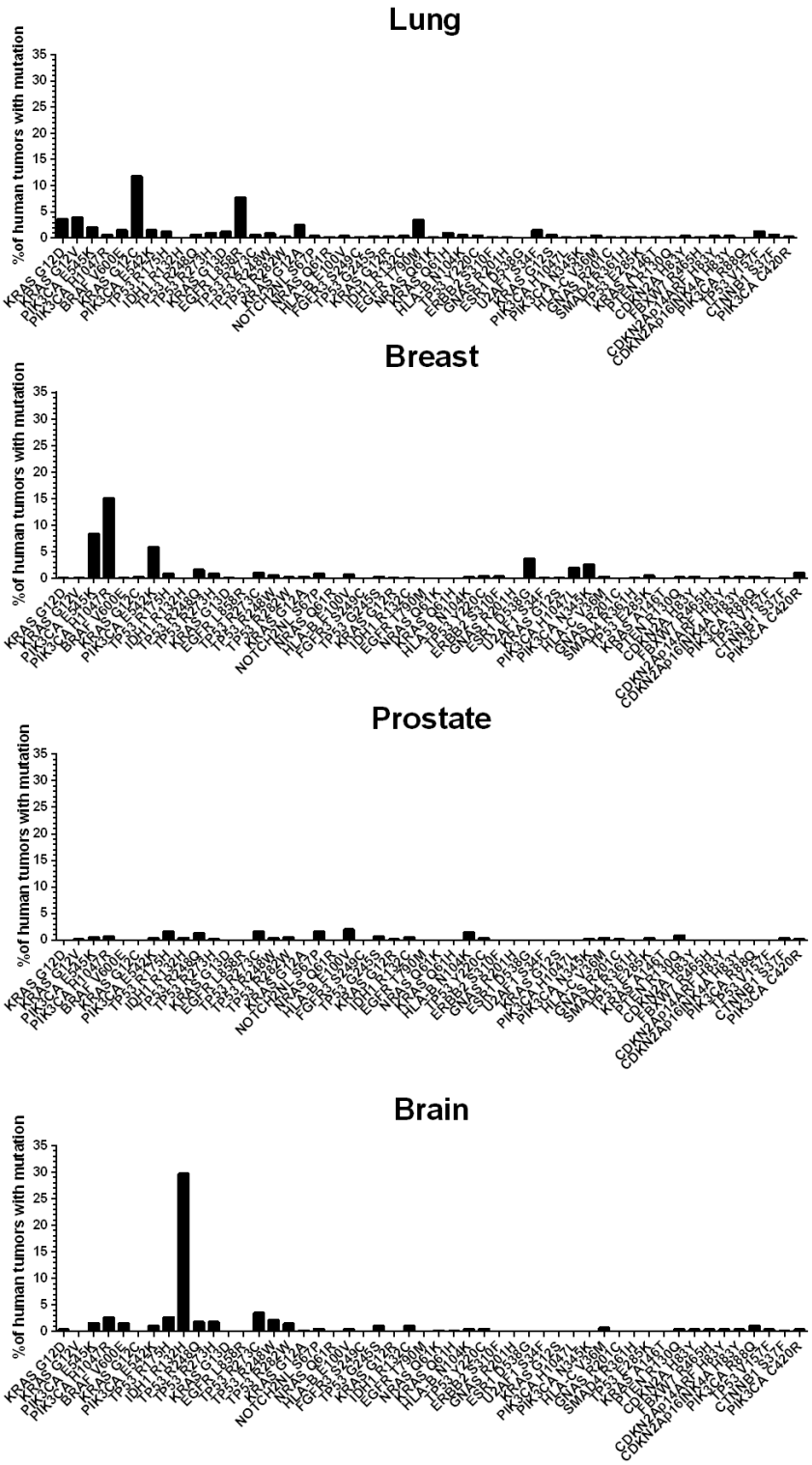

Fig. 4.2 – Diversity of hotspot neoantigens across primary tissues in MSK-IMPACT cohort. Different tissues of origin present with different frequencies of hotspot neoantigens. Sequencing data was filtered for individual primary tissues, and observed frequencies of the top 50 hotspot mutations were plotted for each tissue. Results are very diverse across differing primary tissues. IDH1 R132H dominates in brain tumors, found in >30% of samples. No hotspot mutation is commonly found in prostate tumors. Other tissues present with a greater diversity of hotspot SNV mutations.

antigenic peptide which either strongly or weakly binds these individual MHC isoforms – resulting in a heterogeneity of natural immune surveillance by effector CD8+ T cells that prevents some of these cancers from presenting as often clinically. At the level of individual tumors, a tissue-specific heterogeneity in hotspot antigens can be observed in the MSK-IMPACT cohort – different tissues of origin are more likely to carry certain neoantigen hotspot mutations than others (Fig. 4.2). Pancreatic tumors are especially susceptible to KRAS mutations with over half of patients presenting with either a G12D or G12V mutation. In contrast, breast tumors almost never carry KRAS mutations, but instead carry a >30% incidence risk for one of just a few PIK3CA mutations. Other cancers, such as prostate tumors, share very few neoantigen hotspots with the overall population of tumor samples. These differences likely relate to tissue-specific oncogenesis requirements and demonstrate that targeted neoantigen hotspot arrays or vaccines might not be useful for some tumor types.

Contrary to much of the neoantigen-specific focus of this document, progress toward a generic and widely effective cancer prevention vaccine might not be possible if it depends solely on tumor neoantigens. While a vaccine to the peptides shown above (Fig. 4.1) could in theory prevent some portion of clinically relevant tumors – it would be surprising if such a vaccine were 100% effective. Single letter amino acid changes will not always be immunogenic for some people due to patient MHC diversity [184–186], while in older patients many of these mutations will additionally be carried by normal aged tissues [187]. These otherwise healthy cells displaying tumor neoantigens may unfortunately promote peripheral tolerance against them. In contrast, the severe epigenetic dysregulation commonly observed in cancerous cells [188–190] also results in overexpressed and ectopically-expressed tumor-associated proteins which can prove surprisingly unique to cancerous tissue.

Evidence has grown demonstrating the importance of these non-mutated tumor antigens such as the cancer / testis antigen NY-ESO-1 [21,22,179,191]. In the past when genomic data was harder to obtain, non-mutated tumor antigens such as NY-ESO-1 received most of the attention. More recently the field has shifted away from ectopic and overexpressed tumor antigens due to excitement over neoantigens and the failures of some overexpressed-self clinical trials – such as gp100 peptide combined with anti-CTLA-4 in melanoma [183], and the poor performance of some 'successes' such as Sipuleucel-T (Provenge) for prostate cancer [192]. However, all this might mean is that these vaccines or treatments either failed to induce an adequate and durable response, a poor adjuvant or delivery method, or that the antigen was already recognized by many patients who instead required checkpoint therapy. Interestingly, a recent paper specifically comparing T cell recognition frequency between ectopic tumor antigens and neoantigens demonstrates a higher frequency of T cells targeting ectopic-self tumor antigens than neoantigens [179]. Perhaps the best of these tumor-associated antigens have not yet been appreciated: many may be in retroviruses or other non-canonically transcribed regions of DNA that are often filtered out of mRNA and mass spectrometry analysis because they do not match canonically transcribed genes.

So which tumor antigens are most essential for a successful anti-tumor effector CD8+ T cell response – neoantigens or overexpressed / ectopically-expressed self? In most cases – probably both. In the same way that tumors treated with small-molecule targeted therapies are often able to evade and escape single inhibitors [193,194], it is thought that the immune system's ability to target a tumor simultaneously from several different directions against several different antigens may be key to achieving not just remissions – but actual cures. To determine which targets are most important for both immune response monitoring and future

cancer vaccine design, a large antigen-specific 'Cancer Immune Response Atlas' of both healthy and diseased patients could be made. Our work and that of others suggests that if such an Atlas were built measuring humoral antibody responses, it would also partially represent antigen-specific T cell immunity. By combining hotspot neoantigen analysis with available high-throughput autoantigen discovery methods such as ProtoArray protein microarrays [70,195–197], size exclusion chromatography-microsphere-based affinity proteomics (SEC-MAP) arrays [198], nucleic acid programmable protein arrays (NAPPA) [199–201], or bacteriophage immunoprecipitation sequencing (PhIP-seq) [202,203], it would be possible to determine which antigen and isotype-specific antibody responses correlate most with successful cancer treatments – and perhaps more importantly – to discover which antibodies are associated with a lifetime spent free from cancer.

In addition to pioneering murine studies [204], the hypothesis of cancer immune surveillance is supported by the observation that men are more likely to have clinical cancers than women [4], and women are more likely to suffer from most autoimmune diseases than men [205]. Any antigen-specific antibodies associated with these incidence discrepancies could potentially be observable by methods similar to those reported here, and may represent the effector CD8+ T cell immunity – or lack thereof – underlying some of these immune-based conditions. The results of such surveys could then be applied to potentially improve antigen-specific immune monitoring and cancer vaccine design. There's even a chance this type of work could lead to significant advances for the treatment of non-cancer disorders: many ageing-related degenerative diseases such as Alzheimer's disease, frontotemporal dementia (FTD), and amyotrophic lateral sclerosis (ALS) are known to be inflammatory in nature, involve disappearing cell populations, and yet be of a stubbornly unknown root cause

[206–211]. Meanwhile, many of these same inflammatory diseases have an inverse correlation with cancer incidence [212–217]. Interestingly, large epidemiological studies demonstrate that melanoma survivors are at an increased risk of ALS [218], while some ALS patient neurons are reported to express the normally silent human endogenous retrovirus K (HERV-K) [219] – a known melanoma antigen [23]. Perhaps these observations are interrelated, with conditions such as FTD, Parkinson's, ALS, and Alzheimer's being the direct result of successful and overzealous anti-tumor immune surveillance which unfortunately also attacks normal tissue. The most thorough way to answer such questions would be through population-wide surveys of antigen-specific adaptive immunity; the results presented in this thesis demonstrate such surveys can be accomplished by monitoring humoral immunity with existing technologies.

References:

1. vonHoldt BM, Ostrander EA. The Singular History of a Canine Transmissible Tumor. Cell. 2006;126:445–7.

2. Murchison EP, Schulz-Trieglaff OB, Ning Z, Alexandrov LB, Bauer MJ, Fu B, et al. Genome Sequencing and Analysis of the Tasmanian Devil and Its Transmissible Cancer. Cell. 2012;148:780–91.

3. Bianconi E, Piovesan A, Facchin F, Beraudi A, Casadei R, Frabetti F, et al. An estimation of the number of cells in the human body. Annals of Human Biology. 2013;40:463–71.

4. Jemal A, Ward EM, Johnson CJ, Cronin KA, Ma J, Ryerson AB, et al. Annual Report to the Nation on the Status of Cancer, 1975–2014, Featuring Survival. JNCI: Journal of the National Cancer Institute [Internet]. 2017 [cited 2018 Mar 22];109. Available from: http://academic.oup.com/jnci/article/doi/10.1093/jnci/djx030/3092246/Annual-Report-to-the-Nation-on-the-Status-of

5. Martincorena I, Roshan A, Gerstung M, Ellis P, Van Loo P, McLaren S, et al. High burden and pervasive positive selection of somatic mutations in normal human skin. Science. 2015;348:880–6.

6. Kim JH, Kim HS, Kim BJ. Prognostic value of smoking status in non-small-cell lung cancer patients treated with immune checkpoint inhibitors: a meta-analysis. Oncotarget [Internet]. 2017 [cited 2018 Mar 22];8. Available from: http://www.oncotarget.com/fulltext/18703

7. On behalf of the Spanish Melanoma Group (GEM), Espinosa E, Márquez-Rodas I, Soria A, Berrocal A, Manzano JL, et al. Predictive factors of response to immunotherapy—a review from the Spanish Melanoma Group (GEM). Annals of Translational Medicine. 2017;5:389–389.

8. Sacher AG, Gandhi L. Biomarkers for the Clinical Use of PD-1/PD-L1 Inhibitors in Non–Small-Cell Lung Cancer: A Review. JAMA Oncology. 2016;2:1217.

9. Sclafani F. PD-1 inhibition in metastatic dMMR/MSI-H colorectal cancer. The Lancet Oncology. 2017;18:1141–2.

10. Overman MJ, McDermott R, Leach JL, Lonardi S, Lenz H-J, Morse MA, et al. Nivolumab in patients with metastatic DNA mismatch repair-deficient or microsatellite instability-high colorectal cancer (CheckMate 142): an open-label, multicentre, phase 2 study. The Lancet Oncology. 2017;18:1182–91.

11. Seung SK, Curti BD, Crittenden M, Walker E, Coffey T, Siebert JC, et al. Phase 1 Study of Stereotactic Body Radiotherapy and Interleukin-2--Tumor and Immunological Responses. Science Translational Medicine. 2012;4:137ra74-137ra74.

12. Atkins MB, Lotze MT, Dutcher JP, Fisher RI, Weiss G, Margolin K, et al. High-dose recombinant interleukin 2 therapy for patients with metastatic melanoma: analysis of 270 patients treated between 1985 and 1993. Journal of Clinical Oncology. 1999;17:2105–2105.

13. Grimm EA. Lymphokine-activated killer cell phenomenon. Lysis of natural killer- resistant fresh solid tumor cells by interleukin 2-activated autologous human peripheral blood lymphocytes. Journal of Experimental Medicine. 1982;155:1823–41.

14. Wolchok JD, Kluger H, Callahan MK, Postow MA, Rizvi NA, Lesokhin AM, et al. Nivolumab plus Ipilimumab in Advanced Melanoma. New England Journal of Medicine. 2013;369:122–33.

15. Swanton C. Intratumor Heterogeneity: Evolution through Space and Time. Cancer Research. 2012;72:4875–82.

16. Yap TA, Gerlinger M, Futreal PA, Pusztai L, Swanton C. Intratumor Heterogeneity: Seeing the Wood for the Trees. Science Translational Medicine. 2012;4:127ps10-127ps10.

17. Schumacher TN, Hacohen N. Neoantigens encoded in the cancer genome. Current Opinion in Immunology. 2016;41:98–103.

18. McGranahan N, Furness AJS, Rosenthal R, Ramskov S, Lyngaa R, Saini SK, et al. Clonal neoantigens elicit T cell immunoreactivity and sensitivity to immune checkpoint blockade. Science. 2016;351:1463–9.

19. van Rooij N, van Buuren MM, Philips D, Velds A, Toebes M, Heemskerk B, et al. Tumor Exome Analysis Reveals Neoantigen-Specific T-Cell Reactivity in an Ipilimumab-Responsive Melanoma. Journal of Clinical Oncology. 2013;31:e439–42.

20. Goodyear O, Agathanggelou A, Novitzky-Basso I, Siddique S, McSkeane T, Ryan G, et al. Induction of a CD8+ T-cell response to the MAGE cancer testis antigen by combined treatment with azacitidine and sodium valproate in patients with acute myeloid leukemia and myelodysplasia. Blood. 2010;116:1908–18.

21. Robbins PF, Kassim SH, Tran TLN, Crystal JS, Morgan RA, Feldman SA, et al. A Pilot Trial Using Lymphocytes Genetically Engineered with an NY-ESO-1-Reactive T-cell Receptor: Long-term Follow-up and Correlates with Response. Clinical Cancer Research. 2015;21:1019–27.

22. Wargo JA, Robbins PF, Li Y, Zhao Y, El-Gamil M, Caragacianu D, et al. Recognition of NY-ESO-1+ tumor cells by engineered lymphocytes is enhanced by improved vector design and epigenetic modulation of tumor antigen expression. Cancer Immunology, Immunotherapy. 2009;58:383–94.

23. María G-C, Paola I, Niki K, Mariacarmela S, Julià B, Rafael R. Human endogenous retroviruses and cancer. Cancer Biology & Medicine. 2016;13:483.

24. Cherkasova E, Weisman Q, Childs RW. Endogenous Retroviruses as Targets for Antitumor Immunity in Renal Cell Cancer and Other Tumors. Frontiers in Oncology [Internet]. 2013 [cited 2018 Mar 22];3. Available from: http://journal.frontiersin.org/article/10.3389/fonc.2013.00243/abstract

25. Pardoll DM. The blockade of immune checkpoints in cancer immunotherapy. Nature Reviews Cancer. 2012;12:252–64.

26. Grivennikov SI, Greten FR, Karin M. Immunity, Inflammation, and Cancer. Cell. 2010;140:883–99.

27. Dudley ME. Cancer Regression and Autoimmunity in Patients After Clonal Repopulation with Antitumor Lymphocytes. Science. 2002;298:850–4.

28. Antoniou AN, Powis SJ, Elliott T. Assembly and export of MHC class I peptide ligands. Current Opinion in Immunology. 2003;15:75–81.

29. Lankat-Buttgereit B, Tampé R. The Transporter Associated With Antigen Processing: Function and Implications in Human Diseases. Physiological Reviews. 2002;82:187–204.

30. Dolan BP, Bennink JR, Yewdell JW. Translating DRiPs: progress in understanding viral and cellular sources of MHC class I peptide ligands. Cellular and Molecular Life Sciences. 2011;68:1481–9.

31. Rock KL, Farfán-Arribas DJ, Colbert JD, Goldberg AL. Re-examining class-I presentation and the DRiP hypothesis. Trends in Immunology. 2014;35:144–52.

32. Yewdell JW. DRiPs solidify: progress in understanding endogenous MHC class I antigen processing. Trends in Immunology. 2011;32:548–58.

33. Yewdell JW, Nicchitta CV. The DRiP hypothesis decennial: support, controversy, refinement and extension. Trends in Immunology. 2006;27:368–73.

34. Twitty CG, Jensen SM, Hu H-M, Fox BA. Tumor-Derived Autophagosome Vaccine: Induction of Cross-Protective Immune Responses against Short-lived Proteins through a p62-Dependent Mechanism. Clinical Cancer Research. 2011;17:6467–81.

35. Rammensee H-G, Bachmann J, Emmerich NPN, Bachor OA, Stevanović S. SYFPEITHI: database for MHC ligands and peptide motifs. Immunogenetics. 1999;50:213–219.

36. Hoof I, Peters B, Sidney J, Pedersen LE, Sette A, Lund O, et al. NetMHCpan, a method for MHC class I binding prediction beyond humans. Immunogenetics. 2009;61:1–13.

37. Lemmel C, Weik S, Eberle U, Dengjel J, Kratt T, Becker H-D, et al. Differential quantitative analysis of MHC ligands by mass spectrometry using stable isotope labeling. Nature Biotechnology. 2004;22:450–4.

38. Rozanov DV, Rozanov ND, Chiotti KE, Reddy A, Wilmarth PA, David LL, et al. MHC class I loaded ligands from breast cancer cell lines: A potential HLA-I-typed antigen collection. Journal of Proteomics. 2018;176:13–23.

39. Chen L, Flies DB. Molecular mechanisms of T cell co-stimulation and co-inhibition. Nature Reviews Immunology. 2013;13:227–42.

40. Rudolph MG, Stanfield RL, Wilson IA. HOW TCRS BIND MHCS, PEPTIDES, AND CORECEPTORS. Annual Review of Immunology. 2006;24:419–66.

41. Lythe G, Callard RE, Hoare RL, Molina-París C. How many TCR clonotypes does a body maintain? Journal of Theoretical Biology. 2016;389:214–24.

42. Wherry EJ, Blattman JN, Murali-Krishna K, van der Most R, Ahmed R. Viral Persistence Alters CD8 T-Cell Immunodominance and Tissue Distribution and Results in Distinct Stages of Functional Impairment. Journal of Virology. 2003;77:4911–27.

43. GILLESPIE GMA, WILLS MR, APPAY V, O'CALLAGHAN C, MURPHY M, SMITH N, et al. Functional Heterogeneity and High Frequencies of Cytomegalovirus-Specific CD8ε T Lymphocytes in Healthy Seropositive Donors. 2018;74:11.

44. Cruz FM, Colbert JD, Merino E, Kriegsman BA, Rock KL. The biology and underlying mechanisms of cross-presentation of exogenous antigens on MHC-I molecules. Annual review of immunology. 2017;35:149–176.

45. Blander JM. Regulation of the Cell Biology of Antigen Cross-Presentation. Annual Review of Immunology. 2018;36:717–753.

46. Smyth LA, Hervouet C, Hayday T, Becker PD, Ellis R, Lechler RI, et al. Acquisition of MHC:Peptide Complexes by Dendritic Cells Contributes to the Generation of Antiviral CD8+ T Cell Immunity In Vivo. The Journal of Immunology. 2012;189:2274–82.

47. Wang J, Nanjundappa RH, Shameli A, Clemente-Casares X, Yamanouchi J, Elliott JF, et al. The Cross-Priming Capacity and Direct Presentation Potential of an Autoantigen Are Separable and Inversely Related Properties. The Journal of Immunology. 2014;193:3296–307.

48. Serna A, Ramirez MC, Soukhanova A, Sigal LJ. Cutting Edge: Efficient MHC Class I Cross-Presentation during Early Vaccinia Infection Requires the Transfer of Proteasomal Intermediates between Antigen Donor and Presenting Cells. The Journal of Immunology. 2003;171:5668–72.

49. Zhang J-G, Czabotar PE, Policheni AN, Caminschi I, San Wan S, Kitsoulis S, et al. The Dendritic Cell Receptor Clec9A Binds Damaged Cells via Exposed Actin Filaments. Immunity. 2012;36:646–57.

50. Cerovic V, Houston SA, Westlund J, Utriainen L, Davison ES, Scott CL, et al. Lymph-borne CD8α+ dendritic cells are uniquely able to cross-prime CD8+ T cells with antigen acquired from intestinal epithelial cells. Mucosal Immunology. 2015;8:38–48.

51. Schreibelt G, Klinkenberg LJJ, Cruz LJ, Tacken PJ, Tel J, Kreutz M, et al. The C-type lectin receptor CLEC9A mediates antigen uptake and (cross-)presentation by human blood BDCA3+ myeloid dendritic cells. Blood. 2012;119:2284–92.

52. den Haan JMM, Bevan MJ. Constitutive versus Activation-dependent Cross-Presentation of Immune Complexes by CD8 $^{+}$ and CD8 $^{-}$ Dendritic Cells In Vivo. The Journal of Experimental Medicine. 2002;196:817–27.

53. Segura E, Albiston AL, Wicks IP, Chai SY, Villadangos JA. Different cross-presentation pathways in steady-state and inflammatory dendritic cells. Proceedings of the National Academy of Sciences. 2009;106:20377–20381.

54. Platzer B, Stout M, Fiebiger E. Antigen Cross-Presentation of Immune Complexes. Frontiers in Immunology [Internet]. 2014 [cited 2018 Mar 31];5. Available from: http://journal.frontiersin.org/article/10.3389/fimmu.2014.00140/abstract

55. Baker K, Rath T, Lencer WI, Fiebiger E, Blumberg RS. Cross-presentation of IgG-containing immune complexes. Cellular and Molecular Life Sciences. 2013;70:1319–34.

56. Guilliams M, Bruhns P, Saeys Y, Hammad H, Lambrecht BN. The function of Fcγ receptors in dendritic cells and macrophages. Nature Reviews Immunology. 2014;14:94–108.

57. DiLillo DJ, Ravetch JV. Differential Fc-Receptor Engagement Drives an Anti-tumor Vaccinal Effect. Cell. 2015;161:1035–45.

58. Mills KHG. TLR-dependent T cell activation in autoimmunity. Nature Reviews Immunology [Internet]. 2011 [cited 2017 Jan 18]; Available from: http://www.nature.com/doifinder/10.1038/nri3095

59. Burgdorf S, Schölz C, Kautz A, Tampé R, Kurts C. Spatial and mechanistic separation of cross-presentation and endogenous antigen presentation. Nature Immunology. 2008;9:558–66.

60. Wagner CS, Grotzke J, Cresswell P. Intracellular Regulation of Cross-Presentation during Dendritic Cell Maturation. Kovats S, editor. PLoS ONE. 2013;8:e76801.

61. Grotzke JE, Cresswell P. Are ERAD components involved in cross-presentation? Molecular Immunology. 2015;68:112–5.

62. Imai J, Hasegawa H, Maruya M, Koyasu S, Yahara I. Exogenous antigens are processed through the endoplasmic reticulum-associated degradation (ERAD) in cross-presentation by dendritic cells. International Immunology. 2005;17:45–53.

63. Mehnert M, Sommer T, Jarosch E. Der1 promotes movement of misfolded proteins through the endoplasmic reticulum membrane. Nature Cell Biology. 2014;16:77–86.

64. Cebrian I, Croce C, Guerrero NA, Blanchard N, Mayorga LS. Rab22a controls MHC-I intracellular trafficking and antigen cross-presentation by dendritic cells. EMBO reports. 2016;17:1753–65.

65. Yewdell JW, Reits E, Neefjes J. Making sense of mass destruction: quantitating MHC class I antigen presentation. Nature Reviews Immunology. 2003;3:952–61.

66. Page DB, Hulett TW, Hilton TL, Hu H-M, Urba WJ, Fox BA. Glimpse into the future: harnessing autophagy to promote anti-tumor immunity with the DRibbles vaccine. Journal for ImmunoTherapy of Cancer [Internet]. 2016 [cited 2017 Feb 7];4. Available from: http://jitc.biomedcentral.com/articles/10.1186/s40425-016-0130-4

67. Li Y, Wang L-X, Yang G, Hao F, Urba WJ, Hu H-M. Efficient Cross-presentation Depends on Autophagy in Tumor Cells. Cancer Research. 2008;68:6889–95.

68. Li Y, Wang L-X, Pang P, Cui Z, Aung S, Haley D, et al. Tumor-Derived Autophagosome Vaccine: Mechanism of Cross-Presentation and Therapeutic Efficacy. Clinical Cancer Research. 2011;17:7047–57.

69. Prehn RT, Main JM. Immunity to methylcholanthrene-induced sarcomas. J Nat Cancer Inst. 1957;769–78.

70. Hilton TL. Preliminary analysis of immune responses in patients enrolled in a Phase II trial of Cyclophosphamide with Allogenic DRibble Vaccine Alone (DPV-001) or with GM-CSF or Imiquimod for adjuvant treatment of Stage IIIA or IIIB NSCLC. National Harbor, MD; 2014.

71. Sanborn R. A pilot single institution study of autologous tumor autophagosome (DRibble) vaccination with docetaxel in patients (pts) with stage IV non-small cell lung cancer (NSCLC). Sydney, Australia; 2013.

72. Sancho D, Joffre OP, Keller AM, Rogers NC, Martínez D, Hernanz-Falcón P, et al. Identification of a dendritic cell receptor that couples sensing of necrosis to immunity. Nature. 2009;458:899–903.

73. Yi Y, Zhou Z, Shu S, Fang Y, Twitty C, Hilton TL, et al. Autophagy-assisted antigen cross-presentation: Autophagosome as the argo of shared tumor-specific antigens and DAMPs. OncoImmunology. 2012;1:976–8.

74. Yuan J, Adamow M, Ginsberg BA, Rasalan TS, Ritter E, Gallardo HF, et al. Integrated NY-ESO-1 antibody and CD8+ T-cell responses correlate with clinical benefit in advanced melanoma patients treated with ipilimumab. Proceedings of the National Academy of Sciences. 2011;108:16723–8.

75. Gopalakrishnan V, Spencer CN, Nezi L, Reuben A, Andrews MC, Karpinets TV, et al. Gut microbiome modulates response to anti–PD-1 immunotherapy in melanoma patients. Science. 2017;eaan4236.

76. Routy B, Le Chatelier E, Derosa L, Duong CPM, Alou MT, Daillère R, et al. Gut microbiome influences efficacy of PD-1–based immunotherapy against epithelial tumors. Science. 2017;eaan3706.

77. Su LF, Kidd BA, Han A, Kotzin JJ, Davis MM. Virus-Specific CD4+ Memory-Phenotype T Cells Are Abundant in Unexposed Adults. Immunity. 2013;38:373–83.

78. Mills DM, Cambier JC. B lymphocyte activation during cognate interactions with CD4+ T lymphocytes: molecular dynamics and immunologic consequences. Seminars in Immunology. 2003;15:325–9.

79. Castellino F, Germain RN. COOPERATION BETWEEN CD4 $^{+}$ AND CD8 $^{+}$ T CELLS: When, Where, and How. Annual Review of Immunology. 2006;24:519–40.

80. Clifford M. Snapper, William E. Paul. Interferon-$\gamma $ and B Cell Stimulatory Factor-1 Reciprocally Regulate Ig Isotype Production. Science, New Series. 1987;236:944–7.

81. Hjelholt A, Christiansen G, Sørensen US, Birkelund S. IgG subclass profiles in normal human sera of antibodies specific to five kinds of microbial antigens. Pathogens and Disease. 2013;67:206–13.

82. Banchereau J, Steinman RM. Dendritic cells and the control of immunity. Nature. 1998;392:245–52.

83. Bernasconi NL. Maintenance of Serological Memory by Polyclonal Activation of Human Memory B Cells. Science. 2002;298:2199–202.

84. Pieper K, Grimbacher B, Eibel H. B-cell biology and development. Journal of Allergy and Clinical Immunology. 2013;131:959–71.

85. Mills DM, Cambier JC. B lymphocyte activation during cognate interactions with CD4+ T lymphocytes: molecular dynamics and immunologic consequences. Seminars in Immunology. 2003;15:325–9.

86. Parker DC. T cell-dependent B cell activation. Annual review of immunology. 1993;11:331–360.

87. Noelle RJ, Snow EC. Cognate interactions between helper T cells and B cells. Immunology today. 1990;11:361–368.

88. Stavnezer J, Guikema JEJ, Schrader CE. Mechanism and Regulation of Class Switch Recombination. Annual Review of Immunology. 2008;26:261–92.

89. Basso K, Dalla-Favera R. Germinal centres and B cell lymphomagenesis. Nature Reviews Immunology. 2015;15:172–84.

90. Shulman Z, Gitlin AD, Weinstein JS, Lainez B, Esplugues E, Flavell RA, et al. Dynamic signaling by T follicular helper cells during germinal center B cell selection. Science. 2014;345:1058–1062.

91. De Silva NS, Klein U. Dynamics of B cells in germinal centres. Nature Reviews Immunology. 2015;15:137–48.

92. MacLennan IC. Germinal centers. Annual review of immunology. 1994;12:117–139.

93. Victora GD, Nussenzweig MC. Germinal Centers. Annual Review of Immunology. 2012;30:429–57.

94. Maizels N. Immunoglobulin Gene Diversification. Annual Review of Genetics. 2005;39:23–46.

95. Kawano Y, Noma T, Yata J, Immunol J. Regulation of human IgG subclass production by cytokines. IFN-gamma and IL-6 act antagonistically in the induction of human IgG1 but additively in the induction of IgG2. 2018;12.

96. Snapper CM, Peschel C, Paul WE, Immunol J. IFN-gamma stimulates IgG2a secretion by murine B cells stimulated with bacterial lipopolysaccharide. 2018;8.

97. Olson BM, McNeel DG. Antibody and T-cell responses specific for the androgen receptor in patients with prostate cancer. The Prostate. 2007;67:1729–39.

98. Vidarsson G, Dekkers G, Rispens T. IgG Subclasses and Allotypes: From Structure to Effector Functions. Frontiers in Immunology [Internet]. 2014 [cited 2018 Mar 31];5. Available from: http://www.frontiersin.org/Immunotherapies_and_Vaccines/10.3389/fimmu.2014.00520/abstract

99. Platzer B, Stout M, Fiebiger E. Antigen Cross-Presentation of Immune Complexes. Frontiers in Immunology [Internet]. 2014 [cited 2018 Mar 31];5. Available from: http://journal.frontiersin.org/article/10.3389/fimmu.2014.00140/abstract

100. Baker K, Rath T, Lencer WI, Fiebiger E, Blumberg RS. Cross-presentation of IgG-containing immune complexes. Cellular and Molecular Life Sciences. 2013;70:1319–34.

101. Cha E, Klinger M, Hou Y, Cummings C, Ribas A, Faham M, et al. Improved Survival with T Cell Clonotype Stability After Anti-CTLA-4 Treatment in Cancer Patients. Science Translational Medicine. 2014;6:238ra70-238ra70.

102. Thomas PG, Brown SA, Yue W, So J, Webby RJ, Doherty PC. An unexpected antibody response to an engineered influenza virus modifies CD8+ T cell responses. Proceedings of the National Academy of Sciences of the United States of America. 2006;103:2764–2769.

103. Nagele EP, Han M, Acharya NK, DeMarshall C, Kosciuk MC, Nagele RG. Natural IgG Autoantibodies Are Abundant and Ubiquitous in Human Sera, and Their Number Is Influenced By Age, Gender, and Disease. Tsokos GC, editor. PLoS ONE. 2013;8:e60726.

104. Larman HB, Zhao Z, Laserson U, Li MZ, Ciccia A, Gakidis MAM, et al. Autoantigen discovery with a synthetic human peptidome. Nature Biotechnology. 2011;29:535–41.

105. Meyer S, Woodward M, Hertel C, Vlaicu P, Haque Y, Kärner J, et al. AIRE-Deficient Patients Harbor Unique High-Affinity Disease-Ameliorating Autoantibodies. Cell. 2016;166:582–95.

106. Graff JN, Puri S, Bifulco CB, Fox BA, Beer TM. Sustained Complete Response to CTLA-4 Blockade in a Patient with Metastatic, Castration-Resistant Prostate Cancer. Cancer Immunology Research. 2014;2:399–403.

107. Gnjatic S, Ritter E, Büchler MW, Giese NA, Brors B, Frei C, et al. Seromic profiling of ovarian and pancreatic cancer. Proceedings of the National Academy of Sciences. 2010;107:5088–5093.

108. Messina JL, Fenstermacher DA, Eschrich S, Qu X, Berglund AE, Lloyd MC, et al. 12-Chemokine Gene Signature Identifies Lymph Node-like Structures in Melanoma: Potential for Patient Selection for Immunotherapy? Scientific Reports [Internet]. 2012 [cited 2017 Jan 18];2. Available from: http://www.nature.com/articles/srep00765

109. Affara NI, Ruffell B, Medler TR, Gunderson AJ, Johansson M, Bornstein S, et al. B Cells Regulate Macrophage Phenotype and Response to Chemotherapy in Squamous Carcinomas. Cancer Cell. 2014;25:809–21.

110. Germain C, Gnjatic S, Tamzalit F, Knockaert S, Remark R, Goc J, et al. Presence of B Cells in Tertiary Lymphoid Structures Is Associated with a Protective Immunity in Patients with Lung Cancer. American Journal of Respiratory and Critical Care Medicine. 2014;189:832–44.

111. Chen Y-T. The journey from autologous typing to SEREX, NY-ESO-1, and Cancer/Testis antigens. Cancer Immunity Archive. 2012;12:8.

112. Pfreundschuh M. The genealogy of SEREX. Cancer Immunity Archive. 2012;12:7.

113. Gubin MM, Zhang X, Schuster H, Caron E, Ward JP, Noguchi T, et al. Checkpoint blockade cancer immunotherapy targets tumour-specific mutant antigens. Nature. 2014;515:577–81.

114. Snyder A, Makarov V, Merghoub T, Yuan J, Zaretsky JM, Desrichard A, et al. Genetic Basis for Clinical Response to CTLA-4 Blockade in Melanoma. New England Journal of Medicine. 2014;371:2189–99.

115. Schumacher T, Bunse L, Pusch S, Sahm F, Wiestler B, Quandt J, et al. A vaccine targeting mutant IDH1 induces antitumour immunity. Nature. 2014;512:324–7.

116. Tran E, Robbins PF, Lu Y-C, Prickett TD, Gartner JJ, Jia L, et al. T-Cell Transfer Therapy Targeting Mutant KRAS in Cancer. New England Journal of Medicine. 2016;375:2255–62.

117. Lu Y-C, Yao X, Crystal JS, Li YF, El-Gamil M, Gross C, et al. Efficient Identification of Mutated Cancer Antigens Recognized by T Cells Associated with Durable Tumor Regressions. Clinical Cancer Research. 2014;20:3401–10.

118. Twitty CG, Jensen SM, Hu H-M, Fox BA. Tumor-Derived Autophagosome Vaccine: Induction of Cross-Protective Immune Responses against Short-lived Proteins through a p62-Dependent Mechanism. Clinical Cancer Research. 2011;17:6467–81.

119. Yu G, Li Y, Cui Z, Morris NP, Weinberg AD, Fox BA, et al. Combinational Immunotherapy with Allo-DRibble Vaccines and Anti-OX40 Co-Stimulation Leads to Generation of Cross-Reactive Effector T Cells and Tumor Regression. Scientific Reports [Internet]. 2016 [cited 2017 Jun 29];6. Available from: http://www.nature.com/articles/srep37558

120. Page DB, Hulett TW, Hilton TL, Hu H-M, Urba WJ, Fox BA. Glimpse into the future: harnessing autophagy to promote anti-tumor immunity with the DRibbles vaccine. Journal for ImmunoTherapy of Cancer [Internet]. 2016 [cited 2017 Feb 7];4. Available from: http://jitc.biomedcentral.com/articles/10.1186/s40425-016-0130-4

121. McAlister GC, Nusinow DP, Jedrychowski MP, Wühr M, Huttlin EL, Erickson BK, et al. MultiNotch MS3 Enables Accurate, Sensitive, and Multiplexed Detection of Differential Expression across Cancer Cell Line Proteomes. Analytical Chemistry. 2014;86:7150–8.

122. Käll L, Canterbury JD, Weston J, Noble WS, MacCoss MJ. Semi-supervised learning for peptide identification from shotgun proteomics datasets. Nature Methods. 2007;4:923–5.

123. Calvo SE, Clauser KR, Mootha VK. MitoCarta2.0: an updated inventory of mammalian mitochondrial proteins. Nucleic Acids Research. 2016;44:D1251–7.

124. Feng Z, Jensen SM, Messenheimer DJ, Farhad M, Neuberger M, Bifulco CB, et al. Multispectral Imaging of T and B Cells in Murine Spleen and Tumor. The Journal of Immunology. 2016;196:3943–50.

125. Kreiter S, Vormehr M, van de Roemer N, Diken M, Löwer M, Diekmann J, et al. Mutant MHC class II epitopes drive therapeutic immune responses to cancer. Nature. 2015;520:692–6.

126. Castle JC, Loewer M, Boegel S, Tadmor AD, Boisguerin V, de Graaf J, et al. Mutated tumor alleles are expressed according to their DNA frequency. Scientific Reports [Internet]. 2014 [cited 2017 Jan 18];4. Available from: http://www.nature.com/articles/srep04743

127. Smedley D, Haider S, Durinck S, Pandini L, Provero P, Allen J, et al. The BioMart community portal: an innovative alternative to large, centralized data repositories. Nucleic Acids Research. 2015;43:W589–98.

128. Scrimieri F, Askew D, Corn DJ, Eid S, Bobanga ID, Bjelac JA, et al. Murine leukemia virus envelope gp70 is a shared biomarker for the high-sensitivity quantification of murine tumor burden. OncoImmunology. 2013;2:e26889.

129. Hoof I, Peters B, Sidney J, Pedersen LE, Sette A, Lund O, et al. NetMHCpan, a method for MHC class I binding prediction beyond humans. Immunogenetics. 2009;61:1–13.

130. Nielsen M, Lund O. NN-align. An artificial neural network-based alignment algorithm for MHC class II peptide binding prediction. BMC Bioinformatics. 2009;10:296.

131. Nielsen M, Lundegaard C, Lund O. Prediction of MHC class II binding affinity using SMM-align, a novel stabilization matrix alignment method. BMC Bioinformatics. 2007;8:238.

132. Li Y, Wang L-X, Pang P, Cui Z, Aung S, Haley D, et al. Tumor-Derived Autophagosome Vaccine: Mechanism of Cross-Presentation and Therapeutic Efficacy. Clinical Cancer Research. 2011;17:7047–57.

133. Kim K, Skora AD, Li Z, Liu Q, Tam AJ, Blosser RL, et al. Eradication of metastatic mouse cancers resistant to immune checkpoint blockade by suppression of myeloid-derived cells. Proceedings of the National Academy of Sciences. 2014;111:11774–9.

134. Jensen S. Polarization of a type 1 anti-tumor immune response in the context of a strong tumor antigen results in the regression of the mammary adenocarcinoma, 4T1. Oregon Health & Science University; 2003.

135. Fridman WH, Zitvogel L, Sautès–Fridman C, Kroemer G. The immune contexture in cancer prognosis and treatment. Nature Reviews Clinical Oncology. 2017;14:717–34.

136. Galon J. Type, Density, and Location of Immune Cells Within Human Colorectal Tumors Predict Clinical Outcome. Science. 2006;313:1960–4.

137. Ng SSM, Nagy BA, Jensen SM, Hu X, Alicea C, Fox BA, et al. Heterodimeric IL15 Treatment Enhances Tumor Infiltration, Persistence, and Effector Functions of Adoptively Transferred Tumor-specific T Cells in the Absence of Lymphodepletion. Clinical Cancer Research. 2017;23:2817–30.

138. Kwek SS, Dao V, Roy R, Hou Y, Alajajian D, Simko JP, et al. Diversity of Antigen-Specific Responses Induced In Vivo with CTLA-4 Blockade in Prostate Cancer Patients. The Journal of Immunology. 2012;189:3759–66.

139. Tripathi SC, Peters HL, Taguchi A, Katayama H, Wang H, Momin A, et al. Immunoproteasome deficiency is a feature of non-small cell lung cancer with a mesenchymal phenotype and is associated with a poor outcome. Proceedings of the National Academy of Sciences. 2016;113:E1555–64.

140. Sette A, Moutaftsi M, Moyron-Quiroz J, McCausland MM, Davies DH, Johnston RJ, et al. Selective CD4+ T Cell Help for Antibody Responses to a Large Viral Pathogen: Deterministic Linkage of Specificities. Immunity. 2008;28:847–58.

141. Krzywinski M, Schein J, Birol I, Connors J, Gascoyne R, Horsman D, et al. Circos: an information aesthetic for comparative genomics. Genome research. 2009;19:1639–1645.

142. Narendra D, Kane LA, Hauser DN, Fearnley IM, Youle RJ. p62/SQSTM1 is required for Parkin-induced mitochondrial clustering but not mitophagy; VDAC1 is dispensable for both. Autophagy. 2010;6:1090–106.

143. Snapper CM, Peschel C, Paul WE, Immunol J. IFN-gamma stimulates IgG2a secretion by murine B cells stimulated with bacterial lipopolysaccharide. 2018;8.

144. Bentebibel S-E, Lopez S, Obermoser G, Schmitt N, Mueller C, Harrod C, et al. Induction of ICOS+ CXCR3+ CXCR5+ TH cells correlates with antibody responses to influenza vaccination. Science translational medicine. 2013;5:176ra32–176ra32.

145. Nayak JL, Fitzgerald TF, Richards KA, Yang H, Treanor JJ, Sant AJ. CD4+ T-Cell Expansion Predicts Neutralizing Antibody Responses to Monovalent, Inactivated 2009 Pandemic Influenza A(H1N1) Virus Subtype H1N1 Vaccine. The Journal of Infectious Diseases. 2013;207:297–305.

146. Jäger E, Chen Y-T, Drijfhout JW, Karbach J, Ringhoffer M, Jäger D, et al. Simultaneous humoral and cellular immune response against cancer–testis antigen NY-ESO-1: Definition of human histocompatibility leukocyte antigen (HLA)-A2–binding peptide epitopes. Journal of Experimental Medicine. 1998;187:265–270.

147. GuhaThakurta D, Sheikh NA, Fan L-Q, Kandadi H, Meagher TC, Hall SJ, et al. Humoral Immune Response against Nontargeted Tumor Antigens after Treatment with Sipuleucel-T and Its Association with Improved Clinical Outcome. Clinical Cancer Research. 2015;21:3619–30.

148. Stronen E, Toebes M, Kelderman S, van Buuren MM, Yang W, van Rooij N, et al. Targeting of cancer neoantigens with donor-derived T cell receptor repertoires. Science. 2016;352:1337–41.

149. Routy B, Le Chatelier E, Derosa L, Duong CPM, Alou MT, Daillère R, et al. Gut microbiome influences efficacy of PD-1–based immunotherapy against epithelial tumors. Science. 2017;eaan3706.

150. Gopalakrishnan V, Spencer CN, Nezi L, Reuben A, Andrews MC, Karpinets TV, et al. Gut microbiome modulates response to anti–PD-1 immunotherapy in melanoma patients. Science. 2017;eaan4236.

151. Iida N, Dzutsev A, Stewart CA, Smith L, Bouladoux N, Weingarten RA, et al. Commensal Bacteria Control Cancer Response to Therapy by Modulating the Tumor Microenvironment. Science. 2013;342:967–70.

152. Rafiq K, Bergtold A, Clynes R. Immune complex–mediated antigen presentation induces tumor immunity. Journal of Clinical Investigation. 2002;110:71–9.

153. Srivastava RM, Lee SC, Andrade Filho PA, Lord CA, Jie H-B, Davidson HC, et al. Cetuximab-Activated Natural Killer and Dendritic Cells Collaborate to Trigger Tumor Antigen-Specific T-cell Immunity in Head and Neck Cancer Patients. Clinical Cancer Research. 2013;19:1858–72.

154. Angeletti D, Gibbs JS, Angel M, Kosik I, Hickman HD, Frank GM, et al. Defining B cell immunodominance to viruses. Nature Immunology. 2017;18:456–63.

155. Andrews SF, Kaur K, Pauli NT, Huang M, Huang Y, Wilson PC. High Preexisting Serological Antibody Levels Correlate with Diversification of the Influenza Vaccine Response. Sandri-Goldin RM, editor. Journal of Virology. 2015;89:3308–17.

156. Sasaki S, He X-S, Holmes TH, Dekker CL, Kemble GW, Arvin AM, et al. Influence of Prior Influenza Vaccination on Antibody and B-Cell Responses. Nixon DF, editor. PLoS ONE. 2008;3:e2975.

157. Mongkolsapaya J, Dejnirattisai W, Xu X, Vasanawathana S, Tangthawornchaikul N, Chairunsri A, et al. Original antigenic sin and apoptosis in the pathogenesis of dengue hemorrhagic fever. Nature Medicine. 2003;9:921–7.

158. Su LF, Kidd BA, Han A, Kotzin JJ, Davis MM. Virus-Specific CD4+ Memory-Phenotype T Cells Are Abundant in Unexposed Adults. Immunity. 2013;38:373–83.

159. Coley WB. The Classic: The Treatment of Malignant Tumors by Repeated Inoculations of Erysipelas. Clinical Orthopaedics and Related Research. 1991;NA;3???11.

160. Turnbull S, West E, Scott K, Appleton E, Melcher A, Ralph C. Evidence for Oncolytic Virotherapy: Where Have We Got to and Where Are We Going? Viruses. 2015;7:6291–312.

161. Kaufman HL, Kohlhapp FJ, Zloza A. Oncolytic viruses: a new class of immunotherapy drugs. Nature Reviews Drug Discovery. 2015;14:642–62.

162. Kaisho T, Akira S. Toll-like receptor function and signaling. Journal of Allergy and Clinical Immunology. 2006;117:979–87.

163. Krieg AM. Development of TLR9 agonists for cancer therapy. Journal of Clinical Investigation. 2007;117:1184–94.

164. Hennessy EJ, Parker AE, O'Neill LAJ. Targeting Toll-like receptors: emerging therapeutics? Nature Reviews Drug Discovery. 2010;9:293–307.

165. Dhodapkar MV, Sznol M, Zhao B, Wang D, Carvajal RD, Keohan ML, et al. Induction of Antigen-Specific Immunity with a Vaccine Targeting NY-ESO-1 to the Dendritic Cell Receptor DEC-205. Science Translational Medicine. 2014;6:232ra51-232ra51.

166. Baksh K, Weber J. Immune Checkpoint Protein Inhibition for Cancer: Preclinical Justification for CTLA-4 and PD-1 Blockade and New Combinations. Seminars in Oncology. 2015;42:363–77.

167. Topalian SL, Drake CG, Pardoll DM. Immune Checkpoint Blockade: A Common Denominator Approach to Cancer Therapy. Cancer Cell. 2015;27:450–61.

168. Linch SN, McNamara MJ, Redmond WL. OX40 Agonists and Combination Immunotherapy: Putting the Pedal to the Metal. Frontiers in Oncology [Internet]. 2015 [cited 2018 Mar 29];5. Available from: http://journal.frontiersin.org/Article/10.3389/fonc.2015.00034/abstract

169. Curti BD, Kovacsovics-Bankowski M, Morris N, Walker E, Chisholm L, Floyd K, et al. OX40 Is a Potent Immune-Stimulating Target in Late-Stage Cancer Patients. Cancer Research. 2013;73:7189–98.

170. Gerlinger M, Quezada SA, Peggs KS, Furness AJ, Fisher R, Marafioti T, et al. Ultra-deep T cell receptor sequencing reveals the complexity and intratumour heterogeneity of T cell clones in renal cell carcinomas: Ultra-deep sequencing of T cell repertoires in renal cancer. The Journal of Pathology. 2013;231:424–32.

171. Glanville J, Huang H, Nau A, Hatton O, Wagar LE, Rubelt F, et al. Identifying specificity groups in the T cell receptor repertoire. Nature. 2017;547:94–8.

172. Ott PA, Hu Z, Keskin DB, Shukla SA, Sun J, Bozym DJ, et al. An immunogenic personal neoantigen vaccine for patients with melanoma. Nature. 2017;547:217–21.

173. Ziegler A, Leffell DJ, Kunala S, Sharma HW, Gailani M, Simon JA, et al. Mutation hotspots due to sunlight in the p53 gene of nonmelanoma skin cancers. Proceedings of the National Academy of Sciences. 1993;90:4216–20.

174. Kandoth C, McLellan MD, Vandin F, Ye K, Niu B, Lu C, et al. Mutational landscape and significance across 12 major cancer types. Nature. 2013;502:333–9.

175. Sturm D, Witt H, Hovestadt V, Khuong-Quang D-A, Jones DTW, Konermann C, et al. Hotspot Mutations in H3F3A and IDH1 Define Distinct Epigenetic and Biological Subgroups of Glioblastoma. Cancer Cell. 2012;22:425–37.

176. Forbes SA, Beare D, Gunasekaran P, Leung K, Bindal N, Boutselakis H, et al. COSMIC: exploring the world's knowledge of somatic mutations in human cancer. Nucleic Acids Research. 2015;43:D805–11.

177. Schumacher T, Bunse L, Pusch S, Sahm F, Wiestler B, Quandt J, et al. A vaccine targeting mutant IDH1 induces antitumour immunity. Nature. 2014;512:324–7.

178. Wang QJ, Yu Z, Griffith K, Hanada K -i., Restifo NP, Yang JC. Identification of T-cell Receptors Targeting KRAS-Mutated Human Tumors. Cancer Immunology Research. 2016;4:204–14.

179. Gros A, Robbins PF, Yao X, Li YF, Turcotte S, Tran E, et al. PD-1 identifies the patient-specific CD8+ tumor-reactive repertoire infiltrating human tumors. Journal of Clinical Investigation. 2014;124:2246–59.

180. Gros A, Parkhurst MR, Tran E, Pasetto A, Robbins PF, Ilyas S, et al. Prospective identification of neoantigen-specific lymphocytes in the peripheral blood of melanoma patients. Nature Medicine. 2016;22:433–8.

181. Tran E, Robbins PF, Lu Y-C, Prickett TD, Gartner JJ, Jia L, et al. T-Cell Transfer Therapy Targeting Mutant KRAS in Cancer. New England Journal of Medicine. 2016;375:2255–62.

182. Zehir A, Benayed R, Shah RH, Syed A, Middha S, Kim HR, et al. Mutational landscape of metastatic cancer revealed from prospective clinical sequencing of 10,000 patients. Nature Medicine. 2017;23:703–13.

183. Hodi FS, O'Day SJ, McDermott DF, Weber RW, Sosman JA, Haanen JB, et al. Improved survival with ipilimumab in patients with metastatic melanoma. New England Journal of Medicine. 2010;363:711–723.

184. Maciag PC, Schlecht NF, Souza PSA, Franco EL, Villa LL, Petzl-Erler ML. Major Histocompatibility Complex Class II Polymorphisms and Risk of Cervical Cancer and Human Papillomavirus Infection in Brazilian Women. 2000;10.

185. Marty R, Kaabinejadian S, Rossell D, Slifker MJ, van de Haar J, Engin HB, et al. MHC-I Genotype Restricts the Oncogenic Mutational Landscape. Cell. 2017;171:1272–1283.e15.

186. Marty R, de Prisco N, Carter H, Font-Burgada J. MHC-I genotype drives early immune selection of oncogenic mutations. Molecular & Cellular Oncology. 2018;5:e1409863.

187. Martincorena I, Roshan A, Gerstung M, Ellis P, Van Loo P, McLaren S, et al. High burden and pervasive positive selection of somatic mutations in normal human skin. Science. 2015;348:880–886.

188. Ehrlich M. DNA methylation in cancer: too much, but also too little. Oncogene. 2002;21:5400–13.

189. Jones PA, Baylin SB. The Epigenomics of Cancer. Cell. 2007;128:683–92.

190. Dawson MA, Kouzarides T. Cancer Epigenetics: From Mechanism to Therapy. Cell. 2012;150:12–27.

191. Khong HT, Rosenberg SA. Pre-Existing Immunity to Tyrosinase-Related Protein (TRP)-2, a New TRP-2 Isoform, and the NY-ESO-1 Melanoma Antigen in a Patient with a Dramatic Response to Immunotherapy. The Journal of Immunology. 2002;168:951–6.

192. Kantoff PW, Higano CS, Shore ND, Berger ER, Small EJ, Penson DF, et al. Sipuleucel-T immunotherapy for castration-resistant prostate cancer. New England Journal of Medicine. 2010;363:411–422.

193. Ke X, Shen L. Molecular targeted therapy of cancer: The progress and future prospect. Frontiers in Laboratory Medicine. 2017;1:69–75.

194. Neel DS, Bivona TG. Resistance is futile: overcoming resistance to targeted therapies in lung adenocarcinoma. npj Precision Oncology [Internet]. 2017 [cited 2018 Mar 30];1. Available from: http://www.nature.com/articles/s41698-017-0007-0

195. Kwek SS, Dao V, Roy R, Hou Y, Alajajian D, Simko JP, et al. Diversity of Antigen-Specific Responses Induced In Vivo with CTLA-4 Blockade in Prostate Cancer Patients. The Journal of Immunology. 2012;189:3759–66.

196. Graff JN, Puri S, Bifulco CB, Fox BA, Beer TM. Sustained Complete Response to CTLA-4 Blockade in a Patient with Metastatic, Castration-Resistant Prostate Cancer. Cancer Immunology Research. 2014;2:399–403.

197. Meyer S, Woodward M, Hertel C, Vlaicu P, Haque Y, Kärner J, et al. AIRE-Deficient Patients Harbor Unique High-Affinity Disease-Ameliorating Autoantibodies. Cell. 2016;166:582–95.

198. Kanderova V, Kuzilkova D, Stuchly J, Vaskova M, Brdicka T, Fiser K, et al. High-resolution Antibody Array Analysis of Childhood Acute Leukemia Cells. Molecular & Cellular Proteomics. 2016;15:1246–61.

199. Miersch S, Bian X, Wallstrom G, Sibani S, Logvinenko T, Wasserfall CH, et al. Serological autoantibody profiling of type 1 diabetes by protein arrays. Journal of Proteomics. 2013;94:486–96.

200. Anderson KS, Sibani S, Wallstrom G, Qiu J, Mendoza EA, Raphael J, et al. Protein Microarray Signature of Autoantibody Biomarkers for the Early Detection of Breast Cancer. Journal of Proteome Research. 2011;10:85–96.

201. Gibson DS, Qiu J, Mendoza EA, Barker K, Rooney ME, LaBaer J. Circulating and synovial antibody profiling of juvenile arthritis patients by nucleic acid programmable protein arrays. Arthritis research & therapy. 2012;14:1.

202. Larman HB, Zhao Z, Laserson U, Li MZ, Ciccia A, Gakidis MAM, et al. Autoantigen discovery with a synthetic human peptidome. Nature Biotechnology. 2011;29:535–41.

203. Xu GJ, Kula T, Xu Q, Li MZ, Vernon SD, Ndung'u T, et al. Comprehensive serological profiling of human populations using a synthetic human virome. Science. 2015;348:aaa0698-aaa0698.

204. Mittal D, Gubin MM, Schreiber RD, Smyth MJ. New insights into cancer immunoediting and its three component phases—elimination, equilibrium and escape. Current Opinion in Immunology. 2014;27:16–25.

205. Cooper GS, Stroehla BC. The epidemiology of autoimmune diseases. Autoimmunity Reviews. 2003;2:119–25.

206. Minter MR, Taylor JM, Crack PJ. The contribution of neuroinflammation to amyloid toxicity in Alzheimer's disease. Journal of Neurochemistry. 2016;136:457–74.

207. Oliveira BC de L, Bellozi PMQ, Reis HJ, de Oliveira ACP. Inflammation as a Possible Link Between Dyslipidemia and Alzheimer's Disease. Neuroscience. 2018;376:127–41.

208. Barbeito LH, Pehar M, Cassina P, Vargas MR, Peluffo H, Viera L, et al. A role for astrocytes in motor neuron loss in amyotrophic lateral sclerosis. Brain Research Reviews. 2004;47:263–74.

209. Ramanan VK, Saykin AJ. Pathways to neurodegeneration: mechanistic insights from GWAS in Alzheimer's disease, Parkinson's disease, and related disorders. :31.

210. Radford RA, Morsch M, Rayner SL, Cole NJ, Pountney DL, Chung RS. The established and emerging roles of astrocytes and microglia in amyotrophic lateral sclerosis and frontotemporal dementia. Frontiers in Cellular Neuroscience [Internet]. 2015 [cited 2018 Mar 30];9. Available from: http://journal.frontiersin.org/Article/10.3389/fncel.2015.00414/abstract

211. May C, Nordhoff E, Casjens S, Turewicz M, Eisenacher M, Gold R, et al. Highly Immunoreactive IgG Antibodies Directed against a Set of Twenty Human Proteins in the Sera of Patients with Amyotrophic Lateral Sclerosis Identified by Protein Array. Esteban FJ, editor. PLoS ONE. 2014;9:e89596.

212. Tabarés-Seisdedos R, Dumont N, Baudot A, Valderas JM, Climent J, Valencia A, et al. No paradox, no progress: inverse cancer comorbidity in people with other complex diseases. The Lancet Oncology. 12:604–8.

213. Olsen JH, Friis S, Frederiksen K, McLaughlin JK, Mellemkjaer L, Møller H. Atypical cancer pattern in patients with Parkinson's disease. British Journal of Cancer. 2005;92:201–5.

214. Plun-Favreau H, Lewis PA, Hardy J, Martins LM, Wood NW. Cancer and Neurodegeneration: Between the Devil and the Deep Blue Sea. Horwitz MS, editor. PLoS Genetics. 2010;6:e1001257.

215. Roe CM, Fitzpatrick AL, Xiong C, Sieh W, Kuller L, Miller JP, et al. Cancer linked to Alzheimer disease but not vascular dementia. Neurology. 2010;74:106–12.

216. Olsen JH, Friis S, Frederiksen K. Malignant Melanoma and Other Types of Cancer Preceding Parkinson Disease: Epidemiology. 2006;17:582–7.

217. Devine MJ, Plun-Favreau H, Wood NW. Parkinson's disease and cancer: two wars, one front. Nature Reviews Cancer. 2011;11:813–23.

218. Freedman DM, Curtis RE, Daugherty SE, Goedert JJ, Kuncl RW, Tucker MA. The association between cancer and amyotrophic lateral sclerosis. Cancer Causes & Control. 2013;24:55–60.

219. Li W, Lee M-H, Henderson L, Tyagi R, Bachani M, Steiner J, et al. Human endogenous retrovirus-K contributes to motor neuron disease. Science Translational Medicine. 2015;7:307ra153-307ra153.